Doctoral (PhD) Thesis

University of Sopron

Faculty of Forestry

Roth Gyula Doctoral School of Forestry and Wildlife Management Sciences

Head of the Doctoral School: Dr. Prof. Sándor Faragó

Doctoral program: E7 - Geoinformatics

Head of program : Dr. Kornél Czimber

Discipline: Forestry and Wildlife Management Sciences

APPLICATION OF SATELLITE IMAGE TIME SERIES IN THE HUNGARIAN FOREST DISTURBANCE MONITORING

Author: Tamás Molnár

Supervisor: Dr. Géza Király

Consultant: Dr. Zoltán Somogyi

(Univerity of Sopron, Forest Research Institute)

Sopron

2023

APPLICATION OF SATELLITE IMAGE TIME SERIES IN THE HUNGARIAN FOREST DISTURBANCE MONITORING

Értekezés doktori (PhD) fokozat elnyerése érdekében

Írta: Molnár Tamás

Készült a Soproni Egyetem Roth Gyula Erdészeti és Vadgazdálkodási Tudományok Doktori Iskola E7 Geoinformatika programja keretében.

Témavezetők: Dr. Király Géza és Dr. Somogyi Zoltán (SOE Erdészeti Tudományos Intézet)

Dr. Király Géza: Az értekezés témavezetőként elfogadásra javasolt: igen / nem
_____(aláírás)

Dr. Somogyi Zoltán: Az értekezés témavezetőként elfogadásra javasolt: igen / nem
_____(aláírás)

A komplex vizsga időpontja: 2020. május 15.
A komplex vizsga eredménye: 93 %, summa cum laude

Az értekezés bírálóként elfogadásra javasolt (igen /nem)

1. bíráló: Dr. Czimber Kornél igen / nem _____(aláírás)

2. bíráló: Dr. Burai Péter igen / nem _____(aláírás)

Az értekezés nyilvános védésének eredménye: _____ %

Kelt Sopron, 2023. június

_____
a Bíráló Bizottság elnöke

A doktori (PhD) oklevél minősítése: _____

_____
az EDHT elnöke

5. sz. melléklet

NYILATKOZAT

Alulírott Molnár Tamás jelen nyilatkozat aláírásával kijelentem, hogy az **Application of satellite image time series in the Hungarian forest disturbance monitoring** című PhD értekezésem önálló munkám, az értekezés készítése során betartottam a szerzői jogról szóló 1999. évi LXXVI. törvény szabályait, valamint a Roth Gyula Erdészeti és Vadgazdálkodási Tudományok Doktori Iskola által előírt, a doktori értekezés készítésére vonatkozó szabályokat, különösen a hivatkozások és idézések tekintetében.[1]

Kijelentem továbbá, hogy az értekezés készítése során az önálló kutatómunka kitétel tekintetében témavezetőimet, illetve a programvezetőt nem tévesztettem meg.

Jelen nyilatkozat aláírásával tudomásul veszem, hogy amennyiben bizonyítható, hogy azértekezést nem magam készítettem, vagy az értekezéssel kapcsolatban szerzői jogsértés ténye merül fel, a Soproni Egyetem megtagadja az értekezés befogadását.

Az értekezés befogadásának megtagadása nem érinti a szerzői jogsértés miatti egyéb (polgári jogi, szabálysértési jogi, büntetőjogi) jogkövetkezményeket.

Kelt Sopron, 2023. május 12.

_____

doktorjelölt

[1] **1999. évi LXXVI. tv.** 34. § (1) A mű részletét – az átvevő mű jellege és célja által indokolt terjedelemben és azeredetihez híven – a forrás, valamint az ott megjelölt szerző megnevezésével bárki idézheti.

36. § (1) Nyilvánosan tartott előadások és más hasonló művek részletei, valamint politikai beszédek tájékoztatáscéljára – a cél által indokolt terjedelemben – szabadon felhasználhatók. Ilyen felhasználás esetén a forrást – a szerző nevével együtt – fel kell tüntetni, hacsak ez lehetetlennek nem bizonyul.

Abstract

Remote sensing enables constant monitoring of the state of our forests all over the world. It has constantly increasing importance in forest state monitoring. Since forest damage has become more frequent in Hungary in the last few decades, remote sensing offers a powerful, rapid, and cost-effective tool for monitoring disturbances in forest health.

In this PhD thesis, a novel approach was created to utilize high-resolution Sentinel-2 satellite imagery of the European Space Agency and Google Earth Engine (GEE) cloud computing. The processing, analysing, and visualization of vegetation and water index (Normalized Difference Vegetation Index (NDVI), NDVI change (NDVIch), standardized NDVI (Z NDVI), Normalized Difference Water Index (NDWI), Enhanced Vegetation Index (EVI)) maps and charts derived from satellite images took place online, in the cloud, to ensure the detection of forest disturbances in the three Hungarian study sites (Nagyerdő of Debrecen, Farkas-erdő of Sárvár, and Central Bükk) for the period 2017 – 2020.

My results indicated that the combined dataset of satellite imagery and ground-based reports provided suitable input for forest damage monitoring conducted with GEE. The applied method successfully identified different types of forest damage on Z NDVI maps in the surveyed period with 78 % Total Accuracy

Keywords: forest monitoring, satellite imagery, Sentinel-2, cloud computing, Google Earth Engine, Machine Learning

Kivonat

A távérzékelés segítésével folyamatosan nyomon követhetjük az erdők állapotát világszerte. Egyre fontosabb az erdőmonitoringban betöltött szerepe is. Mivel az erdőkárok gyakorisága megnőtt Magyarországon az elmúlt évtizedekben, az űrfelvételek felhasználása hatékony, gyors és olcsó eszközzé vált az erdők egészségi állapotával összefüggő bolygatások monitorozására.

Ebben a PhD értekezésben egy új módszertant készítettem, ami az Európai Űrügynökség nagyfelbontású Sentinel-2 űrfelvételeinek és a Google Earth Engine (GEE) felhőrendszerének felhasználásán alapul. Az erdőállapotot leíró, műholdképekből előállított vegetációs és vízindex (Normalizált Vegetációs Index (NDVI), NDVI változás (NDVIch), standardizált NDVI (Z NDVI), Normalizált Víz Index (NDWI), Továbbfejlesztett Vegetációs Index (EVI)) térképek feldolgozása, elemzése és megjelenítése online történik a felhőben, ami az erdőkárok kimutatására szolgál három hazai mintaterületen (Debreceni Nagyerdő, Sárvári Farkas-erdő és Központi-Bük) 2017 és 2020 közötti időszakra.

Az eredményeimmel sikeresen kimutattam, hogy a távérzékelt űrfelvételek és a terepi adatok kombinációja megfelelő bemenetet biztosít a Google Earth Engine-ben futtatott erdőmonitoring rendszernek. Az alkalmazott módszertannal sikeresen azonosítottam különféle erdőkárokat a Z ZNDVI térképeken átlagosan 78%-os teljes pontossággal.

Kulcsszavak: erdőmonitoring, űrfelvétel, Sentinel-2, felhő rendszer, Google Earth Engine, Gépi Tanulás

Table of contents

1. Introduction

1.1. Introduction to the Thesis

Modern technologies enable constant monitoring of the state of our Earth. One of the most important and rapidly developing technologies is satellite-based remote sensing. The forest cover of the Earth is around 31.1%, of Europe is 45.9% and of Hungary is 22% due to the large size and huge importance of forests and their monitoring, the remote sensing technologies became real complements of field measurements by providing data with high frequency, accuracy and often free for vast areas.

There are constantly new possibilities for forestry professionals due to the quick progress of remote sensing technologies offering fine-resolution images of the World daily. Large-scale forest monitoring relies on these technologies since forest stands can be found often sparsely and their dynamics can be studied only in the longer run. Satellite images can be used to detect the change in forest expansion and health state and the remote sensing-based forest health monitoring systems are suitable for complementing the field-based monitoring systems coordinated by governmental and research institutes, forestry directorates, and universities in several countries, Hungary included.

One of the main reasons for writing this Thesis is to enhance the previously made Hungarian Remote Sensing based Forest Health Monitoring System ("TEMRE" shortly in Hungarian) which was developed in 2017 by Somogyi et al. (2018) to monitor forest health about environmental changes and climate change (described in detail in chapter 2.6.1.4.) but in time modifications were needed due to the ending lifespan of Terra satellite, carrying the MODIS sensor, which provided data for TEMRE. The final aim is to create a wall-to-wall, constantly updated forest monitoring system for Hungary based on satellite imagery and cloud computing.

In my PhD thesis, I first reviewed the scientific methods (models and indices for vegetation monitoring) applied in Hungary and around the World. Secondly, I surveyed the possible methods to be used, replaced the previous ones, and applied them in case studies, then thirdly create a wall-to-wall forest health state map of Hungary. Fourthly a detailed time-series analysis was made for the three sample areas to show changes in health state. The fifth final

stage was a comparison to existing maps aiming to improve data quality and accuracy for future monitoring.

1.2. Research goals

In my PhD thesis, I focus on novel forest monitoring methods by replacing the old datasets with new ones and proposing health monitoring methods for different forest disturbances.

Replacing the formerly used MODIS data, ESA Sentinel-2 (S-2) seemed to be the most promising solution, and testing this theory several studies were made by us for selected areas of Hungary and the whole county observing abiotic and biotic forest damage.

Abiotic forest damage was surveyed by different methods based on Sentinel-2 in Mountain Bükk to get a clear picture of the extent of the ice brake and windfall (Molnár et al., 2019a). Different vegetation indices derived from MODIS and S-2 images were compared to damage data collected in the field measurements (Molnár et al., 2019b) like Normalized Difference Vegetation Index (NDVI), NDVI change (NDVIch), Z NDVI (standardized NDVI), Normalized Difference Water Index (NDWI), Enhanced Vegetation Index (EVI)). Another type of abiotic damage, drought stress, was analysed by the author in Szigetköz, Püspökladány, Újfehértó, and Debrecen between 2018 and 2020 based on several vegetation and wetness indices.

Biotic forest damage was detected in Sopron as European spruce bark beetle (Ips typographus L) outbreak took place in 2017-2021 (Molnár & Király, 2021). Hopefully, the method used in the study will be suitable to survey the newcomer invasive oak lace bug (Corythucha arcuata) as well (Paulin et al., 2020).

Forest health monitoring proposals were made for Nagyerdő of Debrecen utilizing the Google Earth Engine cloud platform (Molnár et al., 2021, Molnár & Király, 2022b) and Farkas-erdő of Sárvár (Molnár & Király, 2022a) using all previously mentioned methods. These areas were later expanded to Central Bükk, the third study area of the Thesis, and eventually to the whole of Hungary.

1.3. Research plan

My PhD thesis had seven **main objectives**, such as:

1. Review existing scientific methods for forest monitoring applied in Hungary, Europe, and the World such as remote sensing techniques (especially optical satellite imagery) and related vegetation and water indices describing forest state.
2. Analyse the possible methods for forest disturbance monitoring and examine their efficiency via case studies focusing on exact methods and forest damage types.
3. Describe the three study areas of the thesis: Nagyerdő of Debrecen, Farkas-erdő of Sárvár and Central Bükk. Forest health is to be studied with vegetation and water index values in oak, hornbeam, and beech-dominated forests from Hungary's eastern, western, and northern parts.
4. Create a novel forest monitoring system for Hungary based on ESA Sentinel-2 optical imagery, vegetation indices, and GEE cloud computing and test it on three study areas. The monitoring method includes cloud filtering, forest masking, index creation, forest health change detection, visualization, and data export.
5. Analyse the time series of the study areas in detail to identify changes in forest extent and health state between 2017 and 2020. The Z NDVI maps for each year are to be compared to field damage reports.
6. Compare the new maps produced in GEE to the existing ones to check data quality and accuracy for future monitoring.
7. Investigate the expansion of the application of the above mentioned methods to a wall-to-wall system.

1.4. Hypotheses

Connected to the main objectives, I stated seven **hypotheses:**

1. Satellite images can be used to monitor the health state and forest expansion. The remote sensing-based forest monitoring systems are suitable detecting changes and supporting

field-based monitoring. Such systems exist in Europe (Czechia, Norway, Germany) and worldwide, too (USA, Canada, Australia).

2. Forest health can be monitored in Hungary based on a 10x10 m spatial resolution Sentinel-2 L2A (Level-2, surface reflectance) satellite image series in the 2017 – 2020 period using specific indices.
3. Cloudless annual and monthly satellite image composites can be created for the entire vegetation season (from April until November) with spatial, temporal and cloud filtering methods.
4. Interannual forest health disturbances due to biotic and abiotic damage can be detected by vegetation and water indices (NDVI, NDVIch, Z NDVI, NDWI, EVI) derived from annual and monthly composites of Sentinel-2 L2A satellite images. Annual images are used for comparing years and monthly ones for monitoring interannual changes.
5. By developing a specific computer code system, a novel forest monitoring system can be created for Hungary in the GEE cloud computing interface utilizing the above-mentioned Sentinel-2 dataset, cloud filtering, and vegetation and water indices.
6. The Copernicus forest maps can support the system by providing novel, satellite-based forest masks for both the study areas and the whole Hungary. These up-to-date masks could improve monitoring accuracy with the designation of forested areas.
7. The ground-based dataset of the National Forest Damage Registration System can be used as validation of remotely sensed data by comparing damaged forest compartments having both field reports and satellite images.

2. Literature review

In this chapter I described remote sensing basics, remote sensing satellites, indices, image processing, forest damage types, forest monitoring systems, cloud computing and machine learning.

2.1. Remote sensing

By remote sensing (RS) the physical characteristics of Earth and other astronomical objects can be detected and monitored from a distance based on emitted and reflected (mainly solar) radiation. The range of radiation is described in the electromagnetic spectrum, which we can divide into classes based on the frequency, wavelength, and energy of waves (Figure 1). Frequency (f) is the ratio of speed (m/s) and wavelength (m) and is expressed in Hertz (Hz).

$$f = \frac{v}{\lambda} \qquad (1)$$

Wavelength is expressed by the ratio of speed (m/s) and frequency (f) and measured in meters (m).

$$\lambda = \frac{v}{f} \qquad (2)$$

The range of frequency is from 1 to 10^{24} Hz, while in the opposite direction, the wavelength varies between 10^{-16} and 10^{8} meters. The visible part, commonly called light for the human eye, is the portion in this spectrum between 380 – 740 nm (3.8 – 7.4 x 10^{-7} m).

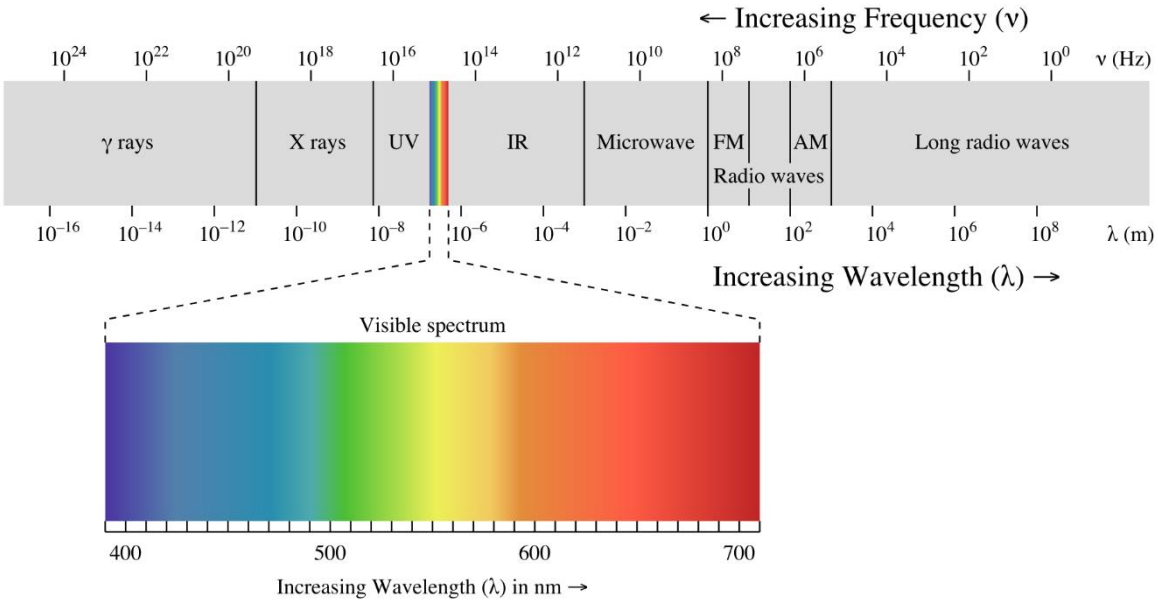

Figure 1. The range of the electromagnetic spectrum with the highlight of visible light

We can divide the electromagnetic spectrum into regions, bands, or channels according to frequency (Hz) and wavelength (nm=10^{-9} m) (Table 1). For remote sensing, visible light, infrared and radio waves are the most often used.

Table 1. Bands of the electromagnetic spectrum.

	Band	Wavelengths (nm)	Frequency (Hz)
1	γ rays	<1	$>3\times10^{17}$
2	X rays	1 – 10	$3\times10^{16} – 3\times10^{17}$
3	Ultraviolet	10 – 400	$7{,}4\times10^{14} – 3\times10^{16}$
4	Visible light	400 – 700	$3{,}8\times10^{14} – 7{,}4\times10^{14}$
5	Infrared	$700 – 10^5$	$3\times10^{12} – 4{,}3\times10^{14}$
6	Microwave	$10^5 – 10^8$	$3\times10^9 – 3\times10^{12}$
7	Radio waves	$>10^8$	$<3\times10^9$

Source: Siyavula

We can utilize different technologies for gathering information about our planet and space environment. There are active and passive remote sensing systems based on the sensor types that instruments are equipped with. Passive ones detect reflected and thermal radiation, while actives first emit radiation, then measuring the time of reflection from the object.

Active systems emit electomagnetic radiation and their sensors detect these signals coming back from the surface. The most important types of active sensors are RADAR (Radio Detection And Ranging), LiDAR (Light Detection And Ranging), Sonar (Sound Navigation Ranging), GPS (Global Positioning System), and GNSS (Global Navigation Satellite Systems). They can be used above and below ground level, in the water, in the air, or the space. The great advantage of using active emitters like Radar is that waves can go through clouds and water and can give a picture of the surface under any weather conditions.

While passive sensors measure reflected and thermal radiation to the instrument from the surface in fixed frequency bands. These bands are based on physical properties and designed for measuring specific features of the objects, like certain wavelengths positioned in natural colours (RGB: red green blue), or NIR (Near-Infrared, λ=700 nm-1000 nm) which are suitable for land monitoring, vegetation cover, aerosol, cloud detection, ocean and soil temperature measurements, etc. A broadband image contains a couple of broader bands (e.g., 4 channels with R, G, B, and NIR) like sensors on-board NASA's Landsat satellites, a multispectral image with more bands (like 36 bands of MODIS), while a hyperspectral has several hundreds of narrow channels, and an ultraspectral has several thousand (Figure 2).

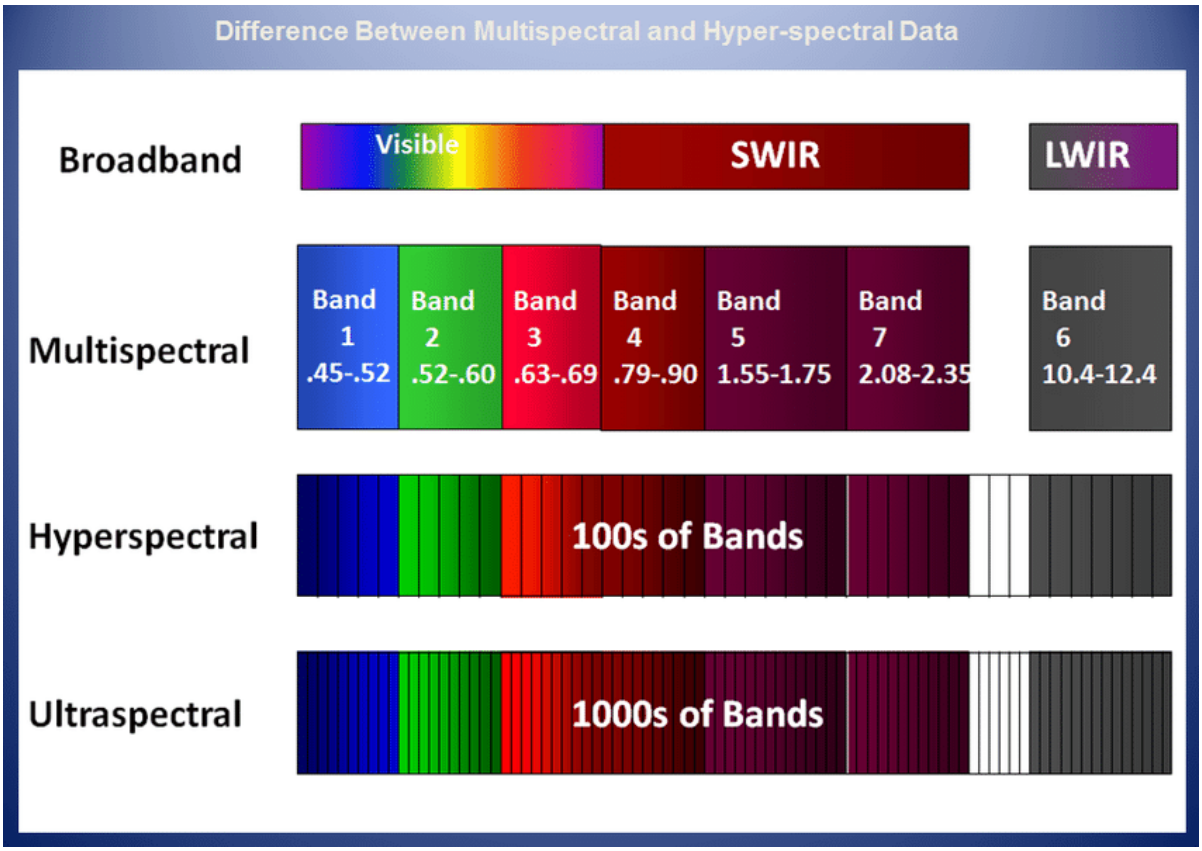

Figure 2. Difference between broadband, multispectral, hyperspectral, and ultraspectral Imaging (Makki, 2017)

2.2. Satellite-based remote sensing

Earth has been studied from space by satellites already for half a century. The first of them was the Soviet Sputnik 1, launched in 1957, which was followed by Explorer 1 of the USA in 1958, and Ariel 1 of the United Kingdom in 1962. In 2019 87 different countries and organizations launched altogether 1957 satellites (UCS, 2019).

Satellites can be classified into several groups according to their use, function, orbit, size, and mass, etc.. The usage of satellites is can be commercial, governmental, military, mixed, and civilly as well.

The main parameter of satellites is a function, that can be remote sensing or Earth observation, astronomy, geodesy, meteorology, telecommunication, navigation, military, and biology as well. Some types carry human like space shuttles and space stations.

Satellites are also classified by orbit types. Orbit is their circular track around the Earth, which satellites reach after being launched by rockets. There are geocentric, and heliocentric

classes according to the object in the centre of the circle. We find satellites in geocentric orbits in the highest number, which observe the Earth. Moon is also on this orbit type, while planets and comets orbit the Sun in a heliocentric track.

We can divide the geocentric orbits according to their altitude into classes: there are low, medium, geosynchronous and high Earth orbits (ESA, 2017). Other classification categories are based on inclination, eccentricity, synchronous and pseudo-orbit characteristics (Riebeek, 2009). Low Earth orbit (LEO) has an orbital altitude of 180 - 2000 km, Medium Earth orbit (MEO) has a 2000 – 35786 km, and Geostationary orbit (GEO) is 35786 km high, with the same rotation period as the Earth during a day with the speed of 11070 km/h at the Equator. Finally, the High Earth Orbit (HEO) is above 35786 km.

According to the inclination of orbits, there are Polar and quasipolar sun synchronous Orbits. The inclination is the orbit's angle to the Equatorial plane, and in the polar case, it is around 90 degrees, crossing both poles. In the case of quasipolar sun-synchronous orbit it passes above the Equator and near the poles always at the same time (Riebeek, 2009).

Eccentricity classification is based on the shape of the orbit. The circular orbit has zero eccentricity, while the Elliptic orbit has between 0 and 1, where zero is the circle and 1 is the ellipse (Swinburne Astronomy Online, 2019). Geosynchronous, geostationary, Molniya, and Tundra Orbits are all elliptic orbits (Xiong & Butler, 2018). Geosynchronous and Geostationary orbits are similar in the respect of the perigee (furthest point of orbit from Earth) of LEO but different in the apogee (closest point of orbit from Earth) with geosynchronous or geostationary altitude. Orbit's inclination is 63.4° and orbital period of half of the day, spending the majority of the time over two areas, Russia and the United States and Tundra orbit has a similar inclination of 63.4° but an orbital period of one day. These satellites are created for observing a single area.

The synchronous classification contains several classes connected to the rotational period of the Earth, the Sun, or Mars (GISGeography, 2018). The synchronous orbit (SO) has the same orbital period as the Earth's rotational period (1 day), while the Semi-synchronous orbit (SSO) has a lower orbit resulting shorter rotational period (half a day). Geosynchronous orbit (GSO) is at 35786 km high, and when the inclination of zero the satellite it looks like staying above the same point always, in this case, we talk about geostationary orbit (GEO). Space programs

2.2.1. NASA missions

The 69 missions of National Aeronautics and Space Administration (NASA) are categorized into 13 topics: atmosphere, climate, continental drift and geodynamics, gravity, hurricanes, ice, land and vegetation, oceans, ozone, Sun and its Influence on Earth, water cycle, weather, and wildfires (NASA, 2017). For forest monitoring purposes land and vegetation satellite missions are the most interesting, they are the following: Aqua, ICESat, ICESat-2, Landsat, LDCM, NPP, Operation Ice Bridge, Orbiting Carbon Observatory-2, Radiation Belt Storm Probes, Shuttle Radar Topography Mission, Soil Moisture Active Passive, TDRS, and Terra.

2.2.2. ESA missions

European Space Agency (ESA) has recently had 18 missions and three cooperative missions with NASA (ESA, 2020a). Earth observation missions are amoung others the Aeolus, the CryoSat, the Sentinel-1, 2, 3, 5P, and the Swarm. Sentinels are part of the Copernicus Earth observation program.

In 2024 Biomass (ESA, 2019) and in 2025 Flex missions (ESA, 2020b) will be launched for estimating forest biomass and vegetation fluorescence and photosynthetic activity.

2.2.3. Remote sensing satellites

Regarding the equipment carried by remote sensing satellites, we can talk about passive (e.g. optical), and active (e.g. SAR, LiDAR) systems, based on sensing reflected radiation of the electromagnetic spectrum or emitting and after sensing the time of returning waves. The image created in a certain spectrum by sensors is described by spatial (pixel size), spectral (bandwidth in the electromagnetic spectrum), and temporal (revisiting time) resolution.

Respecting forest monitoring the most important satellites will be described below, which are widely used due to beeing free and having optimal parameters for this aim. The satellite Terra & Aqua were used in the Hungarian Forest Monitoring System (Somogyi et al., 2018) and several studies concerning forest monitoring all accross the World, providing 20-year long time series. While the satellites of the Landsat program have been on orbit for even longer time, since 1972. Eventually the Sentinel-2 provides higher spatial resulution which gives new perspective of forest research.

2.2.4. The satellites of the Landsat program

The history of remote sensing satellites starts in 1972 with the launch of the first Landsat satellite operated by the NASA of the USA. For almost fifty years the longest continuous dataset of Earth observation was collected by Landsat satellites and nowadays Landsat-7 and -8 are operational and 9 was launched in 2021 (USGS, 2019).

Regarding the technical parameters, the temporal resolution is 18 days for Landsat 1-3 (in the followings indicated with L) and 16 for L4-8, while the spatial resolution is 15-100 m in 4-11 bands (4 for L1-3, 7 for L4-5, 8 for L7, and 11 for L8). These features together create a suitable base for forest monitoring as Banskota et al. (2014), Saarinen et al. (2018), Barka and Bucha (2010), Wulder et al. (2022) presented.

According to Banskota et al. (2014), current state and temporal dynamics are the most significant attributes of forest monitoring. The structure and composition of forests describe their state and the temporal dynamic shows the change in it. Changes occur due to short-term (biotic or abiotic), and long-term events (climate change, anthropogenetic activities). The combination of these two types of forest state changes results in differences in biophysical conditions and vegetation phenology as well.

To monitor these changes by satellite data the correction of raw images is needed for improving quality. For this aim atmospheric, topographic, and geometric corrections are used to minimising the effect of temporal variation in atmospheric properties, brightness variations of terrain (or terrain shading), and inaccuracy by registration and correction of geometry.

The availability of corrected images enables the calculation of different kinds of indices that are used to describe numerically the forest state and changes. Such indices are NDVI NDWI, EVI, etc.

Based on them, Banskota et al. (2014) categorized forest ecosystems into three groups: abrupt changes (clearcut, crown fire, defoliation), partial changes (fire, insects, diseases), and subtle changes occurring gradually through time (e.g., forest degradation, tree mortality, and forest successional dynamics).

Different approaches can be used for the classification, such as Image Classification-based Analysis and Trajectory-Based Change Detection. In the first case, post-classification is

applied at end of investigated time interval by comparison of independently produced images, then the comparison is made to detect changes. In the second case ,the temporal patterns of spectral variables are used by the following methods: threshold-based change detection, single curve fitting, hypothesized curve fitting, or trajectory segmentation.

An application of these methods is fundamental in a forest monitoring system. A country-based monitoring system is needed to have a dataset covering the whole country for a sufficiently long period. Landsat imagery is suitable for that goal since the launch of Landat 4 in 1982, 30x30 m resolution data is available and Landsat-9 was launched in 2021 to provide data for additional 10 – 20 years.

2.2.5. Terra & Aqua

The data provided by the MODIS sensor onboard satellite Terra and Aqua cover the whole world every 1-2 days in 36 narrow spectral bands at 250 – 1000 m spatial resolution (NASA, 2019a). Terra is equipped with five instruments: ASTER, CERES, MISR, MODIS, and MOPITT, while the sister ship Aqua has: AIRS, AMSU, CERES, MODIS, and AMSR-E (NASA, 2019b).

For forest monitoring MODIS is one of the most widely used devices, several studies were made based on the data of this sensor, examining abiotic and biotic forest damage, heat stress, climate change, phenological phases, and land cover changes. MODIS images are applied all over the World. In the forest monitoring chapter (2.6.) I give examples which might be similar to our methods due to similar climatical and ecological conditions.

2.2.6. Sentinels

European Space Agency launched the first Sentinel mission in 2014 in the framework of the European Union's Copernicus Earth observation program which has been developed since 1998 and originally was called Global Monitoring for Environment and Security (GMES), while in 2012 the European Commission changed the name to Copernicus. The program offers freely available satellite images of the Earth in medium and high spatial and temporal resolution. In 2022 Sentinel-1, -2, -3, and -5P provided data for research. Sentinel-2 and -3 are described here as the most promising ones for forest monitoring.

Sentinel-2 satellites (Figure 3) were launched in 2015 and 2017 (A and B satellites), and they have the highest potential for monitoring purposes with a 1 – 5 days revisit time and free

and open data policy, and high 10x10 – 60x60 m resolution (Table 2). On- board the Sentinel-2 satellites took place the Multispectral Instrument (MSI) (ESA, 2020c) which measure the radiance of Earth in 13 spectral bands. Different S-2 products are provided by ESA such as Level-0 (raw image), Level-1 (L1C, Top Of Atmosphere reflectances) and Level-2 (L2A, Bottom Of Atmosphere), this latter is derived from Level-1C products.

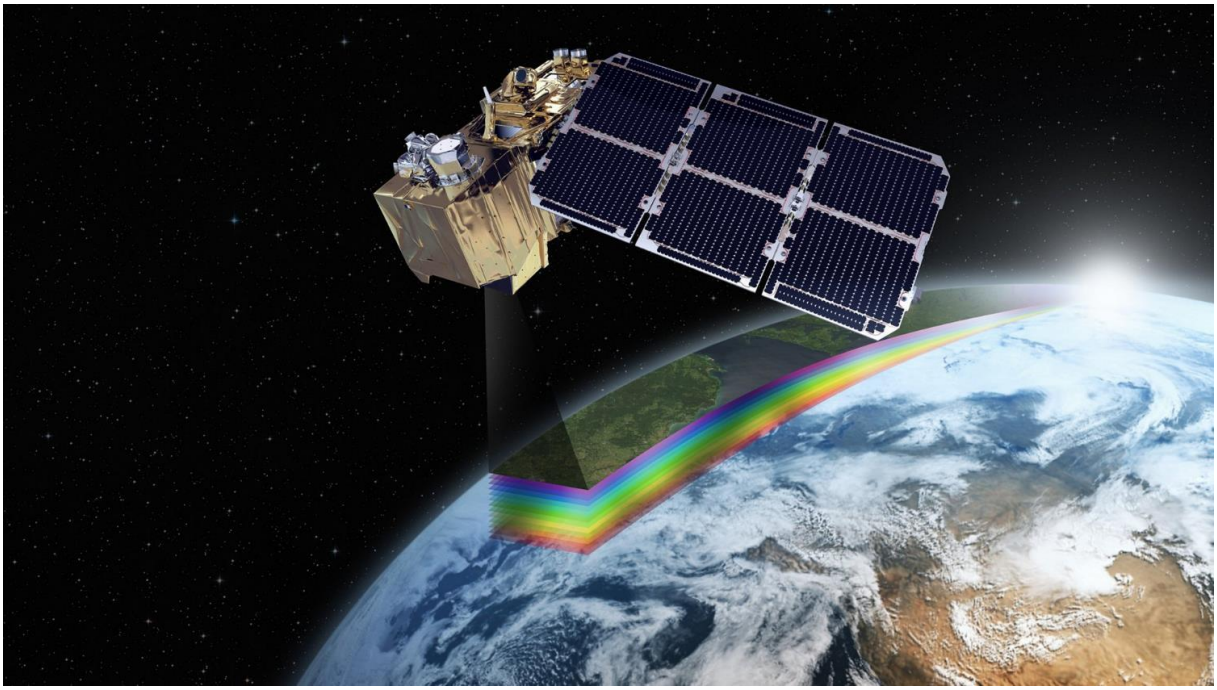

Figure 3. The Sentinel-2 satellite is observing the Earth. Source: ESA.

Table 2. Spectral bands for the Sentinel-2 MSI sensor

Sentinel-2 Bands	**Central Wavelength (µm)**	**Bandwith (nm)**	**Spatial resolution (m)**
Band 1 - Coastal aerosol	0.443	20	60
Band 2 - Blue	0.490	65	10
Band 3 - Green	0.560	35	10
Band 4 - Red	0.665	30	10
Band 5 - Vegetation Red Edge	0.705	15	20
Band 6 - Vegetation Red Edge	0.740	15	20
Band 7 - Vegetation Red Edge	0.783	20	20

Band 8 - NIR	0.842	115	10
Band 8A - Vegetation Red Edge	0.865	20	20
Band 9 - Water vapour	0.945	20	60
Band 10 - SWIR - Cirrus	1375	30	60
Band 11 - SWIR	1610	90	20
Band 12 - SWIR	2190	180	20

2.3. Satellite-derived vegetation indices

Satellite-derived Vegetation Indices (VIs) have been widely used for monitoring the extent and state of vegetation-covered surfaces. Spectral remote sensing provides this type of data based on the ratio of absorbed and reflected solar radiation in different bands (Stacher, 2019). The high absorption of healthy vegetation in the red wavelength (due to the secondary absorption of green colour of chlorophyll-A, chlorophyll-B, and carotenoids) and high reflectance of vegetation due to internal leaf structure in the Near-Infrared (NIR) band. The higher photosynthetic activity means higher absorption and a denser, healthier state. While unhealthy or less dense vegetation reflects more visible and less NIR lights than healthy vegetation (NASA, 2000). In the following subchapters, I describe the VIs used in the Thesis. Besides the most commonly used NDVI (Huete, 2012) and its variations, I tested more complex VIs like the EVI, which is optimized to minimize VI biases from soil background and aerosol variations. Since the sensing of vegetation liquid water (Gao, 1996) has great importance nowadays due to climate change, the NDWI was used to investigate this issue.

2.3.1. NDVI

Normalized Difference Vegetation Index (NDVI) (3) is calculated from atmospherically corrected reflectances detected in the (NIR) and visible red (RED) bands:

$$NDVI = \frac{NIR-RED}{NIR+RED} \qquad (3)$$

where values vary between -1 and +1 indicate the photosynthetic activity of the forests. A healthy forest usually has a value between 0.8 – 0.9, while 0 stands for vegetation-less land area, and negative numbers mark cloudy or water surface (Rouse et al., 1974).

During the process of leaf loss or discolouration (Caccamo et al., 2011, Spruce et al., 2011, Hlasny et al., 2014) these values drop significantly. After serious forest damage, this state lasts for a longer period (weeks, months, years) to 0.3 – 0.7 but there are changes even in the healthy forest called inter-annual variation. During the vegetation period, NDVI rises from about 0.4 to 0.9, reaching the maximum in the middle of summer. Photosynthetic activity decreases during the autumn and in the winter it reaches the minimum (Figure 4) (Kern et al., 2022).

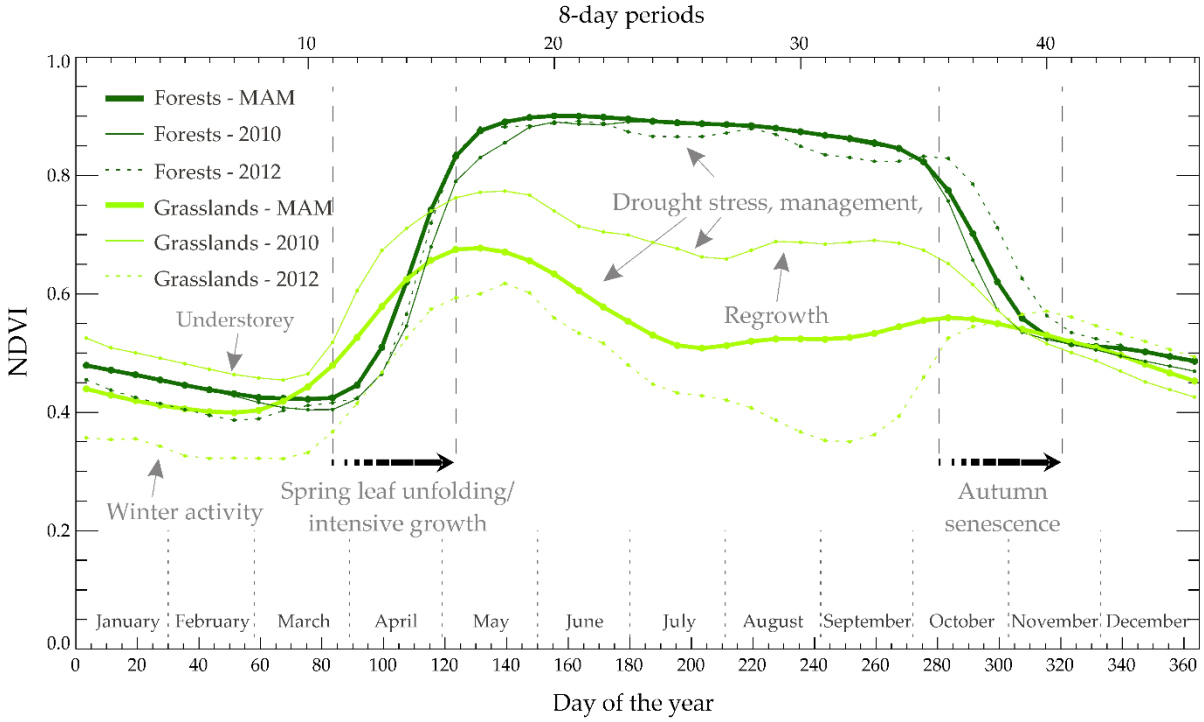

Figure 4. A typical phenological curve of a broadleaf forest (sessile oak with hornbeam) based on multiannual mean NDVI values. Source: Kern et al. (2022)

2.3.2. NDVI change

The NDVI change index (4) is calculated from two NDVI images by subtraction of a given year's value (second year) from the previous year's value (first year).

$$NDVI_{change} = NDVI_{second\ year} - NDVI_{first\ year} \qquad (4)$$

NDWI and EVI changes were calculated similarly to this, the range is from -2 to +2. However, these change indices only show the difference in forest state between two exact dates and might not be enough to detect forest damage due to interannual variation of index values, especially for the beginning and end of vegetation period.

2.3.3. Z NDVI

However, NDVI shows the state of the forest on an exact date, which is not enough to point out damage due to variation of NDVI. To reduce the inter-annual variation of NDVI value standardized version (Z NDVI) (5) is used instead of the simple version (Peters et al., 2002) calculated on pixel level by this formula:

$$NDVI\ Z = \frac{NDVI - \mathrm{NDVI_{mean}}}{\mathrm{NDVI_{std}}} \qquad (5)$$

where Z NDVI is the standardized NDVI, NDVI is the actual year (2017, 2018, 2019 or 2020), $NDVI_{\mathrm{mean}}$ is the multiple-year average of NDVI (period between 2017 – 2020), and $NDVI_{\mathrm{std}}$ is the standard deviation of NDVI values through (also the period between 2017–2020). According to my experiences the Z NDVI could vary appreciably between the end values, in Hungary most often between -3 and 3.

2.3.4. EVI

The Enhanced Vegetation Index (EVI) (6) is considered an enhanced vegetation index with several correlation factors aiming to achieve results where NDVI is insufficient (Justice et al., 1998) due to saturation of soil (Huete et al., 2006). It has the following formula:

$$EVI = \mathrm{G} * \frac{(NIR - RED)}{(NIR + C1 * RED - C2 * BLUE + L)} \qquad (6)$$

where NIR, Red, and Blue have atmospherically corrected surface reflectances , L is the soil background adjustment for differential NIR and red radiant through a canopy, and C1, and C2 are the aerosol resistance coefficients, which utilize a blue band to correct aerosol influences in the red band. The coefficients adopted for MODIS and Sentinel EVI are; L=1, C1 = 6, C2 = 7.5, and G (gain factor) = 2.5. The value of healthy vegetation ranges between 0.2 – 0.8 depending on the vegetation type. EVI was made for MODIS originally, but it can be used

for Sentinel-2 and -3 images as well where damaged forest (EVI = 0.4 – 0.6) stands to diverge from healthy ones (Molnár et al., 2020).

2.3.5. NDWI

Normalized Difference Water Index (7) (also called Wetness or Moisture Index) is sensitive to changes in vegetation canopy water content with similar formula (Gao, 1996) but at different wavelengths, 820 for NIR and 1600 for SWIR (Index database, 2020b).

$$NDWI = \frac{NIR-SWIR}{NIR+SWIR} \quad (7)$$

NIR (near-infrared) is band 8 and SWIR (short-wave infrared) is band 11 in the case of Sentinel-2. High NDWI values correspond to high vegetation water content and cover while low index values to low vegetation water content and cover. During the period of water stress or after logging NDWI decreases. The range of NDWI is similar to NDVI, where -1 refers to the driest and +1 to the wettest state. Important to mention that NDWI is suitable for coniferous-broadleaf separation and the SWIR band has 20x20 m resolution unlike the other bands used in the above-mentioned indices.

2.4. Image processing

Processing satellite image requires several interdependent steps. The workflow starts with the image acquisition (downloading or accessing), followed by pre-processing including atmospheric, geometric, and radiometric correction, main processing, including filtering, masking, calculation of VIs, classification, information extraction, etc., and eventually post-processing, analysis, visualization and data export (Jensen, 2016). The detailed algorithm I used in GEE is similar to this workflow and described in detail in the methods (Chapter 3.3.).

2.5. Cloud computing

Google Earth Engine is a cloud-based geospatial, interactive, and big-data processing platform used for multipurpose scientific data analyses and visualization including forest monitoring, land cover, and land-use changes (Gorelick et al., 2017; Google, 2019). The GEE is available since 2010 for free and the multi-petabyte catalogue covers 40 years of series of satellite imagery, having over eight petabytes size (eight million gigabytes). Datasets can be found in the Earth Engine Data Catalog in either raster (satellite imagery, climate, weather, terrain) or

vector format (country boundaries, land cover types, water bodies, etc.). Besides datasets, JavaScript and Python Guides and tutorials are also available with sample codes included.

még általános hivatkozás

The GEE has four main components:

- datasets of remote sensing imagery,
- computational power for processing geospatial data,
- Application Programming Interface (API) in JavaScript and Python languages for creating requests to the Earth Engine servers,
- and code editor or dashboard**:** an online Integrated Development Environment (IDE) for visualization of spatial analyses.

The application of GEE-based method is described in detail in chapter 3.3.

2.6. Machine Learning

Machine Learning (ML) is an application of Artificial Intelligence (AI) (Figure 5) that is based on the useage of data and algorithms to imitate the way of human learning and improving the accuracy gradually. ML can be used in GEE (Bar et al., 2020) to expand the possibilities to find forest disturbances as well as to classify tree species, which can support the proper interpretation of forest change maps.

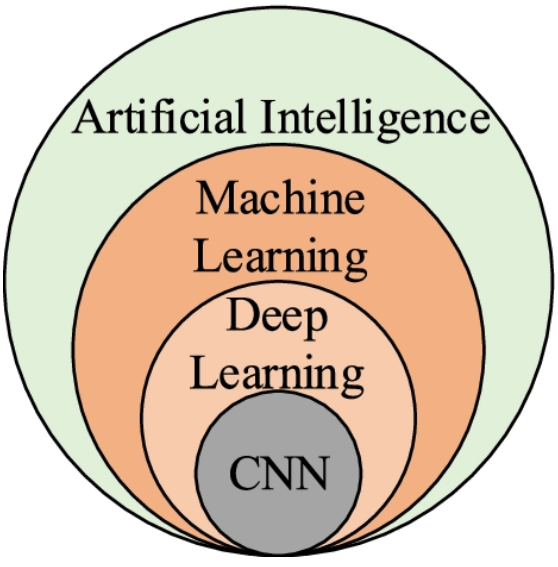

Figure 5. Relationship between AI, ML, Deep Learning, and Convolutional Neural Network (CNN). Source: Zhang et al. (2022)

ML is based on training data that is given by the user and the model predictor uses that to make decisions and predictions. There is a supervised and unsupervised form of ML, in the first case, the dataset includes inputs and outputs as well, while in the second only outputs.

Several ML algorithms such as Random Forest , Minimum Distance Estimation, Support-Vector Machine, k-Nearest Neighbour Regression, and Gradient Boost Regression Tree can be utilized to achieve these goals (Zhang et al., 2019). The Random Forest algorithm can be used for tree species classification, which has supervised, unsupervised and regression type as well, which are based on decision trees to classify data (Ho, 1995). The supervised version builds decision trees on the training sample and creates classes. The classifed maps provide valuable information about forests species or health differentiating healthy and damaged strands. Hence, they can be used for predicting future state as well, which could further enhance monitoring efficiency.

2.7. Forest damage types

2.7.1. Abiotic forest damage types

Regarding abiotic damage types, I described here the most frequently occurring ones, which are capable of massive destruction of forests on such a scale which is detectable by RS.

- Snow break: breakage of branches and parts of crown mostly due to the pressure of wet snow. In the worst case due to the accumulating weight of snow, the whole crown or the stem could break or bend, this latter result in damage to the roots as well which is irreversible (Csóka et al., 2013).
- Winter ice and hoarfrost damage: rather rarely happens due to required specific weather conditions. When after a strong, dry cold period, warmer and wetter air mass flows to the supercooled surfaces the rain freeze to the trees resulting in heavy pressure on branches which leads to branch and crown breakage. Besides the thick ice, hoarfrost can precipitate out too which results in less serious damage. However, the

combination of these can occur at the same time as it took place in Northern Hungary, Börzsöny, and Pilis Mountains in 2014.

- Frost damage: Spring frost causes damage to fresh buds and sprouts making them wizen and brown. In worse cases, the bark can break open resulting in tree mortality.
- Windfall and break: storm-wind could cause different damage. Windfall occurs in areas with shallow, wet soil where trees have a horizontal root system, which falls to the ground with the roots. On contrary, in drier and heavier soil the stem and crown break is more frequent.
- Drought: permanent high temperatures and dry periods induce drought damage both in young and mature stands. Leaves wit and turn yellow and dry. Some species react with defoliation to heat stress.

2.7.2. Biotic forest damage types

In this section I described three insect species which recently has great importance in forest monitoring since there are all able to cause severe health issues and eventually mortality.

- European bark beetle (*Ips typographus,* Linnaeus, 1758) is a 4 – 5 mm long bug feeding mainly on *Picea*, but sometimes on *Pinu*s and *Larix* too. It has 2 – 4 generations per year resulting in massive, several millions of m^3 spruce mortality all over Europe.
- Gypsy moth (*Lymantria dispar, L.*) is one of the most serious pests in forests being polyphagous and feeding on several hundreds of species. During gradation, the leaf-eating moth can cause total defoliation in vast areas for years. Outbreaks take place in Hungary periodically, every 4 – 12 years. The last major one occurred in 2003 – 2006.
- Oak lace bug (*Corythucha arcuata,* Say 1832) has 2 – 4 generations per year and causes damage mainly on oak species but can occur on *Acer* and *Castanea* as well. Known impacts of the bug are early leaf abscission and the general weakening of infested trees. Since 2019 in Hungary, we can talk about gradation since it occurred everywhere in the country in high numbers.

2.8. Forest monitoring systems

This section was made to overview the characteristics of different forest monitoring techinques (Lausch et al., 2016) and systems (listed in 2021) based on the:

- development stage of satellite-based forest monitoring: methods, development directions (machine learning), technical possibilities, obstacles, and solutions
- technical parameters and applicability of MODIS, Landsat 8, Sentinel-2, and -3 images for forest monitoring purposes
- different vegetation indices (NDVI NDWI, EVI, etc.) are used for short and long-term measurements.

The European forest monitoring systems (Table 3) are listed in chapters 2.8.1 and 2.8.2. which utilize satellite imagarey and ground-based datasets.

Table 3. European satellite-based forest monitoring systems.

Material	**Hungarian**	**Polish**	**Czech**	**Slovak**	**German**	**Slovenian**	**Norwegian**	**Finnish**
MODIS	☒	☐	☒	☐	☒	☒	☐	☐
Landsat 8	☐	☐	☒	☒	☐	☒	☐	☒
Sentinel-2	☒	☒	☒	☒	☐	☒	☒	☐
Sentinel-3	☒	☐	☐	☐	☐	☐	☐	☐
Planet	☐	☐	☒	☐	☐	☐	☐	☐

2.8.1. Hungarian forest monitoring systems

In this chapter I wrote about monitoring systems used in Hungary, both the ground-based and the RS-based ones.

2.8.1.1. Forest Protection Measuring and Observation System

In Hungary, the Forest Protection Measuring and Observation System (in Hungarian Erdővédelmi Mérő- és Megfigyelő Rendszer, shortly EMMRE) runs since 1987 and coordinated by the Forestry Research Institute of University of Sopron and Forestry Department of Hungarian National Land Centre (in Hungarian NFK EI) (NFK, 2018). The ground-based Forest

Damage Registration System (in Hungarian Országos Erdőkár Nyilvántartási Rendszer, shortly OENyR or NFDRS in English) is an integrated part of EMMRE since 2012. Aggregated forest damage can be also viewed on dedicated maps of NFDRS from 2013 and updated every year.

The forest protection damage reports of NFDRS contain data on damage date, type, frequency, intensity, code, tree species and damaged area given for each forest compartment of Hungary, which is systematically collected and reported at least four times per year at the end of each quarter, except for quarantine pests that have to be reported at once (Hirka 2018). The damage data registered in forest protection damage reports are available on the NFDRS website (Hirka, 2019) and in annual reports (Figure 6). In every year around 25 000-150 000 ha damage takes place according to Koltay (2006). The forest protection damage reports of NFDRS has data on damage frequency and intensity given for each forest compartment of Hungary.

The damage frequency (11) is the number of damaged given trees compared to all trees in the same species in the compartment expressed in the percentage (0-100%), i.e. if 30 oak is damaged in the compartment of 100 trees then the frequency is 30 %.

$$Damage\ freqency = \frac{damaged\ trees}{total\ trees} * 100 \qquad (11)$$

While the damage intensity shows the severity of damage and health deterioration compared to the healthy state, given in percentage (0-100%). Intensity shows if i.e. half of the canopy is missing due to defoliation in the compartment then the intensity is 50%.

Damage area and total forest compartment area are given in hectares. As a novel parameter, damage ratio (12) was introduced according to the following formula to enchance spatial agreement between the datasets, measured on a 0-100% scale:

$$Damage\ ratio = \frac{damaged\ area}{total\ area} * 100 \qquad (12)$$

Trends were calculated from the annual reports and according to Hirka et al. (2019, 2023), the frequency of droughts showed an increasing trend in Hungary in the last 50 years. The yearly values of the forest drought damage showed a significant response for the yearly values of two drought indices, namely Pálfai and Forest Aridity index (R^2=0.8 and 0.56). Droughts also have major indirect effects on forest health by causing damage chains, which could result in forest insects outbreaks as well.

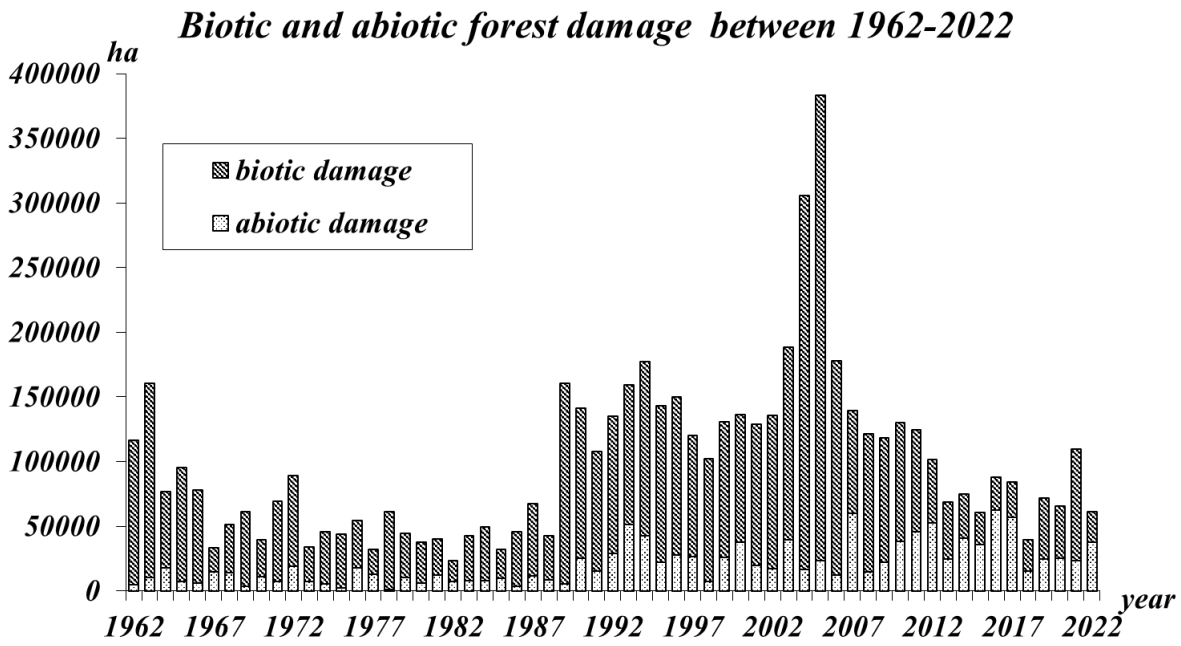

Figure 6. Biotic and abiotic forest damage between 1962 – 2022 (Hirka, 2023).

2.8.1.2. Spectral forest monitoring system

Király (2007) developed methods for modern, satellite-based forest monitoring at the University of Sopron and successfully tested them in the area of the Sopron Mountains. The spectral databank classification method based on forest compartments and the vegetation indices using SPOT P (Satellite Pour l'Observation de la Terre), and ASTER (Advanced Spaceborne Thermal Emission and Reflection Radiometer), and Landsat satellite images showed remarkable results, thus the usage of them would be useful in Hungarian forest monitoring.

2.8.1.3. Climate change monitoring

Climate change created a growing interest among scientists and aimed to investigate the effects on forests. Kovács & Gulácsi (2018) studied the usage of MODIS tiles in a study area of Mid-Danube-Tisza Plain in Hungary, in connection of this enviornmental issue. The area suffered a 1.2 – 1.5 °C temperature increase (Lakatos et al., 2014), and then vegetation period phases (start and end) shifted (1.9 – 4.4 days) (Varga et al., 2012). The forest cover map was

taken from the Corine Land Cover database, and MODIS images were collected from summer periods (81 – 273 DOY) between 2000 and 2017. Different vegetation indexes, such as NDVI, EVI, and standardized EVI were calculated for the study area. Coniferous, deciduous, and mixed forests were examined separately, and results were compared to each other and represented on a time-series graph. According to the results EVI was proven to be more sensitive to external impacts, but standardization is needed to examine differences between years. By this method, drought periods were shown in 2003, 2009, and 2012, and a wet year also in 2010. Validation happened using the PADI dataset of the CARPATCLIM database, and high correlation (R^2=0.72–0.86) values were observed with NDVI and EVI. However, 4/5 of forests are affected by drought, trends were not identified here either, only descending amounts of biomass.

2.8.1.4. TEMRE

In 2017 Somogyi et al. (2018a) created the Remote sensing based Forest Health Monitoring System (in Hungarian: Távérzékelésen alapuló Erdőállapot Monitoring Rendszer, shortly TEMRE) to monitor forest health about environmental changes and climate change. The system utilizes filtered and forest-masked Terra MODIS NDVI image composites with 250x250 m spatial and 16 days temporal resolution. The forest state is described by standardized NDVI Z, which is based on the actual, long-term (2000 – 2020) average, and the standard deviation of forest pixel values (Figure 7). These maps are regularly published at http://www.temre.hu supported by tree species map layers and site factors (Somogyi et al. 2018b, Molnár et al. 2018) (Figure 8).

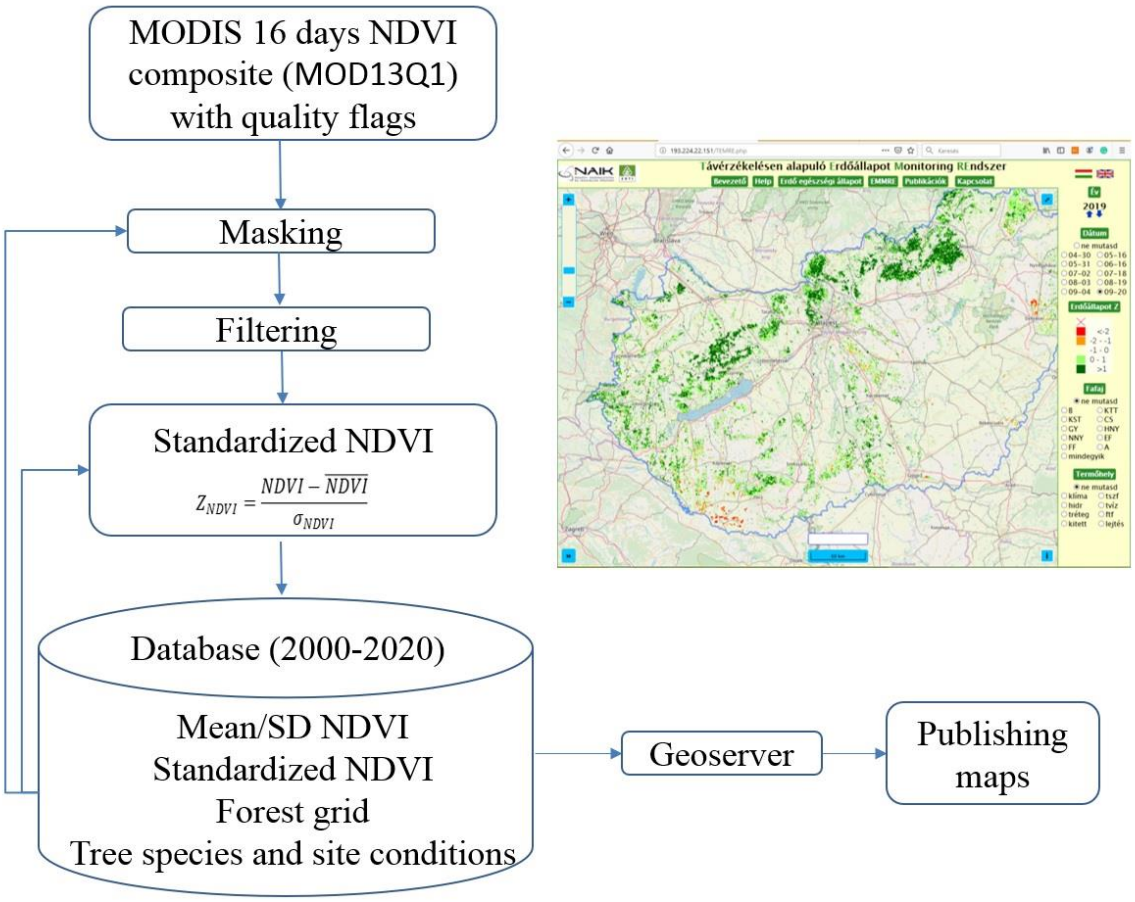

Figure 7. Structure of TEMRE

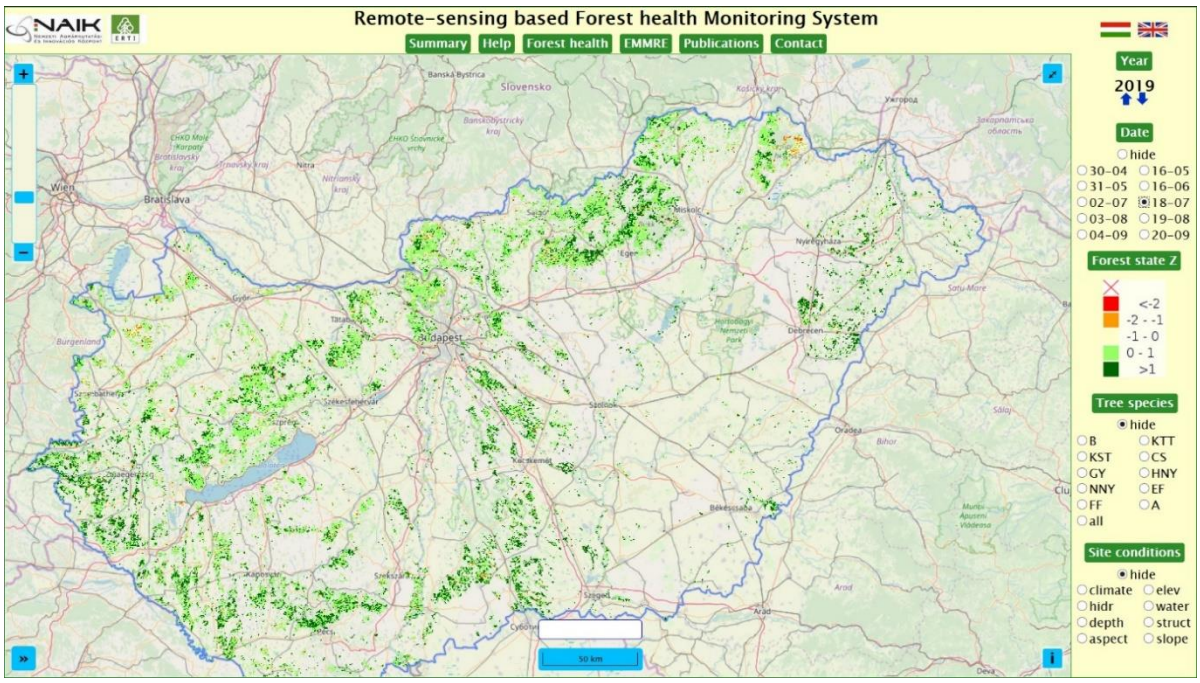

Figure 8. The health state of Hungarian forests in July 2019 in TEMRE

According to the experiences, TEMRE detected the European gipsy moth damage in 2003-2006 in the Northern Medium Mountains and Southern Hungary, drought in Keszthely mountains in 2012, sleety rain in Pilis and Börzsöny mountains in 2014, and snow break effects in Bükk mountains in 2017. Pixels over the damaged areas showed discolouration through the year of the damage in large areas but in the following years, they started to disappear due to regeneration and reforestation.

Experience has shown that the system can monitor most of the forest area of Hungary and detect forest health issues across space and over time (Figure 9). For example, TEMRE could detect the effects of the large-scale windfall and snow break in Bükk in 2017 (Figure 9a), the sleety rain (glaze) that loaded trees with heavy ice in Pilis and Börzsöny mountains in North Hungary 1-3 December 2014 (Figure 9b) (Zoltán et al., 2021). Other examples of abiotic damage are from 2017 when spring frost, snow, and wind damaged some mountainous areas above about 400 m, and from 2012 when forests of Veszprém county of Western Hungary suffered larger scale drought (Móricz et al., 2018). Biotic agents can be also observed with TEMRE such as European gipsy moth (Figure 9c) (Nádor et al., 2007) and oak lace bug outbreaks from 2012-to 2013 and 2019 onwards (Figure 9d) (Kern et al., 2021).

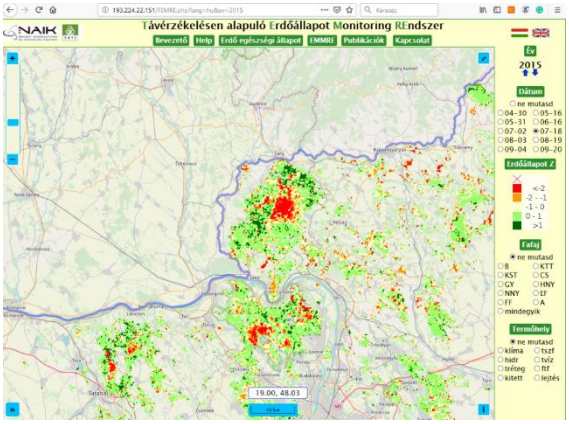

a

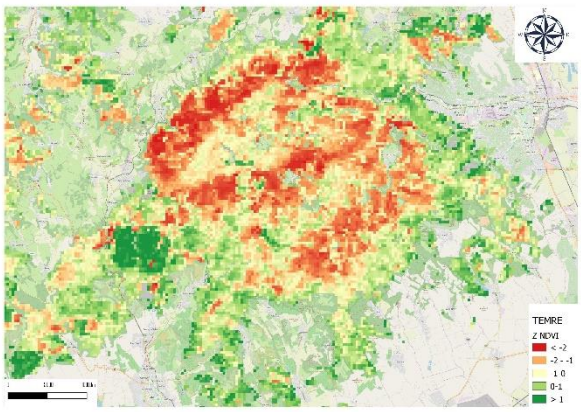

b

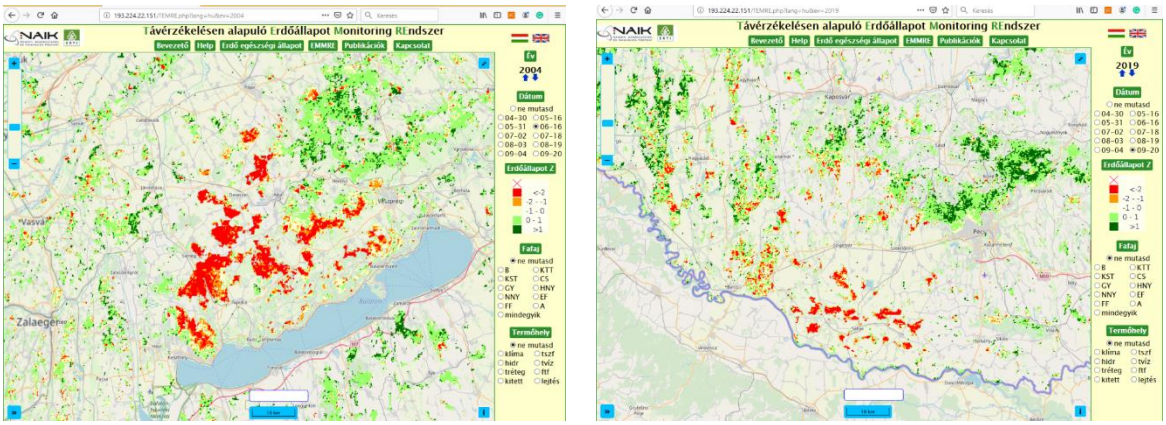

c d

Figure 9. Abiotic and biotic forest damage observed in TEMRE: windfall and snow break in May 2017 (a), ice break in July 2015 (b), gipsy moth in June 2004 (c), and oak lace bug in September 2019 (d).

TEMRE products were used in a case study when Barka et al. (2019) demonstrated a multipurpose application of the normalized difference vegetation index (NDVI) derived from MODIS products for forest monitoring across the Central-European macro-region (the Western Carpathians and Pannonian basin), where NDVI values could identify the location and extent of forest damage caused by snow break and windbreak. The article is based on Hungarian and Slovak RS forest monitoring methods, see the latter in detail in chapter 2.8.2.

Enhancement of TEMRE was made in two steps, in which I participated. The first one was the replacement of MODIS products with Sentinel-3 and 2, and took place in 2020, which was the theoretical end of life of the Terra satellite, but it still operated in 2022 when constellation exit maneuver was made. Having similar attributes (300x300 m spatial and 1-2 days temporal resolution in the case of Sentinel-3) made possible the creation of 12 days NDVI composites for the vegetation period at a higher frequency. Sentinel-3 was used to cover the entire country and Sentinel-2 was used in two study areas (Central Bükk and Fekete-víz Plain) where the original resolution was reduced to 20x20 m and published for the period 2018-2021.

2.8.1.5. Hungarian Earth Observation Information System

The Hungarian Earth Observation Information System (in Hungarian: Földmegfigyelési Információs Rendszer, (FIR)) is a new system, which is available in the beta stage for the public in 2022 at this website: https://efold.gov.hu/. It is under development by the consortium of

the Hungarian Governmental Agency for IT Development, Lechner Knowledge Centre, National Infocommunications Services Company, and the Ministry of Foreign Trade and Foreign Affairs. A wide range of ESA satellite products are available on the geoportal such as RGB, NDVI, EVI, NDWI, etc., derived from Sentinel-1, 2, and 3, 5P for viewing and downloading.

2.8.2. Forest monitoring systems in Europe

International Co-operative Programme on Assessment and Monitoring of Air Pollution Effects on Forests (ICP Forests, http://icp-forests.net/) is one of the World's largest biomonitoring networks with the collaboration of 42 countries, which provides information on forest condition, air pollution, climate change, and biodiversity (ICP, 2011). The program was launched in 1985 by the Convention on Long-range Transboundary Air Pollution of the United Nations Economic Commission for Europe (UNECE).

This ground-based monitoring provides useful data on two levels. Level I is based on 6000 observation plots on a systematic 16 x 16 km grid of Europe and Level II with 500 intensive monitoring plots represents selected forest ecosystems to clarify cause-effect relationships. Data from both levels are useful for the validation of satellite-based forest monitoring systems

ICP Forest plots are included in the Hungarian ground-based forest monitoring systems (EMMRE, OENyR) and fields measurements are made regularly, but nowadays the lack of human resources and availability of remote sensing data drives us to develop this system with satellite data to make the nationwide monitoring rapidly, automatically and with low cost. However completely satellite-based systems can be found yet in a few numbers.

2.8.2.1. Slovak forest monitoring system

The forest monitoring system of the Slovak National Forest Centre called „Forest cover change detection by satellite scenes" is a system (Barka et al., 2018) aiming to visualize actual and historical Landsat and Sentinel-2 satellite compositions to monitor forest state and to identify changes by using ArcGIS (http://www.nlcsk.sk/stales/m_aplikacia_en.html) (Figure 10). It has four applications: visualization of satellite scenes and forest health state, comparison of satellite scenes from different periods, dynamic visualization of actual and historical satellite scenes, and dynamic visualization of forest health state classifications. The dynamic

visualization of forest state classifications based on satellite scenes contains maps from 1990 to 2019, where health status can be observed over time with damage classification colours within forest boundaries.

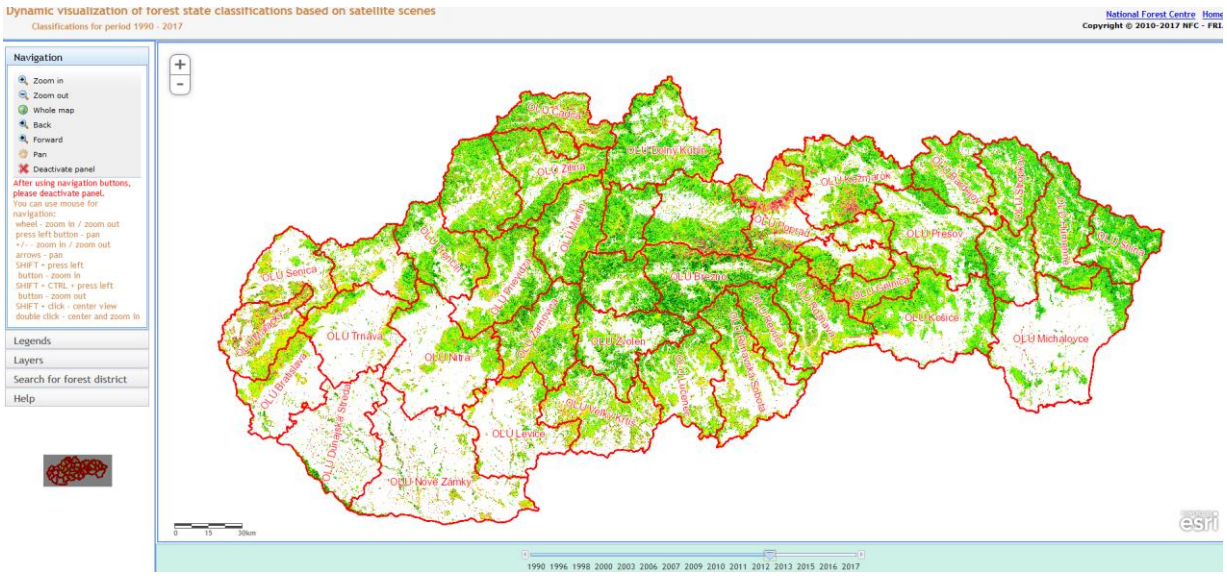

Figure 10. Slovak forest monitoring system showing dynamic visualization of forest state classification based on satellite scenes for the period 1990-2017.

The nationwide forest health assessment was made in an automatized way, which is fast, accurate, and based on free Sentinel-2 images and two-phase regression used for detecting forest damage, especially windstorms and biotic agents. In this method, the first phase of forest health estimation happens from satellite images (mosaiced Landsat and Sentinel-2 from the last 40 years) and in the second phase, ground defoliation is described based on 112 ground data plots, where defoliation was the main indicator of tree health. Different spectral reflectivity in forest stands connected to their foliage and linear regression showed strong correlation. Significant forest health changes were found and described by foliage loss and health state decrement. The 1st phase (correlation of satellite and defoliation in the previous year) was R^2= 0.4 – 0.7 and between the 1st and 2nd phases 0.85 – 0.97. Eventually, this method showed 15% of damaged forests and the promising results can be further optimized using Sentinel-1 images, as the authors suggested.

Barka and Bucha (2010) also presented a synergy of satellite data from Terra, Landsat, SPOT. The focus was on the evaluation of the ecological and productive state of forests based on the identification of damaged areas and biophysical and structural properties. A

combination of SPOT and ASTER (compared to Landsat showed the best results in damage detection, while Terra MODIS was utilized most successfully in biophysical and structural properties identifying. The biophysical and structural identification is based on vegetation indices (NDVI, EVI, LAI), and photosynthetic active radiation absorbed by vegetation calculated from satellite image bands. Both methods of subsystems were successfully applied to different tree species such as European beech (*Fagus sylvatica*), Norway spruce (*Picea abies*), and Turkey oak (*Quercus cerris L*.).

Bucha & Koreň (2014) constructed a phenological model, which predicts phenological events by NDVI during the whole year. The period between 2000 and 2015 was used in the study, and 803 MODIS tiles were collected for model input. NDVI modelling was made on a sigmoidal logistic curve, where v(t) stands for the day of the year, and it is calculated using the minimum and maximum NDVI (V_{min}, V_{max}), and spring and autumn amplitude controls (m_{1-4}). After the average and standard deviation of NDVI were calculated first then the second derivate was created to model these curves, especially the phenophases onset. By this method minimum, maximum and extreme points were given and marked on the curve through the vegetation season. Finally, time series analysis was made by regression, but significant trends were not observed in any phases, only a very slight shift (0.8-1.9 days). Despite the lack of trends, the phases were successfully identified proving the efficiency of the model and it is used in the forest monitoring system of the Slovak National Forest Centre.

2.8.2.2. Czech forest monitoring systems

In Czechia, several forest monitoring approaches can be found in different institutes. The Czech Forest Management Institute (in Czech: Ústav pro hospodářskou úpravu lesů Brandýs nad Labem, or shortly 'ÚHÚL') developed a method using Sentinel-2 data and NDVI, LAI (Leaf Area Index) for forest health evaluation. The LAI was calculated on 189 ICP plots, which are based on field LAI measurements and supported by remote sensing as well for the years 2015 and 2017. Only the best-quality pixels were chosen with a decision tree based on the lowest cloud cover and highest biomass values. Then vegetation indices were calculated like NDVI, Red Edge Inflection Point (REIP), Normalized Difference Infrared Index (NDII), Difference Index (DI), wetness component of Tasseled Cap, and LAI. Finally, categories were classified (I.-V.: significant increase – decrease in forest health). As a result, ground-based LAI correlated

mostly to NDII, DI, and Wetness component of Tasseled Cap with R^2=0.57–0.63 and the method showed 15% of damaged forests (Lukeš et al., 2018).

This method was developed and extended into a monitoring system having four main components: the most important one is PlanetScope satellite image collection (with 3x3 m spatial and 1-day temporal resolution) used for calculating VIs, and the second one is Sentinel-2 data for tree species classification and ICP Forest monitoring plots for its validation. Orthophotos and maps of clearcuts made by ÚHÚL are the third and fourth components of the system used to exclude misclassification of damaged forests due to forest operations. Based on these components plus LIDAR and base map datasets, 20 different layers are available on their geoportal (http://geoportal.uhul.cz/mapy/MapyDpz.html) (Figure 11).

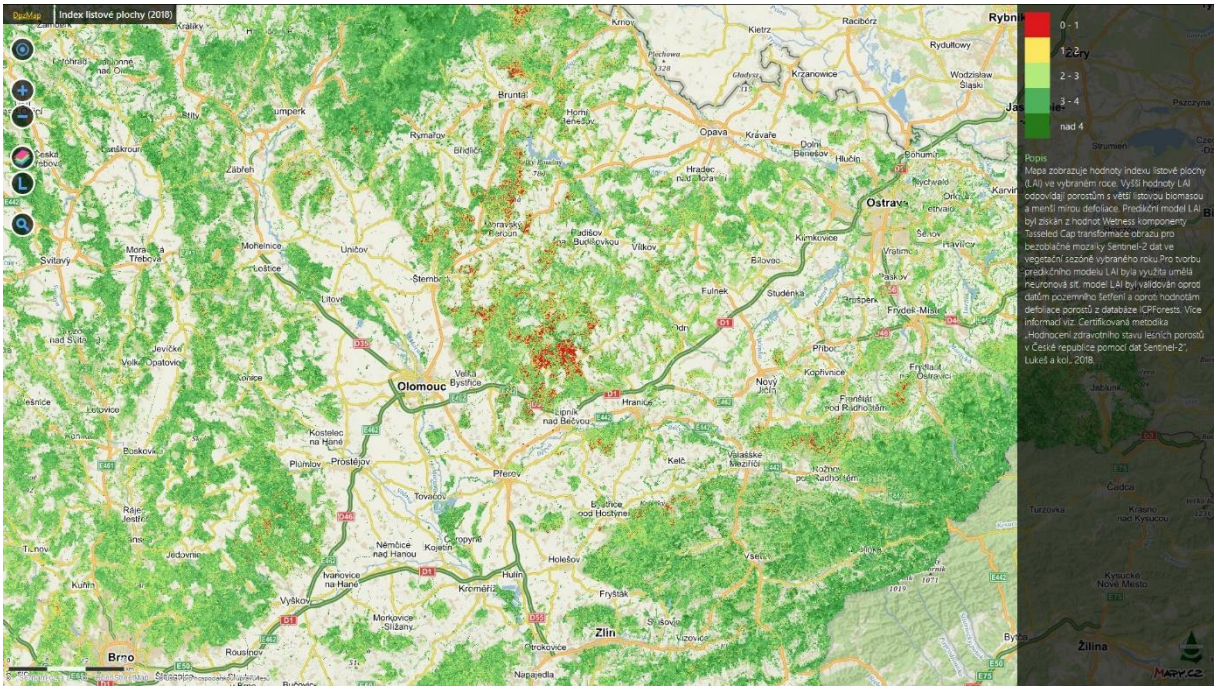

Figure 11. Forest state near Olomouc in 2018 from the Czech forest monitoring system.

The forest state and development maps are categorized into groups. The forest health state is described by annual LAI composite maps from 2015 and changed by four classes (state increment, steady-state, slight decrease, significant decline) showing differences between years. There are dedicated maps to the European spruce bark beetle (*Ips typographus L.),* which endangers 80% of Czech forests by attacking Norway spruce (*Picea Abies*), Scots pine (*Pinus syvestris*), silver fir (*Abies alba*), douglas fir (*Pseudotsuga menziesii*) and European larch (*Larix decidua*) as well. ÚHÚL created two separate geoportals called bark beetle maps (found

at: http://www.kurovcovamapa.cz) and bark beetle info (available at: http://www.kurovcoveinfo.cz/), where remotely sensed and ground collected data is visible.

The Global Change Research Institute (CzechGlobe) of the Czech Republic has a service called Mapserver where hyperspectral, LiDAR, orthophoto, thermal, and other thematic data is published (CzechGlobe, 2019) for 55 areas of the country on certain dates, where ecosystem types are categorized into the forest, urban, agro-ecosystem and water classes. Datasets can be visualized by selecting them, in the forest ecosystem menu, carotenoids, chlorophyll, water content and LAI values are published on the webpage: http://mapserver.czechglobe.cz/en/map.

Hlásny et al. (2014) examined the heat and drought stress in oak and beech forests by MODIS-based NDVI for the years between 2000 and 2010 and explored differences in stress response connected to climate change. 21 experimental plots were established with data about the site: altitude, slope, aspect, age, density, and altitudinal and horizontal distances from meteorological stations. 121 MODIS pixels covered the same area. Dry periods were examined carefully by comparing meteorological (daily temperatures and rainless days) and satellite data by regression fitting and correlation coefficients showed strong connections. NDVI curves also declined significantly during the dry periods, thus the method is suitable for indicating variations in NDVI, but not for verifying climate change, according to the authors.

2.8.2.3. Polish forest monitoring system

The Polish Forest Research Institute (Instytut Badawczy Leśnictwa) runs a mapping portal that offers a wide range of products divided into ten categories (IBLES, 2019), which contains several map layers. Categories are the followings: regional boundaries by IBL, regional boundaries by Warsaw University of Life Sciences, ForBioSensing project results with Digital Terrain Models, monitoring of Polish forests by defoliation and monitoring points on two levels, monitoring of mountains forests, forest protection prognosis and others. These datasets are both from ground-based measurements and satellites.

Hawryło et al. (2018) in Poland made a study focusing on Scots pine (*Pinus sylvestris*) defoliation with the method of machine learning. 50 field plots were chosen based on Landsat EVI values, where defoliation was observed and given in % values. The remote sensing data

contains Sentinel-2 tiles from 2015 and 2016, and three methods were chosen for creating regression and classification models: k-Nearest Neighbours (kNN), Random Forest (RF), and Support Vector Machine (SVM). These methods were tested with 23 different vegetation indices, which gave 38 predictor variables after running the best predictor selecting algorithm. MERIS Terrestrial Chlorophyll Index (MTCI), and Green Normalized Difference Vegetation Index (GNDVI) proved to be the most important ones (with 79-100%) in all three methods. But moderate accuracy was shown by all stand defoliation regression models (R^2=0.53-0.57). The study showed that other indices than NDVI are more robust and sensitive to forest changes.

Bartold (2012) showed the effect of large-scale abiotic damage, in a hurricane in a Polish forest where large areas were severely damaged. The large time scale (11 years) allowed him to use the Corine Land Cover database for validation, which showed where the forest disappeared. Firstly, MODIS NDVI values were compared before and after the disaster, then calculated Moisture Stress Index was calculated and finally Tasseled Cup transformation was applied to gain information in four channels: brightness, greenness, wetness, and vegetation condition. All three methods were tested for all pixels and after converted the rasters to vectors to be comparable with control data. The results with very high accuracy (96%) showed the utility of the methods.

2.8.2.4. Slovenian forest monitoring systems

The Slovenian Ministry of Agriculture, Forestry and Food have a Public Graphical Data Viewer system (http://rkg.gov.si/GERK/WebViewer), which contains several map layers connected to forests (MKGP, 2019), like orthophotos, actual land use of agricultural and forestry maps (RABA), digital terrain models (DDM), hydrological maps, pedological maps and so on.

The forest data viewer of the Slovenian Forest Service (ZGS, 2019) offers eight large map categories with maps of forest regions, units, characteristics, ecological functions, social functions, production functions, areas affected by damage, and cartographic base. Damage is displayed by time and cause.

2.8.2.5. Finnish forest monitoring system

Saarinen et al (2018) examined the opportunities in Finland by creating a dataset of 30 076 images in 185x185 km tiles and 30x30 m resolution from 45 years and all Landsat satellites (1–

7) were used in this research. Filtering was applied to have pictures that are suitable for forest monitoring. In the temporal scale, it means the vegetation season peak (±30 days of August 1 in the northern hemisphere summer) and in the spatial scale excluding cloudy pixels. The dataset acquired by this method contains gaps but Saarinen et al. also pointed out that Landsat and Sentinel-2 satellite image combinations are possible since robust compositing algorithms exist, and there is spatial and spectral complementarity between these satellites. With all these remote sensing data field monitoring plots can be complemented with new information for forest monitoring.

2.8.2.6. German forest monitoring system

The German Forest Condition Monitor (in German: Waldzustandsmonitor, https://waldzustandsmonitor.de/en/forest-condition-monitor/) was made to visualize the condition of forests in Germany and Europe. MODIS 8 days NDVI composites are used to determine the greenness of the vegetation and compared to long-term observations (Waldzustandsmonitor, 2019). The greenness is described by relative and absolute values as well. The quantiles represent the positive and negative extreme values, which can indicate favourable or unfavourable (forest damage) environmental conditions, while they represent the absolute deviation of the greenness from the long-term mean value in percent. These maps are available for the whole of Europe in the selected years of 2003, 2015, and 2018, when extreme drought damage happened (Buras et al. 2020, 2021).

2.8.2.7. Norwegian forest monitoring system

The Kilden system of the Norwegian Institute of Bioeconomy Research consists of online maps for multi-purposes, one of them is the forest portal (“Skogportalen”, https://kilden.nibio.no/), where dedicated maps can be made for bark beetle The Kilden system of the Norwegian Institute of Bioeconomy Research consists of online maps for multi-purposes, one of them is the forest portal (“Skogportalen”), where dedicated maps can be made for bark beetle alerts in Southern Norway. Two thematic layers show the probability of damage in percentage for each 10x10 m Sentinel-2 pixel and the 1x1 km squares with aggregated damage. Both are coloured according to the severity on a scale from white to dark red, where dark red stands for the highest probability of damage. These probabilities are calculated in a program written in Python language using the Extreme Gradient Boost machine learning method to classify

each pixel into the clearcut, healthy forest, and damaged forest categories based on ground-based and aerial datasets. The maps are automatically updated whenever new satellite images are available (Figure 12).

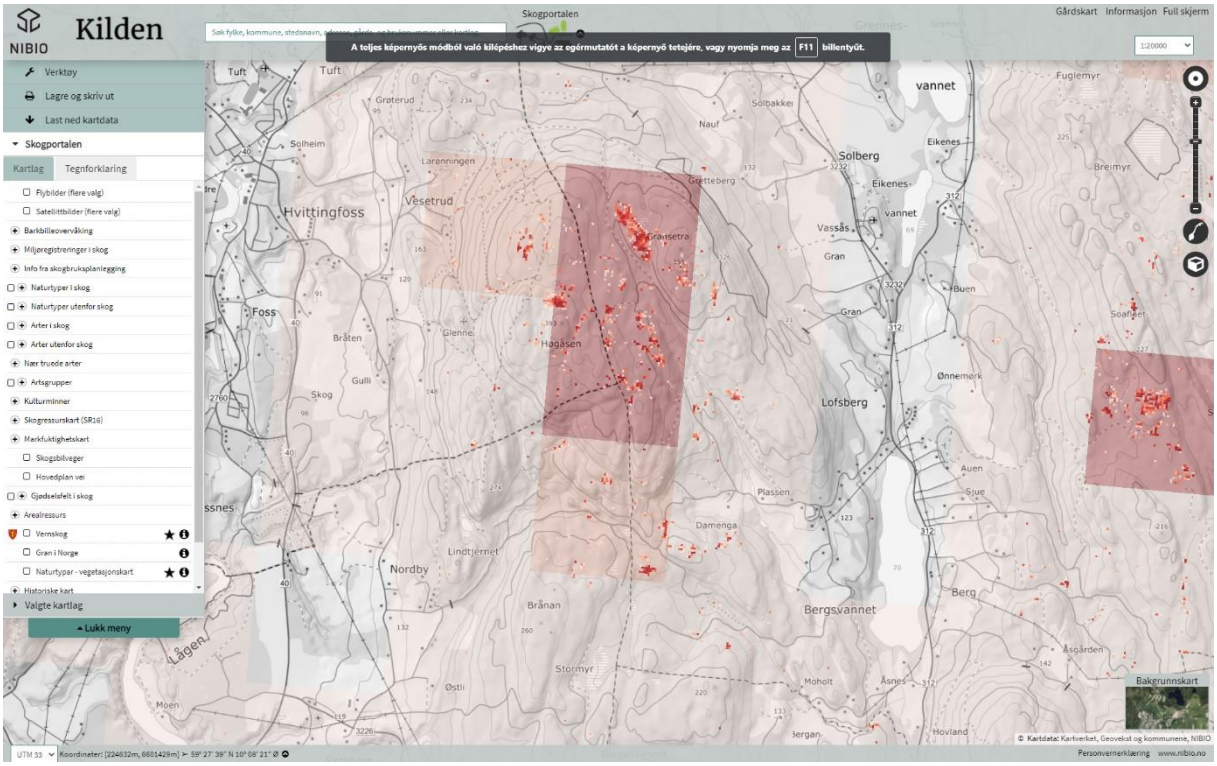

Figure 12. Kilden system shows damaged forest stands based on Sentinel-2 images around Hvittingfoss, Southern Norway in August 2021.

2.8.3. Forest monitoring systems worldwide

The Global Forest Watch (GFW, https://www.globalforestwatch.org), 2019) of the USA is an online platform providing the largest dataset in the world for monitoring forests in real-time giving information about where and how forests are changing around the World. The global and local datasets are shown on maps, analyses, and dashboards in several classes like forest change (gain, loss cover, deforestation, and fire alerts), land cover change (tree cover, land cover, plantations), land-use changes (logging, mining, mills, gas concessions, dams, roads, population density), climate change (CO_2 emissions, biomass density, soil C density, C storage), biodiversity (hotspots, extinction sites, conservation landscapes, and areas). On the interactive maps, countries or counties can be selected for detailed analysis with graphs and they can be downloaded in Excel tables.

The ForWarn II was made by United States Department of Agriculture (USDA) Forest Service (2020) and used as a vegetation change recognition and tracking system which provides near real-time change maps for the United States of America updated every eight days made of MODIS NDVI data. Biotic, abiotic damage, antropogentetic and meteorological disturbances are visible on these maps and with the tracking system, the recovery plus the cumulative effects of multiple disturbances over time are also detectable. From 2000 till today 46 NDVI maps are published every year using the 24-day window rule. Forest health decline was monitored systematically in the last few years by Norman & Christie (2020) and evidence of forest stress was proved as well. The monitoring will continue in the new version of the system, the ForWarn III based on Sentinel-3 since 2022.

Other monitoring systems are not open to the public in 2021 such as the one in Australia called the Continental Forest Monitoring Framework (Wood et al., 2006), in Canada the National Deforestation Monitoring System (CNDMS, 2015), and in Russia the KEDR (WWF 2017). The KEDR utilizes GEE algorithms to automatically compare multi-temporal satellite images in a pixel-by-pixel way, and the imaginary database is explained with statistical values, thus the system can detect deviations from the median values for each pixel. This information is sent in real-time to rangers to identify and respond to violations of forestry legislation.

In Africa and South America, the GEE was also utilized for forest monitoring, for example in Ghana (Osei et al., 2019), Mozambique, Peru, and Bolivia (Hamunyela et al., 2020). The Global Forest Watch also utilizes GEE, which is available for all the above-mentioned countries.

2.9. Forest damage types

Forest damage can be divided into three groups according to its origin. Abiotic damage is caused by non-living, natural factors such as wind, snow or fire. They are often triggered by certain meteorological and climatological events, like forest fire could be caused by drought (Tobak et al., 2017) or flood is by extra amount or intensity of precipitation. While biotic damage is caused by living creatures such as insects, fungi, viruses, or bacteria. Under unfavourable abiotic conditions trees are more vulnerable to biotic agents as well, thus these damage types are connected in certain cases (Teshome et al, 2020). Eventually there are anthropogenic damage as well caused by humans, which can be done by inexpert forestry operations, infrastructure construction or illegal logging.

3. Material and methods

This section contains the description of study sites, the general application of Sentinel-2 images for Hungary, and the specific method developed in this Thesis based on GEE. The time-series analysis also contains methods for evaluating maps, graphs, and tables. Machine learning is also briefly described in this section which is applied for tree species classification and the validation sets are also presented. These ground-based datasets contain abiotic and biotic damage types, and a damage threshold was created to identify them. Eventually, in the confusion matrix, the RS and ground-based datasets were compared.

3.1. Study sites

In this thesis forest health was studied with remote sensing methods in three selected study areas: Nagyerdő of Debrecen, Farkas-erdő of Sárvár, and Central Bükk (Figure 13) (Table 4). These areas differ in size (1092, 5665 and 49152 ha), terrain (plain and mountainous), location (eastern, western, and northern parts of Hungary), and typical forest communities (oak with Lily of the valley (*Convallario-Quercetum roboris*), oak-hornbeam (*Querco robori-Carpinetum*), submontane beech (*Melittio-Fagetum*) as well. The study areas were selected to represent typical forest ecosystems of Hungary and also due to accessibility and data availability (forestry database, site descriptions, field reports). The Nagyerdő is easily accessible (in the city of Debrecen), relatively small, flat and dominated by oak, which made it ideal for monitoring. While the Farkas-erdő on the other side of the country is larger and has mixed forest communities, the location also plays role since the headquarters of the Hungarian Forest Research Institute are in Sárvár, close to the forest. While the mountainous Bükk is the largest contagious forest in the country and several forest studies took place there in the past, also serious forest damage happened in the past few years which made it an interesting place to be monitored.

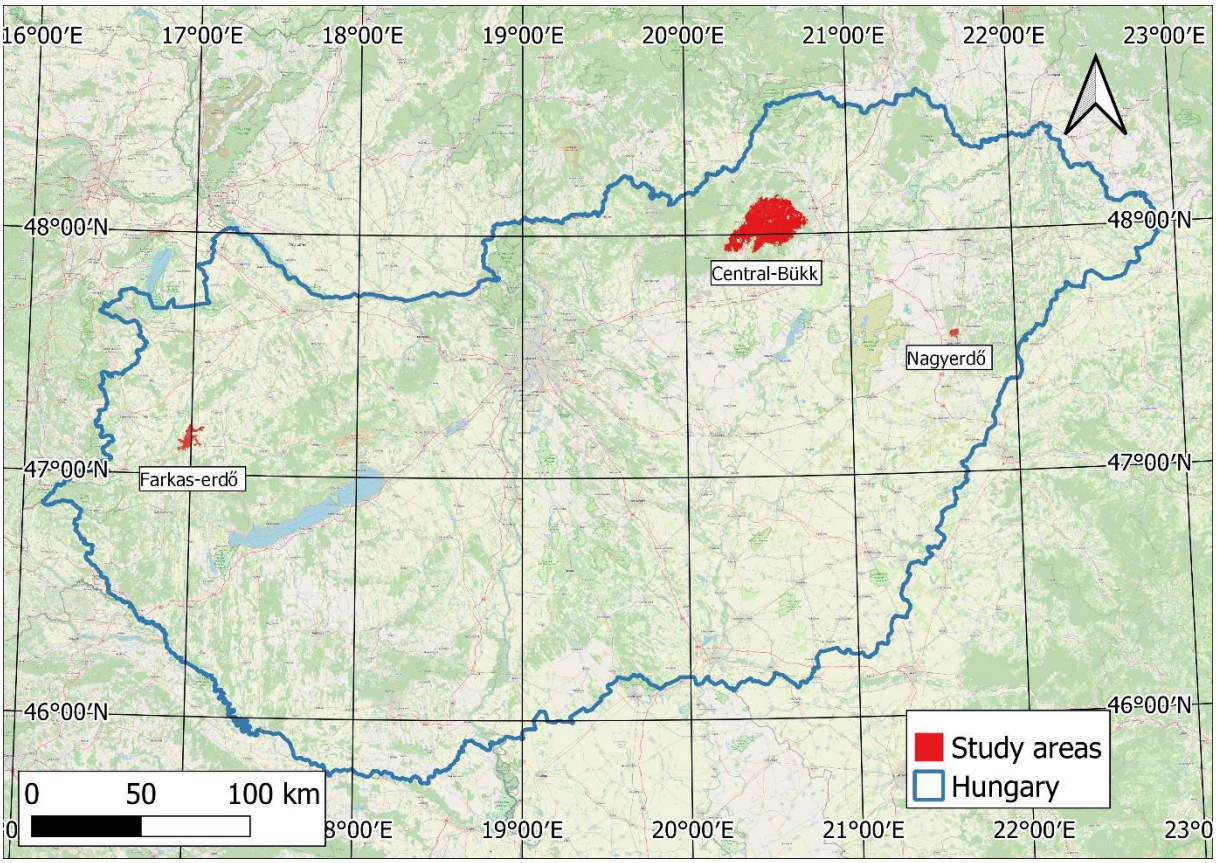

Figure 13. Study areas of the thesis: Farkas-erdő (west), Central Bükk (north) and Nagyerdő of Debrecen (east).

Table 4: Characteristics of study sites.

Name	**Nagyerdő**	**Farkas-erdő**	**Központi-Bükk**	
Area (ha)	1092	5665	49152	
Forest microregion	Nagyalföld	Nyugat-Dunántúl	Északi-középhegység	
Forest mesoregion	Hajdúság (West), Nyírség (East)	Kemeneshát	Bükk	
Forest microregion	Hajdúság (West), Nyírség (East)	Kemeneshát	Központi-Bükk	
Forestry Authority	Nyírség Forestry PLC.	Szombathely Forestry PLC.	Északerdő Forestry PLC. (East)	Egererdő Forestry PLC. (West)
Forest management unit	Debrecen	Sárvár	Lillafüred, Délbükk, Keletbükk	Eger, Felsőtárkány Szilvásvárad
Protected	Yes	Yes	Yes	
Climate	Sessile-oak – Turkey- oak type	Hornbeam- sessile oak type	Beech and hornbeam-sessile oak type	
Topography	Plain	Mostly plain, partly hilly	Mountainous	
Forest communities	Oak with Lily of the valley	Oak-hornbeam Turkey oak - Sessile oak	Submontane beech Oak-hornbeam Turkey oak - Sessile oak Lime-ash Ravine forests Rocky forests	

Since the study areas differ not just in the geographical conditions but in the tree species composition as well, a query was made from Hungarian National Forestry Database to determine the five dominant ones in each forest giving information about tree species name, code, area and the number of compartments (Table 5).

Table 5: Dominant tree species of the study sites expressed in area and percentages.

		Nagyerdő		Farkas-erdő		Central Bükk	
Tree species	Code	area	area	area	area	area	area
		(ha)	(%)	(ha)	(%)	(ha)	(%)
Black locust	A	66.85	6.12	505.68	8.93		
European beech	B					16634.75	33.84
Hornbeam	GY					2295.32	4.67
Norway spruce	LF					1112.03	2.26
Pedunculate oak	KST	653.81	59.87	1531.71	27.04		
Red oak	VT	150.33	13.77				
Scots pine	EF	66.49	6.09	734.48	12.97		
Sessile oak	KTT			705.97	12.46	20201.75	41.10
Turkey oak	CS			989.01	17.46	3475.67	7.7
Other		154.52	14.15	1197.77	21.14	8835.22	11.05
Total		1092	100	5664.62	100	49152.11	100

Dominant tree species were filtered from the Hungarian Forest Database based on the index (‘jelzőszám’ in Hungarian, JSZ shorty) and tree species mixture (‘elegyedés módja’ in Hungarian, ELM shorty) attributes referring to forest stand levels where the selected number 1 stands for “first or only forest stand level, or first and only topmost stand-level” and “main species” (FAFN) according to the list of forestry description sheet (‘Leíró lap nyomtatvány kódjegyzéke’). For the filtering, the topoXMap 1.22.3.1 software was used and the five most frequent species were selected (Table 5). In this example Scots pine (EF code) was filtered from the database with the following code line (Code 1):

```
[efafs.JSZ] = "1" & [efafs.ELM] = "1" & [efafs.FAFN] = "EF"
```

Code 1. Tree species selection from the Forestry Database by index, mixture and name.

where efafs is the Forestry Database with species code, JSZ is index and ELM is mixture and FAFN is the tree species name.

3.1.1. Nagyerdő of Debrecen

The Nagyerdő (“Grand Forest”) is situated inside the administrative border of Debrecen, northwards from the centre, on a 1092 ha large area (HNP, 2020). Geographically it lies at the meeting of three microregions: Hajdúhát, Dél-Hajdúság and Dél-Nyírség. On the loess and

sandy soils, there were favourable water supply conditions and large coherent forests, which only remained nowadays in smaller patches after the second world war, river regulations, and forest cutting. Typical forest communities were willow (*Salicetum tríandrae*), willow-poplar gallery forest (*Salicetum albae-fragilis*), oak-ash-elm gallery forest (*Fraxino pannonicae-Ulmetum*), oak-hornbeam (*Querco robori-Carpinetum*), open oak forest on sand (*Festuco rupicolae-Quercetum roboris*), and oak with Lily of the valley (*Convallario-Quercetum roboris*) (Gencsi, 2021).

Pedunculate oak with Lily of the valley (*Convallaria majalis*) is the most important and typical community, in which the indicator species marks habitats with partial shade, warm summers, and moderately alkaline silty or sandy soils with a plentiful amount of humus. While gallery forests disappeared after the water regulations and water level decreased (Zöld Kör, 2019).

The Nagyerdő has been used for 700 years and the degrading condition in the 19th century demanded renewal of forest management. In 1939 a 31 ha large part of the forest was nominated for nature protection area which was expanded in the next decades, resulting in that 1992 the whole forest is under protection with 1092 ha under the supervision of Hortobágy National Park marked as Nagyerdő TT (249/TT/92).

The local forest management authority is the Debrecen Forestry Unit of Nyírerdő PLC. which handles a 9457 ha area, from which 7498 ha is inside the municpality borders. The regulatory authority of the Nagyerdő is the Government Office for Hajdú-Bihar County Forestry Directorate, based in Debrecen (Nyírerdő, 2020). The currently existing forest management plan from 2017 consists of forest compartments of Debrecen from 34-73, with protection as a primary function, and park-like forest as a secondary function under the protection of the Natura2000 area of EU with cutting and transitory tree utilization modes.

The forest tree composition includes several species, but the most important, largest (20-30 m high), and eldest (100-300 years) pedunculate oaks (*Quercus robur*) can be found in the old forest (Figure 14). Domestic compound species are silver poplar *(Populus alba),* wild cherry *(Prunus avium),* Tatar maple *(Acer tataricum),* field maple *(Acer campestre),* field elm *(Ulmus minor),* wych elm (Ulmus glabra), European crab apple *(Malus sylvestris),* European wild pear *(Pyrus pyraster),* large-leaved lime *(Tilia platyphyllos) and* silver lime *(Tilia tormentosa)*. The foreign species are black locust *(Robinia pseudoacacia),* Scots pine *(Pinus sylvestris),* and northern red oak *(Quercus rubra)*. Under the trees, special flowers can be

found such as the Lily of the valley, Turk's cap lily *(Lilium martagon),* a lesser butterfly-orchid *(Platanthera bifolia),* white helleborine *(Cephalanthera damasonium),* steppe iris *(Iris aphylla subsp. hungarica).*

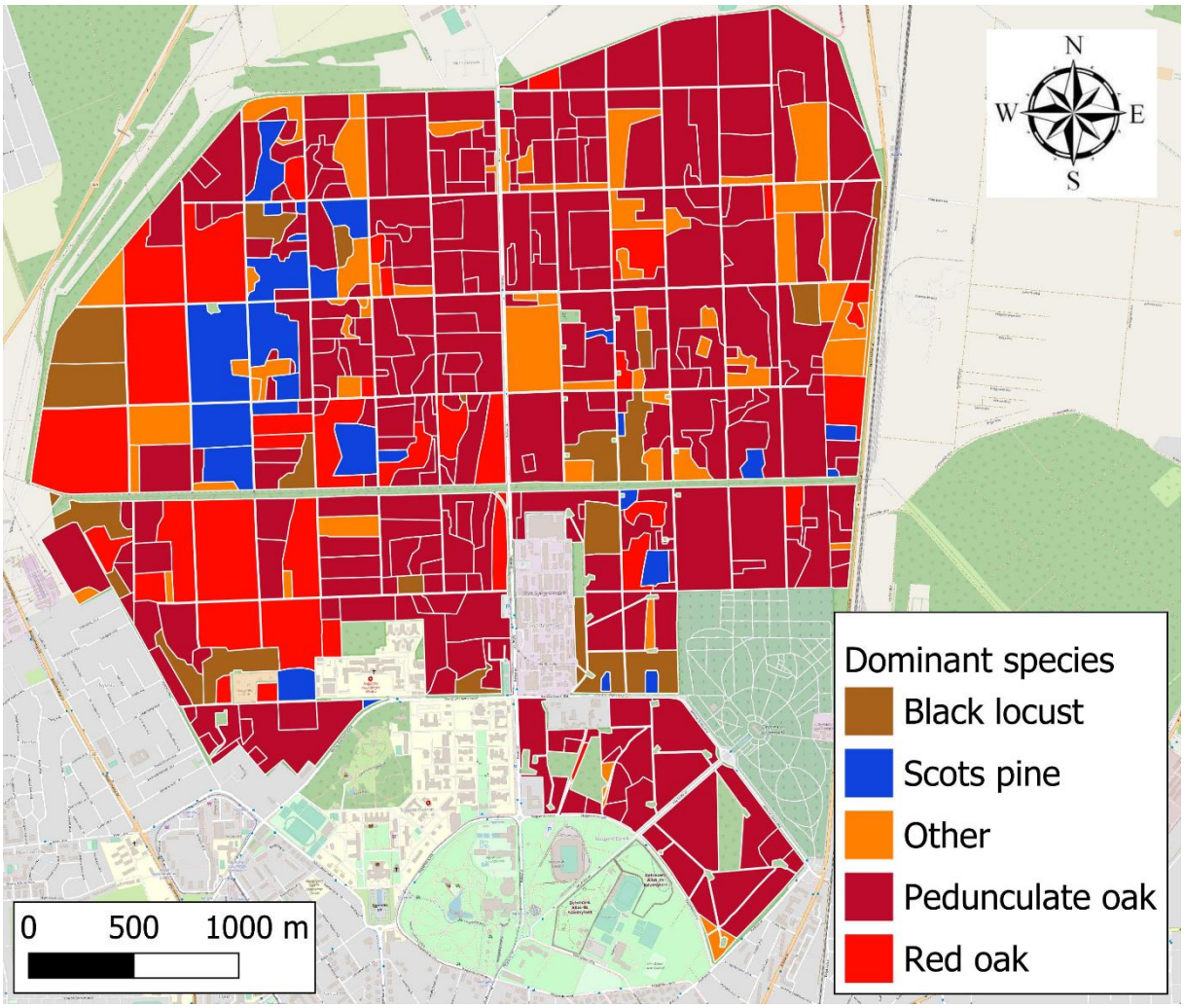

Figure 14. Dominant tree species of Nagyerdő.

3.1.2. Farkas-erdő of Sárvár

The Farkas-erdő ("Wolf Forest") lies between the settlements of Sárvár and Káld on a 7200 ha large area, in Western Hungary, being the largest forest in Vas county. The 5500 ha large contiguous part of the forest south of Sárvár is protected. The mixed oak-beech-hornbeam forest belongs to the Sárvár Forestry Unit of Szombathely Forestry PLC. (Szombathelyi Erdészet, 2020).

The most typical forest communities are oak-dominated ones: *Quercetum petreae-cerris* and *Querco robori-Carpinetum,* while the most important tree species are pedunculate oak, and sessile oak, Turkey oak, European beech, European hornbeam, black locust, and Scots

pine (Figure 15). The forest was famous for the 300 years old large, pedunculate oaks called hagtrees (‘banyafa’ in Hungarian) and the red deer (*Cervus elaphus*) colony.

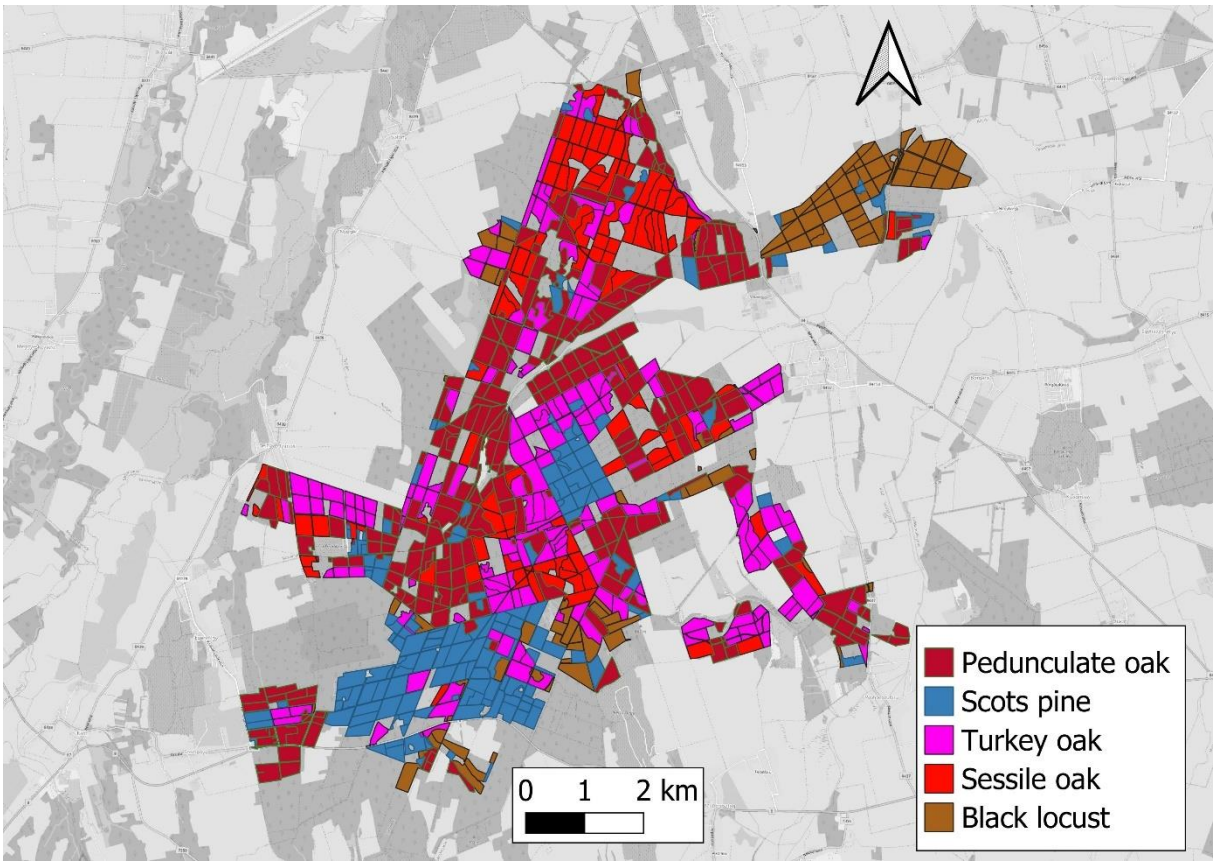

Figure 15. Dominant tree species of Farkas-erdő

3.1.3. Central Bükk

The Bükk Mountains are located in Northern Hungary on a 100.000 ha area which is the largest contiguous forest body in Hungary and is entirely protected by Bükk National Park Directorate. The Central Bükk studied in this Thesis covers around half of this area (52,000 ha) and is managed by two forestry companies, Egererdő PLC. (on the west side) and Északerdő PLC. (on the east). Both have three-three forestry units such as Eger, Szilvásvárad, Felsőtárkány belonging to Egererdő, and Lillafüred, Délbükk, Keletbükk to Északerdő.

Due to the various types of elevation (200-900 m), slope, and aspect conditions almost every type of Hungarian forest community can be found here (Egererdő, 2021), and the dominant tree species are European beech (which the mountain was named after in Hungarian) and Pedunculate oak covering 2/3 of the forested areas (Északerdő, 2021) (Figure 16).

The zonal distribution of forest communities is visible in form of belts in the Bükk Mountains (Vojtkó, 2002). At the height of 250 – 400 m, Turkey oak - Sessile oak (*Quercetum petraeae-cerris*) forest can be found which has the largest extent as a community in Bükk Mountains. The main species are mixed with several species like chequers (*Sorbus torminalis*) and field maple (*Acer campestre*) wild pear (*Pyrus pyraster*) and wild apple (*Malus sylvestris*). This belt is followed by the hornbeam-oak stands (*Carici pilosae-Carpinetum*) between 400 – 600 m. Even higher submontane beech forests (*Melittio-Fagetum*) can be found mixed with sessile oak (*Quercus petraea*), hornbeam (*Carpinus betulus*), sycamore maple (*Acer pseudoplatanus*), Norway maple (*Acer platanoides*), silver birch (*Betula pendula*), and European ash (*Fraxinus excelsior*).

On special terrain conditions, we can find different communities like in steep ravines ravine forests (*Phyllitidi-Aceretum*), on the mountain tops lime-ash (*Tilio-Fraxinetum excelsioris*), or rocky beech forests (*Seslerio hungaricae-Fagetum*) with ice-age relicts. Bedrock also affects the distribution of forests creating brooms-oak (*Genisto pilosae-Quercetum*) or acidofrequent oak stands (*Luzulo-Quercetum*).

Water availability has also of great importance, theisare xerophile (drought tolerant) communities dominated by downy oak (*Quercus pubescens*) in stands with mahaleb cherry (*Ceraso-Quercetum pubescentis*), another type of oaks (*Corno-Quercetum*), or false-brom (*Cirsio pannonici-Quercetu*m). With more water, supply willows (*Salicetum albae-fragilis*) and alders (*Aegopodio-Alnetum)* grow mixed with European ash (*Fraxinus excelsior*) or European white elm (*Ulmus laevis*).

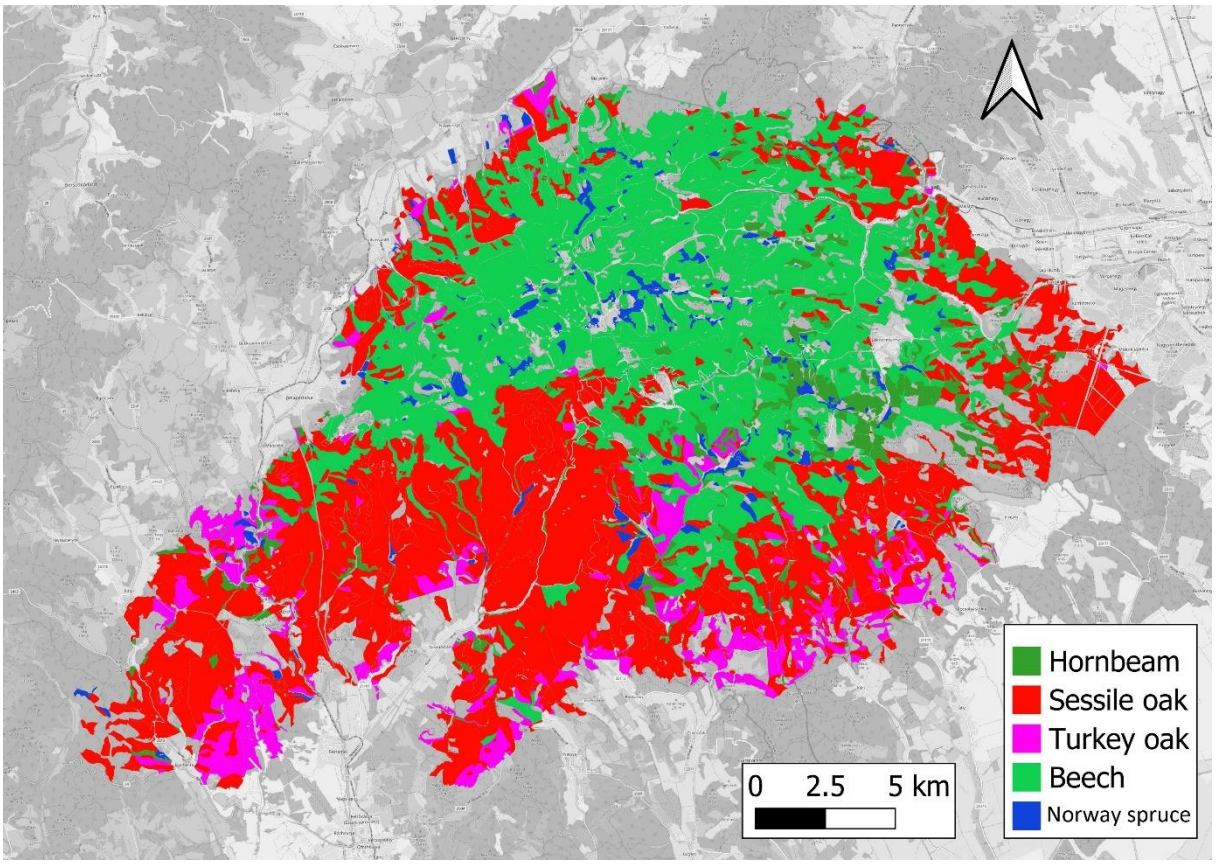

Figure 16. Dominant tree species of Central Bükk

3.2. Sentinel-2 satellite imagery

The number of available Sentinel-2 images for Hungary is a crucial part of the monitoring system. According to the map of Barton et al. (2017b) about the number of cloud-free Sentinel-2 images, it seems clear, that both Bükk Mountains and Farkas-erdő of Sárvár are covered with a few (9-16) cloud-free images between 2015 and 2017. Nagyerdő of Debrecen is better with 22-28 images. This has great importance in setting the thresholds for cloud cover masking and the creation of time series. I used S-2 L2A imagery (with both Sentinel-2 A és B satellites) which is available for Hungary since 2017 in GEE, where tile 33 TXN covers Farkas-erdő, 34 TET does Nagyerdő and 34 UDU does Central Bükk (Figure 17).

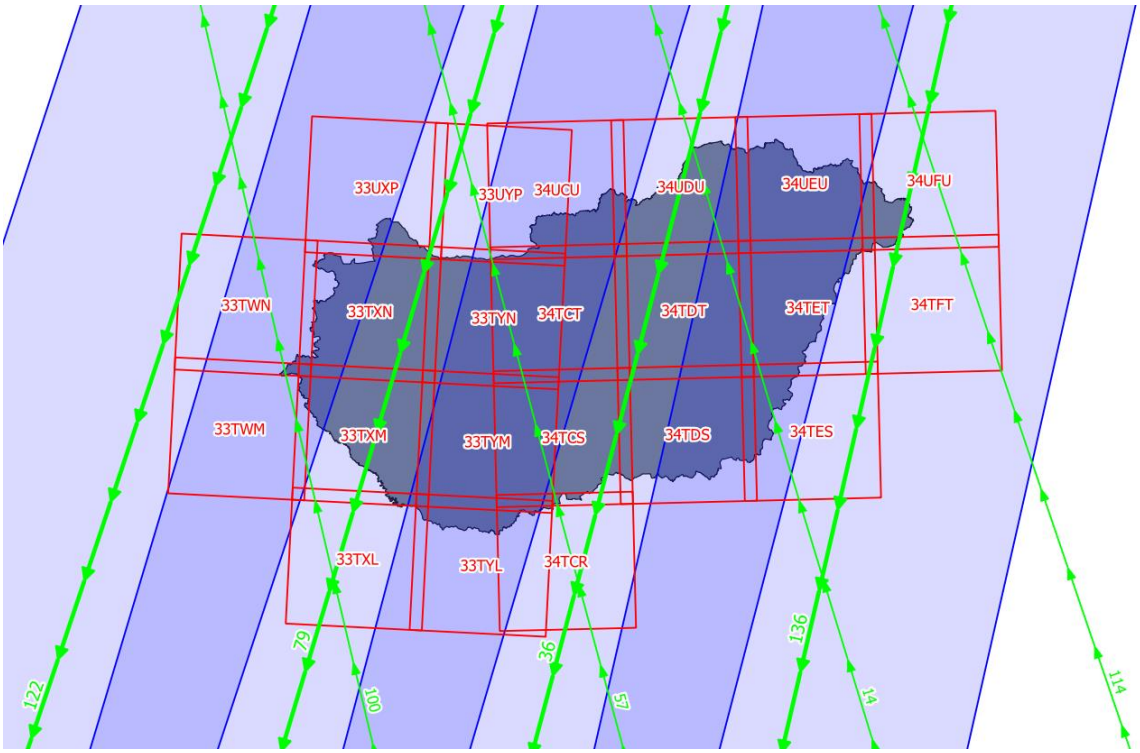

Figure 17. Sentinel-2 tiling grid in Hungary.

3.3. Google Earth Engine

3.3.1. General description

The reason behind choosing GEE for this Thesis was the quick and flexible processing capability which is ideal for research purposes. Huge asset is the online storing, computing and visualizing capacity of the system which helped to avoid a lack of storage capacity on hard disks and buying expensive hardware and software to perform geospatial analysis. Google also provides wide range of online datasets and tutorial material which helped a lot in the coding and fastened the whole monitoring process. On the other hand, several questions emerged in connection with GEE which had to be tested in practice such as:

- platform: if it is suitable for running a wall-to-wall forest monitoring system,
- computing capacity limits: achieving monitoring goals without exceeding limitations,
- data policy: uploading and downloading non-public data,
- data security: public version without sharing the code.

3.3.2. Algorithm

As a novel approach to Hungarian forest monitoring, I created a GEE-based method in the code editor (dashboard) to make maps and charts. This algorithm is written in JavaScript language and consists data query, filtering, masking, reduction, visualization and export as well. The steps of processing can be seen in the flowchart (Figure 18).

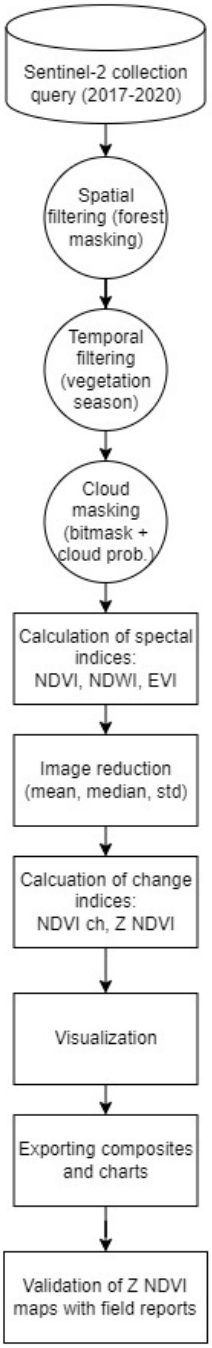

Figure 18. GEE system flow chart for Hungarian forest monitoring.

The flowchart contains these elements of the monitoring:

- Data collection query: Sentinel-2 surface reflectance collection (10x10 m) on which filtering and masking were applied
    - bound filtering: set Region of Interest (ROI) by shapefiles
    - time filtering: set start and end date (04.01-10.30.)
    - cloud filtering: bitmask with band QA60 (cloud mask, 60x60m)
    - forest masking: by Hungarian forest boundaries and ESA forest cover mask (10x10 m) by shp
- Reducing collection: minimum, mean, median, maximum, and standard deviation (std) with image reducers
- Calculating vegetation indices: NDVI, NDVI ch, Z NDVI, NDWI, EVI.
    - Reducing vegetation indices: NDVI mean, NDVI median, NDVI std.
    - Comparing years:
        - by subraction → ch NDVI
        - by standardization → Z NDVI
- Visualization parameters: palettes, borders, bands (colour, width, centre, etc.)
- Display
    - Display in GEE platform: RGB and VI maps and charts
    - Public display by App Engine
- Image export
    - maps to Google Drive in TIFF format
    - charts in CSV and PNG for further analysis.

3.3.3. Spatial filtering

Proper filtering of the Sentinel-2 L2 SR dataset (Google, 2020a) by boundary is needed at the initial stage to set Region of Interest (ROI) aiming to work with data that is interesting for us. For this, we can use built-in datasets like international boundary polygons (USDOS/LSIB_SIMPLE/2017 collection) or global administrative unit layers (Google, 2020b). In the case of the Hungarian state border, OpenStreetMaps were used (OSM, 2021). Spatial filtering also means forest masking in this case, described in the next chapter.

3.3.4. Forest masking

Forest masking is a crucial part of the monitoring system. Both vector and raster-based solutions can be utilized depending on the goal. The below-mentioned datasets are not yet available directly in GEE, but by downloading from the website and uploading to the GEE it is possible to utilize them even in combined form.

One solution is the usage of vector polygons. To get the most accurate forested area the forest compartment polygons created by Forestry Companies were filtered by type not to contain the ones which do not cover actual forests like roads (ÚT), openings (NY) , clearings (TI), buildings (ÉPÖ, feeding ground (VF), water bodies (VI), barren earth (TN), shrubs (CE), other forestry establishments (EY). These compartments belong to areas serving forestry activities and areas that belong to forestry establishments but are not covered by forest. In the Hungarian Forestry Management Guide (NFK, 2004) these codes refer to the filtered areas: ÚT, NY, TI, ÉP, VF, VI, TN, CE, and EY.

Raster-based forest masks could be also used such as high-resolution forest layers of Copernicus (2021), which consist of three types of status products and two types of change products at 10x10 and 20x20 m resolution. These are available for 2012, 2015, and 2018 and 2012-2015, 2015-2018 respectively. There are Tree cover density (TCD) (level of tree cover density, 0-100%), Dominant leaf type (DLT) (broadleaved or coniferous majority), and Forest type product (FTY), which is a combination of the dominant leaf type, the size of at least 0.5 ha, 10% tree cover density, plus trees under agricultural use from Corine Land Cover (CLC). Besides the status maps change layers are also available such as Tree Cover Change Mask (TCCM) and Dominant Leaf Type Change (DLTC).

I have used both methods for different reasons. The polygons are more accurate and more frequently updated but also have bigger sizes, which could cause problems after a certain limit in GEE, yet suitable for sample areas. While rasters are smaller and could be loaded faster, thus they might be more suitable for country- or continent-wide monitoring, on the other hand for certain functions they must be converted to vectors. I tried different methods, see the method of country wide maps in chapter 3.9.

3.3.5. Temporal filtering

In the case of time series, the size of data is always considered for filtering. Setting the proper start and end date of the image collection is advised to process only useful data. In the case of forest monitoring, the vegetation period (or growing season) is the window from spring to late autumn to exclude the months when photosynthesis is low or does not occur at all.

The growing season length (GSL) varies depending on geographical location and in Hungary is supposed to be between mid-April and the end of September as we applied in TEMRE. However several studies were made to prove that GSL could be longer. According to Garonna et al. (2015) the GSL increased significantly by 18 – 24 days/decade over 18 – 30% of the area of Europe, depending on methodology, but observed both by satellite and ground-based observations. I observed on my GEE graphs made of NDVI time-series of study areas (in chapter 3.5) that GS ends around mid-October instead of the previously used end of September, thus at least two weeks longer.

The start of the growing season (SOS) is also shifted earlier by weeks as Hamunyela et al. (2013) stated in their research and the satellite SOS estimates derived from NDVI time series of MODIS data and ground observations showed the same results. The change of SOS is not visible on my graphs thus I expanded the time window from 15.4 – 1.10 as it was in TEMRE to 01.04 – 31.10 to have more cloud-free data.

3.3.6. Cloud masking

A perfect Sentinel-2 cloud masking solution does not exist yet, but the QA60 band is suitable for filtering suggested by Google (2020c) developers. Bits 10 and 11 of QA60 refer to clouds and cirrus, where flags should be set to zero indicating clear conditions. Prefiltering is also advised by Google setting *CLOUDY_PIXEL_PERCENTAGE* property with *ee.Filter.lte* function. The percentage was set to less or equal to 5 % in every case except Central Bükk in 2017 where it had to be increased to 20% to have available images, otherwise, a data gap occurred. The combination of a bitmask and a cloudy pixel percentage proved to be a suitable method even in this above-mentioned case.

Another solution is setting cloud probability with which clouds can be mostly removed (Google 2020c). An advanced solution, the Fmask (Function of mask for cloud filtering) 4.0 has been implemented for Sentinel-2 (Qiu et al., 2020) and in GEE too, however, it was not created originally for this satellite, and there is a need to make it available for this type of dataset as well.

3.3.7. Collection reducing

Reduction of the collected dataset (i.e., image collection) is necessary due to the computing limitations of GEE. This method is called *ee.reducer()* creates a single image from several images based on *minimum, maximum, minMax, mean, median*, or *standard deviation*. For forest monitoring, all of them are useful while calculation of spectral indices takes place, especially indices where current values are compared to aggregated long-term values. This image reduction has high importance and often solves capacity problems, which are listed in chapter 5.8. about GEE limitation.

3.3.8. Calculating vegetation indices

Using the reduced images one could calculate VIs like NDVI, NDVI change, Z NDVI, EVI, and NDWI in my case. Some are available as separate bands or with a shortcut function like NDVI with *ee.image.normalized difference() (Code 2)* , other indices (Z NDVI, EVI) have to be created with combinations of mathematical operators (like *add(), subtract() or divide()*) or with *ee.image.expression()* where the formula is described in a variable. *Image.expression()* was used for more complicated formulas such as EVI (Code 3):

```
.normalizedDifference(['B8', 'B4'])
```

Code 2. Computation formula of NDVI with *normalizedDifference()* function.

```
var evi = image.expression(
  '2.5 * ((NIR - RED) / (NIR + 6 * RED - 7.5 * BLUE + 1))', {
    'NIR': image.select('B8'),
    'RED': image.select('B4'),
    'BLUE': image.select('B2') });
```

Code 3. Computation formula of EVI with an *image.expression* function.

3.3.9. Visualization parameters

Proper visualization of maps helps the developer and the users to easily evaluate their content of them. For the VI raster maps, it is typical to use colour palette. In the case of my maps from red to green palette was used where red marks the lowest NDVI values, orange the lower, yellow is the middle ones, while light green stands for higher and dark green for the highest values. These can be set in a variable for maps and referenced by name: palette: ['red', 'orange', 'yellow', 'green', 'dark green']. Satellite image bands can be selected to be visualized such a true colour (red, green, blue – RGB) image too like B4, B3, and B2 in the case of Sentinel-2 referring to real red, green and blue colours (Figure 20). The vector maps also can be coloured like the border of ROI by attributes of line width, filling colour, and transparency.

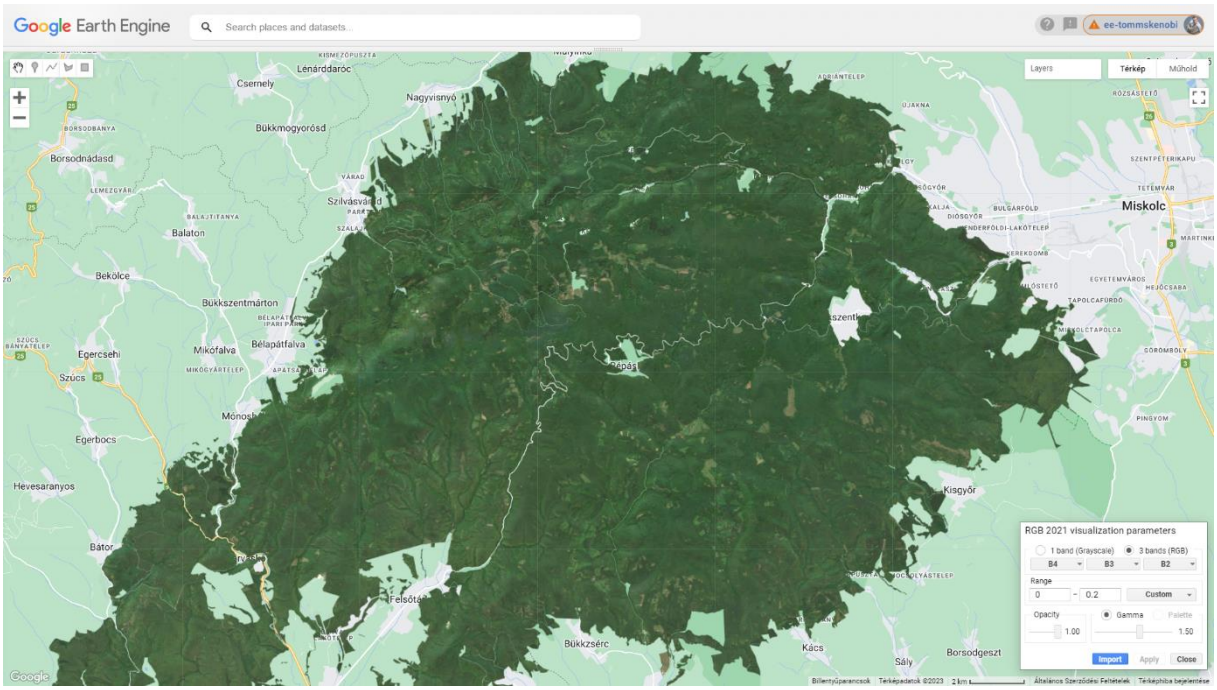

Figure 19. True colour map of Central Bükk in 2021.

Setting the centre of the map is important as well to show and zoom to the ROI, otherwise, by default, it will be the USA. This setting can be done in two ways: by setting longitude, latitude, and zoom level in *Map.setCenter()* function or by zooming to the centre of a given polygon: *Map.centerObject().* I used the latter solution with the forest masks and country borders.

3.3.10. Display

Maps can be displayed in the API below the code editor which makes it easy to check the results for the developers: the RGB, the VI maps, and charts are available in real-time with the command *Map.addLayer()*. While the public version of these maps could meet security issues since by Google App Engine (Google, 2021) it is easy to share and publish a map, on the other hand, it is not possible to do so without sharing the code, which is not desirable from the developers and data owners side. Another disadvantage of App Engine is not being free after the trial.

3.3.11. Image export

To the previously mentioned problem, one solution is exporting the data from GEE. The raster maps can be transferred to Google Drive or cloud storage in TIFF format, the charts in CSV, SVG, and PNG, the polygons in KML and Sh but tables and videos as well for further analysis in any GIS program. The coordinate reference system is WGS84 (EPSG:4326) at default but the Hungarian EOV projection (EPSG: 23700) was used in this Thesis. Limitations also occur here since the large files cannot be exported. For exporting files *Export.image.toDrive()* or *Export.image.to cloud storage()* commands can be used.

3.4. Time-series analysis of sample areas

The detailed time-series analysis of three Sentinel-2 satellite image-covered study areas gave information about the health state of forests in the years between 2017 and 2020. The NDVI values were smoothed with 10 days time window with. flatten*()* function, which converts feature collections into a feature collection based on date. The *S2_CLOUD_PROBABILITY* collection was merged with the S2_SR collection in this section.

The series of analyses aimed to point out forest disturbances (damage, deforestation) and reforestation as well. Each dominant tree species (ten in total) got a dedicated chart, where NDVI data was visualized, with which I managed to discover changes in forest state.

3.5. Machine learning

Machine learning is suitable for tree species classification providing maps which show the spatial distribution of species with high resolution. The Random Forest classifier was tested on a median Sentinel-2 composite of the vegetation season of 2021 to distinguish the main species of Nagyerdő such as Pedunculate oak, black locust, Scots pine, and red oak, plus clearcuts.

The *ee.Classifier.smileRandomForest* function used every S-2 band in the classification and combined it into a single median raster as an input. The sampling approach was based on the manually selected training points on the WorldView RGB image provided by Google and these points were used as training input for tree species classification. Five classes were defined by the 123 points (with geometry imports function) which were based on the tree species dataset of the Hungarian Forestry Database, and the Random Forest classification was completed with the training samples (15 black locust, 22 red oak, 27 Scots pine, 40 pedunculate oak, 19 clearcut) and 100 decision trees. The different tree species layers were also merged into one. The classified map was exported with the *image.toDrive* function to Google Drive and PC.

3.6. Establishing the new monitoring system

The above-mentioned studies pointed out that the 10x10 m resolution is suitable as a base for a new monitoring system since both biotic and abiotic damage was shown on the satellite images. However, the method has a rather large need for computing capacity which could result in exceeding available memory when the Area of Interest is too vast, the image collection is too dense, or the resolution is too fine. The online image analysis with algorithms on cloud platforms is problematic in the case of Bükk which is roughly seven times larger than Farkas-erdő which is also seven times larger than Nagyerdő. Due to this testing of new methods always started with Nagyerdő, and then transferred to other study sites.

3.7. Analysing maps and charts

NDVI charts were created for the period 2017-2020 using different masks based on tree species classes. Five classes were made of a dataset of the Hungarian Forest Database for Nagyerdő according to the dominant tree species: pedunculate oak, black locust, Scots pine, northern red oak, and other species. In the Farkas-erdő the most typical species were:

pedunculate oak, sessile oak, Turkey oak, black locust and Scots pine, while in Central Bükk European beech, sessile oak, Turkey oak, hornbeam and Norway spruce were present.

The different coniferous and deciduous species have typically different NDVI values, they may also differ depending on the site conditions, thus they were analysed separately. Each dominant species got a dedicated curve on the graph. The NDVI values were also exported into a table and further filtered in the form of monthly mean composites. These monthly values were compared to each other with subtraction showing different types of forest damage. When forest damage took place according to the ground-based reports another column was added to the NDVI values with the specific damage type. These tree species and damage-specific values were calculated for all four years and all study areas. In addition, a mean value was added to describe the impact of each damage type, i.e., how severely impacted the NDVI of the forest.

The NDVI values were tested for normality, outliers, and linear trends. Normality was tested with the Shapiro-Wilks test (1965) (8) on 100 randomly selected points from all four Z NDVI rasters of all study areas. This method was described in the original paper of the Z NDVI formula (Peters et al., 2002). The sample points were created with random points in the layer bounds and sample raster values functions of QGIS and analysed in Past 4.11 statistics software (Hammer et al., 2001).

$$W = \frac{(\sum_{i=1}^{n} a_i \, x_{(i)})^2}{(\sum_{i=1}^{n} (x_i - \bar{x})^2} \qquad (8)$$

where a_i is coefficient (Shapiro & Wilks, 1965) and $\overline{x}$ is sample.

The outlier test was made with Grubbs' method (9) (1969) based on the largest absolute deviation from the sample mean in units of the sample standard deviation, according to this formula:

$$G = max|x - u| \,/\, s \qquad (9)$$

where x stands for the actual NDVI value and u and s for sample mean and standard deviation, respectively. The Grubbs-test was performed in Past software which indicated if there were significant outliers from normal distribution. The outliers were removed from the samples.

Linear trend (10) was estimated by this formula:

$$y = mx + b \qquad (10)$$

where x is the independent and y is the dependent variable, while m marks the slope of the line and eventually b does the y-intercept.

3.8. Validation with forest damage reports

3.8.1. National Forest Damage Registration System

The ground-based dataset is from the Hungarian National Forestry database, and the forest protection damage reports of the National Forest Damage Registration System of which description can be found in chapter 2.8.1.1.

3.8.2. Damage thresholds

Thresholds were selected to focus on more severe forest damage; thus, when the damage frequency, ratio and intensity were above 30%, it was classified as damaged, marked with 0, otherwise it got 1. The 30% was based on the distribution of registered damage in the reports, where the majority of damage events could be categorised into two larger groups: the first with slight (1-30%) and the second with severe damage (60-90%). Since remote sensing is not suitable to detect slight damage in every case, the focus was on the more severe ones.

Similarly, when the Z NDVI was below -0.5, it was claimed as damaged, otherwise not. According to these rules, every pixel was reclassified and was given a value of 0 in the case of damage and 1 in the case of no damage. The selection of the -0.5 Z NDVI damage threshold was based on empirical tests, the original scale (<-1 for damage and <-2 for serious damage) used in TEMRE was not suitable for most of the maps made for my Thesis (Somogyi et al., 2018). The reason behind this was the significantly shorter time series (4 years vs 22 years) for calculating mean and std from NDVI and the different resolutions as well (10x10 m vs 250x250 m, S-2 vs MODIS).

3.8.3. Accuracy assessment

Accuracy parameters were calculated based on classified (RS-based) and reference (ground-based) datasets in a confusion matrix. In this matrix every pixel is classified as true positive (where the model correctly predicts the positive class), true negative (where the model correctly predicts the negative class), false positive (model incorrectly predicts the positive class) and false negative (model incorrectly predicts the negative class) (Congalton 2019, 2021).

In the confusion matrix, True Positive (TP) signifies damage by both methods, False Positive (FP) signifies damage shown by the RS method but not ground-based reports, while True Negative (TN) stands for damaged by ground-based reports but no RS, and False Negative (FN) is for undamaged by both methods. In the confusion matrix, the true positive pixels show when the model correctly predicted the positive class (TP), while the true negatives show where the model correctly predicted the negative class (TN). False positive (FP) indicates the cases when the model incorrectly predicts the positive class. The pixel is a false negative (FN) when the model incorrectly predicted the negative class. The elements of the matrix are calculated as:

- P = TP+ FN;
- N = FP + TN;
- Pc = TP+ FP;
- Nc = FN +TN;
- SUM = P + N = Pc +Nc.

The matrix elements are derived as:

- Sensitivity = Probability of true positive P(TP) = TP/P,
- Specificity = Probability of true negative P(TN) = TN/N,
- Precision = Positive predictive value P(TP) = TP/Pc,
- Negative predictive value P(TN) = TN/Nc,
- Total Accuracy = Probability of accurate classification: P(Acc) = (TP + TN)/SUM.

Producer's Accuracy (PA) (or sensitivity) shows how often features on the ground are correctly shown on the classified map, while the User's Accuracy (UA) (or reliability) gives

information about that, how often a class on the map is present on the ground. Eventually, Total Accuracy (TA) is the sum of the true positives plus true negatives divided by the total number of individuals tested (Jensen, 1996).

The accuracy assessment chapter (4.2.) contains the confusion matrices based on these calculations, where all study areas and years are described.

3.9. Country-wide maps

Copernicus tree cover density, dominant leaf type, forest type, and expert product maps are published on the Pan-European level for 2018, based on Sentinel-2 imagery and RF classifier. The tree cover density maps provide information on crown coverage at 10x10m resolution pixel level and 0-100% range (Copernicus, 2022). Filtering was applied on the rasters to keep pixels with at least 75% of forest cover, which was converted to vectors and compared to the forest map made by the Hungarian Forest Database, as reference.

Forest masks had to be simplified due to the limitation of vertexes and distance-based Douglas-Peucker simplifying function of QGIS was used for that with 20 m threshold. The simplified polygons were corrected by fix geometries function, after they were dissolved into a single piece. The unnecessary attributes were deleted, and the shape was converted to WGS 84 which the GEE can handle.

4. Results

In this section, I summarize the results of my PhD based on the analysis of study areas, accuracy assessment, statistics, time-series analysis, comparison, and expansion of methods.

4.1. Analysis of study areas

According to the forest protection damage reports of the NFDRS maps were made for each year and study sites to show ground-based damage. The results are shown on compartment level in chapters 4.1.1-3.

State and change index maps were derived from S-2 composites for each year: 2017 - 2020 and each study area in chapters 4.1.5-7. The actual condition of forests in the given year was described by state index maps, while the change index showed the difference between the

sequential years (2017-2018, 2018-2019, 2019-2020). To show deviation from four years, mean Z NDVI values were calculated utilizing the entire time series, showing greater inter-annual and spatial changes, thus they were analysed in detail.

Analysis of Z NDVI maps showed forest disturbance in several compartments of every study area and year. Negative changes appeared partly due to forest damage, but the most severe disturbances were clearcuts since they followed the borders of forest compartments. On the other hand, positive anomaly was detected as well after the artificial plantings on the area of clearcuts, and the regeneration was visible in the index values.

Natural differences have been observed between the studied years due to meteorological conditions. Several forest compartments were damaged by drought and detected by both methods, resulting in generally lower Z NDVI values all over the forests. However, these differences are less evident in given years, even if that year was drier than the previous, and the whole forest appeared to be in worse condition according to the Z NDVI values. This can be due to the long-lasting effect of drought which is not always visible right after the damage.

4.1.2. Ground-based damage of Nagyerdő

According to the forest protection damage reports of the Hungarian National Forest Damage Registration System in 2017, frost damage occurred in young stands, while in 2018 and 2019, and 2020 (Hirka 2019, 2020) the Nagyerdő suffered from drought, frost, and game damage.

Both geographical and temporal overlapping of different damage types is visible in the Nagyerdő in the case of game, drought, and frost damage as well. This damage occurs mostly in the Northwest and Northeast quarters, but also in the other two quarters in lower numbers (Figure 20). One hundred thirty-one damaged compartments were reported from the 394 total compartments, which means 33% damage.

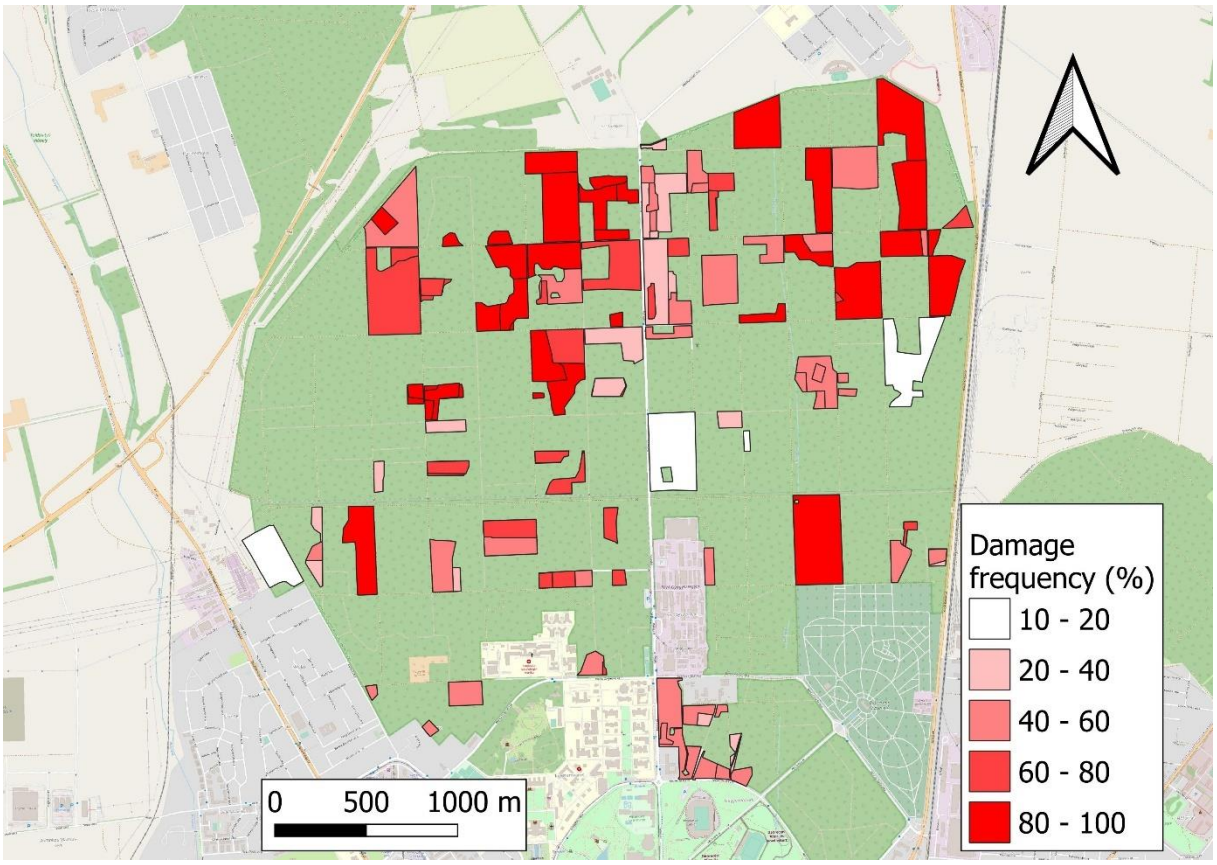

Figure 20. Aggregated damage frequency map of Nagyerdő of Debrecen based on field surveys from 2017 to 2020. Mostly the northern half of the forest shows considerably serious damage, but overall, 33% of the area of Nagyerdő was damaged for at least one year.

4.1.3. Ground-based damage of Farkas-erdő

According to the field data of four studied years (2017-2020), in 2017 frost and game damage occurred, while in 2018 and 2020 drought and game, damage was detected in several forest compartments. In total 277 were damaged of 1068 compartments, thus ~26% (Figure 21).

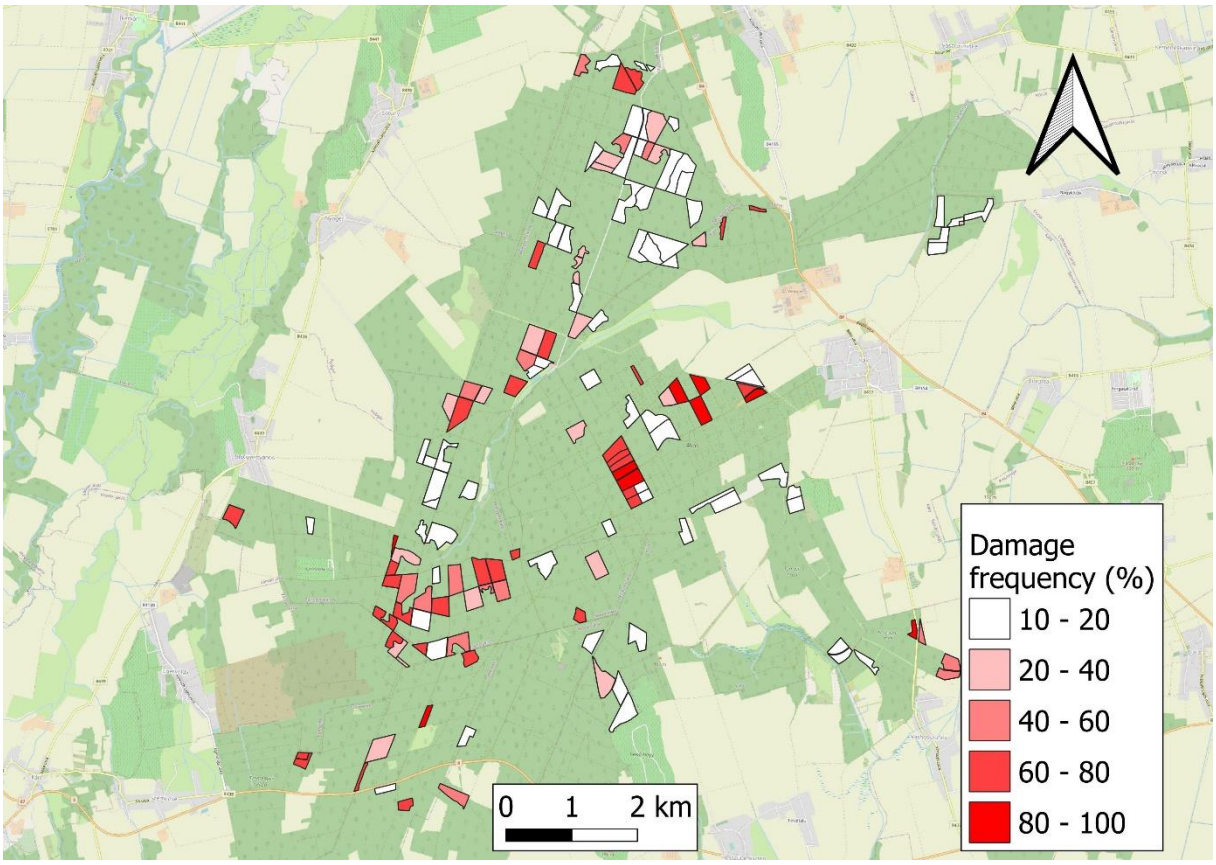

Figure 21. Aggregated damage frequency map of Farkas-erdő based on field surveys from 2017 to 2020. Mostly the central part showed more severe damage, but the northern half also suffered from various disturbances.

4.1.4. Ground-based damage of Central Bükk

According to the NFPDR reports, in 2017 2235 compartments were damaged, while in 2018 it was 573, in 2019 472 and in 2020 646 of the total 7758. The severe windfall and snow break (also some game damage and frost) in 2017 affected 29% of the area of Central Bükk. Even though the 29% seems to be large enough to be easily detected by RS and matched with field reports, the study area is also large (~50000 ha) and managed by two forest companies thus the damage reports came from different sources and the registered damage frequency and intensity varies from 1-100 % all around the mountain. It has to be noted as well that, for instance, Szilvásvárad and Nagyvisnyó is missing from the NFPDR reports and the data gap had to be filled by asking data from the local forestry company (Figure 22).

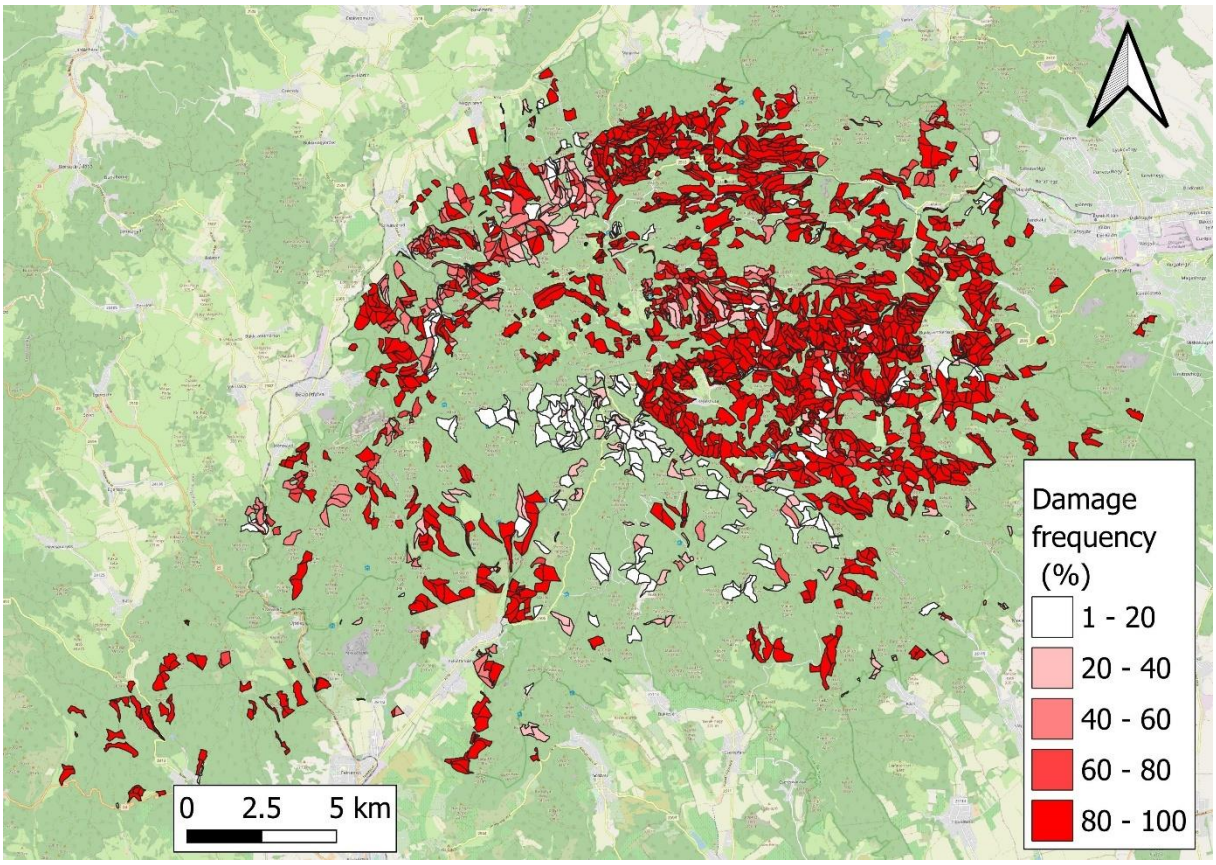

Figure 22. Aggregated damage frequency map of Central Bükk based on field surveys from 2017 to 2020.

4.1.5. Satellite-based damage of Nagyerdő

From the VI composites state and change indices were derived for each year: 2017, 2018, 2019, 2020, and 2021. The state index means the actual state of the forests in the given year and the change index shows the difference between the sequential years (2017-2018, 2018-2019, 2019-2020, 2020-2021), in addition, standardized values were calculated.

Analysis of Z NDVI maps (Figure 23) showed that the composite of the base year 2017 indicated high Z NDVI values but areas with clearcuts and other sparsely vegetated forest compartments. In 2018 general Z NDVI decrement is detected (orange colour) in most of the forest with new red areas, standing for clearcuts following the borders of forest compartments. While in 2019 and 2020 generally positive anomalies is experienced on the maps as a result of artificial plantings after clearcuts and regeneration of less forested areas. Despite the general positive changes, negative ones were also noticed. New clearcuts were made every year, marked with red, and in 2020 the northeast part of the forest started to become orange coloured on the map, thus it changed negatively. The difference between VI

values is also due to different dominant tree species which are visible in 2017 and 2018 in the NW part of the forest.

However, there is no perfect match of ground-based on RS damage, which could be due to natural differences between years in 2017 many forest compartments were damaged which is shown by both methods but 2018 was a dryer year generally where differences are not so evident since the whole forest seemed to be in the worse state according to the Z NDVI values. While 2019 was a better year with more positive values and much fewer damage reports, however, 2020 seemed to be worse again with more reports and lower VI values and a visible phenomenon in quarter NE, which is mostly pedunculate oak-dominated and known for being under heat and drought stress for decades already. Accuracy assessment for damage detection is described in Table 5, in chapter 4.2.

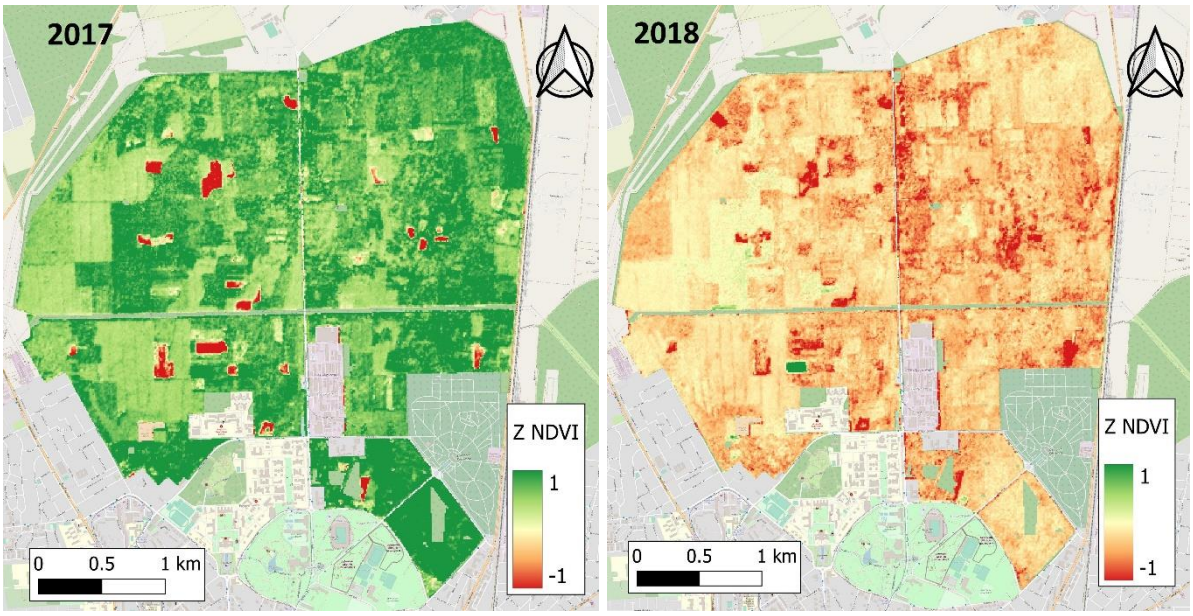

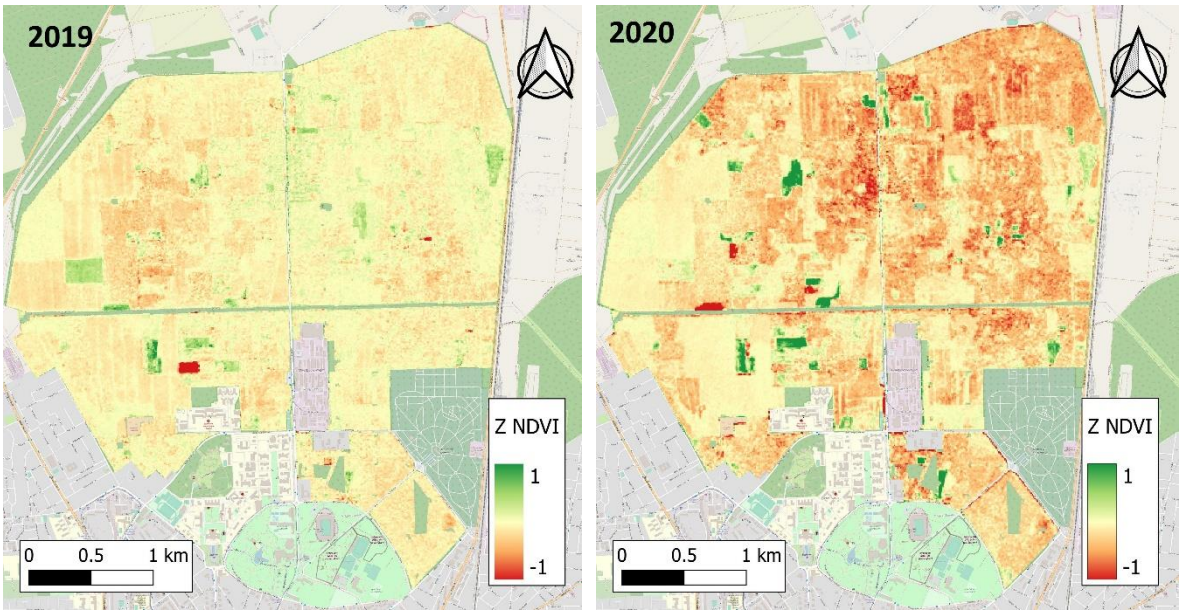

Figure 23. Annual Z NDVI composites of Nagyerdő of Debrecen in 2017 (a), 2018 (b), 2019 (c), and 2020 (d). Clearcuts (with dark red) drought and frost damage (orange or yellow) are visible on every map marking a significant photosynthetic activity drop in the given years compared to the long-term mean. The difference between VI values is also due to different dominant tree species. Regeneration was detected as well with green colours.

Graphs were made from the time series as well, showing the median NDVI values of Nagyerdő between 2017 and 2020 (Figure 24). Deviations from the ideal state of the vegetation period can be detected when the actual values are compared to the ideal NDVI curve. If forest damage takes place, the shape of the NDVI curve will be changed according to the severity of the damage. Drought affected the NDVI curve in 2018, 2019, and 2020, which is visible on the graph in the form of a decline.

A comparison of years was made with charts showing the differences in NDVI curves for each year. Deviations from the normal state are visible every year. In April and May 2017 frost damaged the younglings and in August drought was experienced. Similarly in 2018 and 2019 in June and August, drought was registered. In April, May and June of 2020 frost damage took place again.

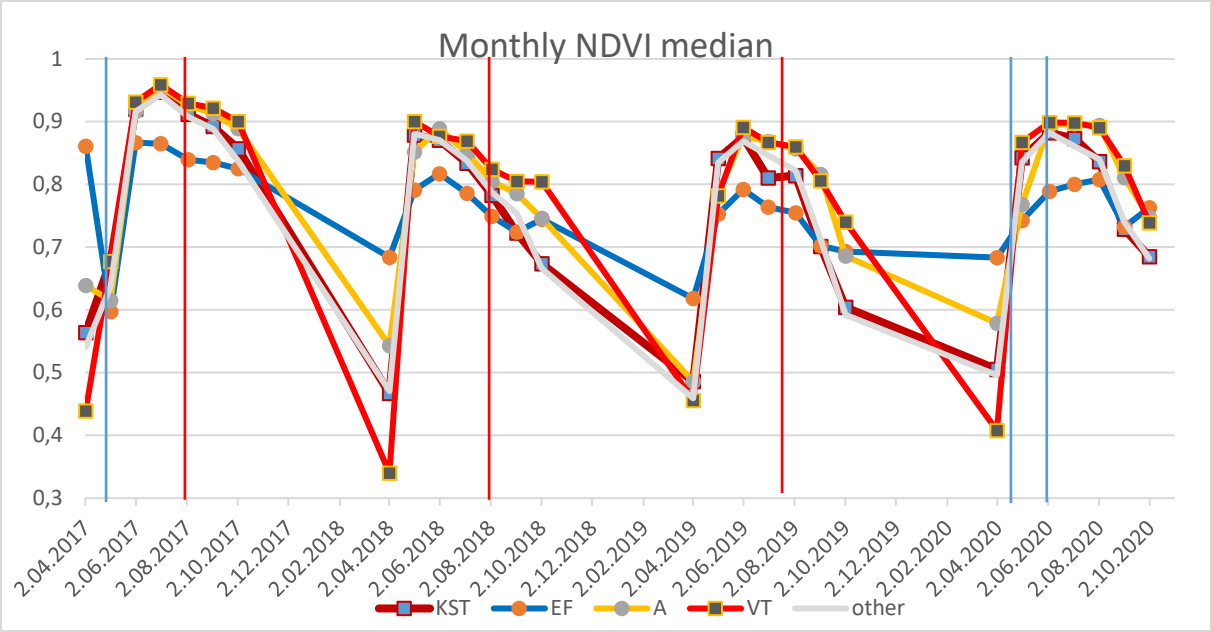

Figure 24. NDVI median chart of dominant tree species of Nagyerdő for 2017-2020. The vertical red lines stand for drought events and the blue ones for a late frost. Legend: KST (pedunculate oak), EF (Scots pine), A (black locust), VT (red oak).

Different tree species were detected both on the VI (Figure 23) and the Random Forest-based classified (Figure 25) maps. Road Pallagi divides the forest into western and eastern halves, while an unnamed road does the same in north and west directions, resulting in four quarters. The presence of black locusts is outstanding in quarter NW, red oak and Scots pine, and black locust in quarter NE compared to more homogenous pedunculate oak-dominated quarters SW and SE (Figure 23). Scots pine and pedunculate oak show significantly higher Z NDVI values (with dark green) compared to the above-mentioned others, however at certain forest compartments, especially in quarter SW, larger orange areas appeared in 2020 probably due to drought stress (Figure 23). Visual comparison of maps of main tree species and SE showed that there is a connection between them, and different species react differently to biotic or abiotic damage resulting in different VI values. I not here that this method aimed to classify the most important and dominant tree species, there are several compartments with secondary, tertiary, or even quaternary mixed species.

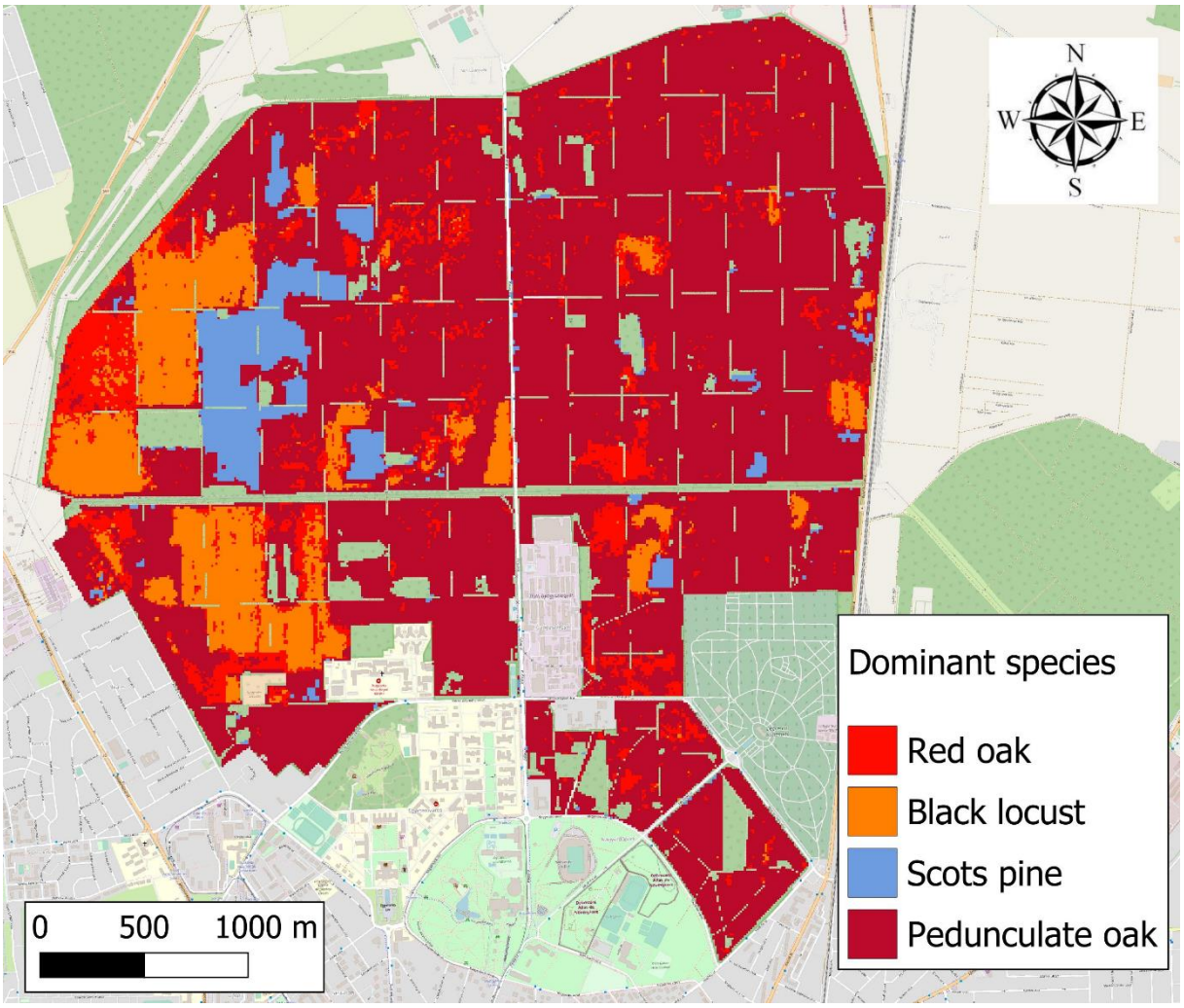

Figure 25. Main tree species of Nagyerdő made with Random forest classification of a Sentinel-2 image from July 2020.

Forest compartments differ in tree species; thus, the different VI values do not mark necessary damage but heterogeneity in species, which was detected both on the RF-based classified and the VI maps. Tree species classification of Nagyerdő by RF-based method showed the dominant presence of pedunculate oak in the western part of the forest while coherent patches of black locust, red oak, and Scots pine were detected in the eastern quarters of the forest (corresponding to forest compartment borders).

The majority-based tree species comparison on forest compartment level indicated 76.1% accuracy in the case of five classes: four dominant tree species and clearcut. In 258 compartments we found agreement on the species from the 339 total. It is worth mentioning that we aimed to classify only the dominant tree species while there are several compartments with secondary, tertiary, quaternary, or even more mixed species, which made

the result less accurate. It is also important to note that there is ongoing tree species change in several compartments due to nature conservation when black locust and Scots pine are exchanged with pedunculate oak. This process resulted in compartment-sized clearcuts and lower classification accuracy. removing the clearcut class and only focusing on forest-covered compartments. Removing clearcuts resulted in 81.79% accuracy instead of 76.1 %.

4.1.6. Satellite-based damage of Farkas-erdő

Composites created for the period 2017-2020 showed interesting results on its own and in comparison. Analysing the median Z NDVI maps (Figure 26) of vegetation periods, it could be stated that in 2017 (Figure 26) inside the administrative boundaries of Nyőgér, Bejcgyertyános, Egervölgy, Hosszúpereszteg, and Káld (central and southern part) several forest compartments were spotted referring to lower photosynthetic activity, marked with orangish-reddish colours, but generally, the majority of the Farkas-erdő was healthy with high Z NDVI values. The damaged forest compartments showed signs of improvement in 2018 (Figure 26) and 2019 (Figure 27) with higher index values (greener colours), however, in 2018 and 2019 the general state worsened which was marked by yellowish-orangish colours. In 2019 Egervölgy and Csipkerek (southern part) forest damage took place again which resulted in a decline in index values. In 2020 it was still visible but with lower intensity, also new damage was observed in Bejcgyertyános (Figure 27).

The severe damage and the logging showed on the map with red colour on every map, which is isolable clearly. However, damage with lower intensity or frequency is harder to detect. In 2018 and 2019 less damage can be shown on satellite images and even regeneration was visible in Bejcgyertyános and Csipkerek.

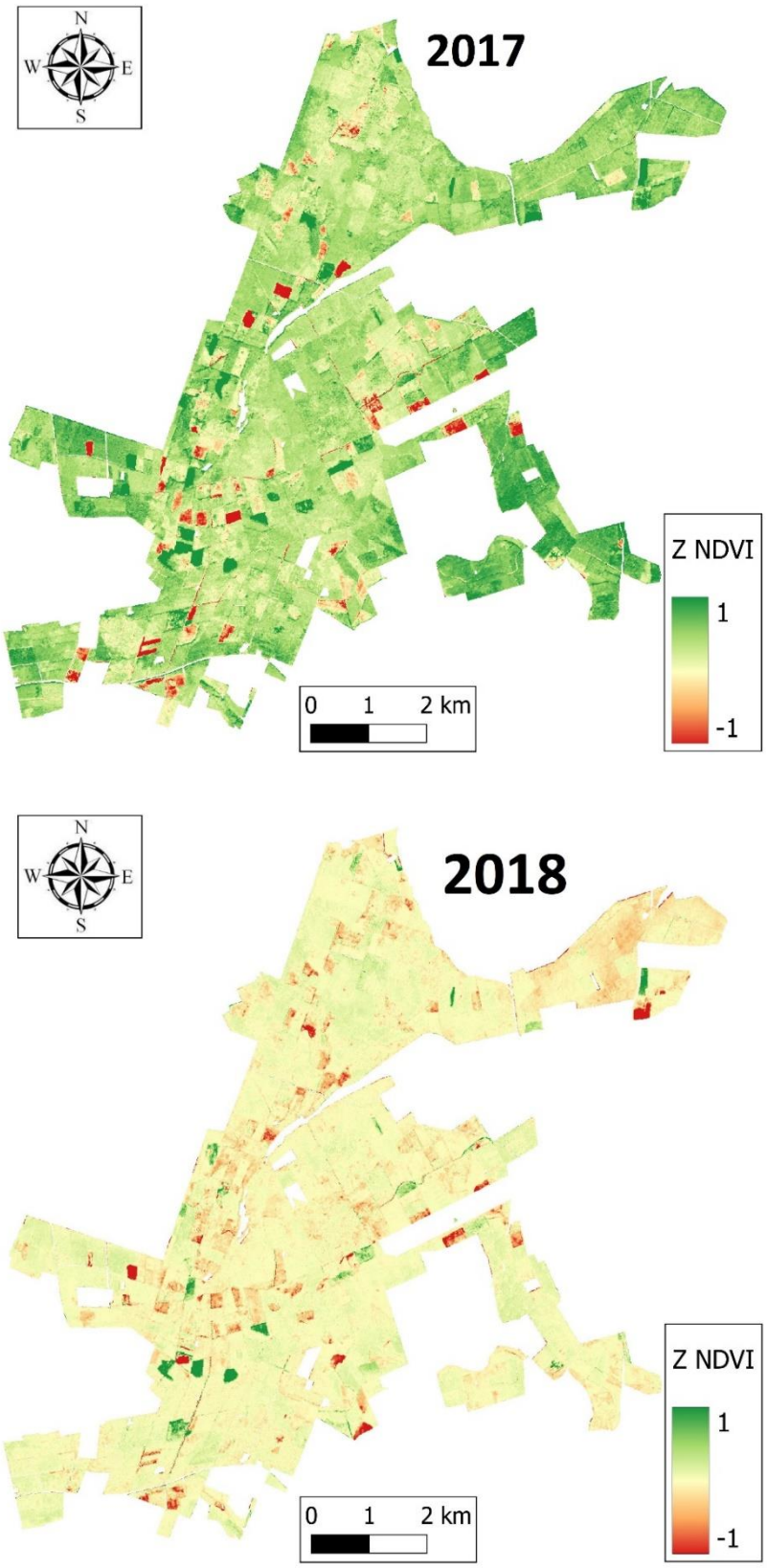

Figure 26. Z NDVI maps of Farkas-erdő of Sárvár in 2017, 2018 in the GEE monitoring system.

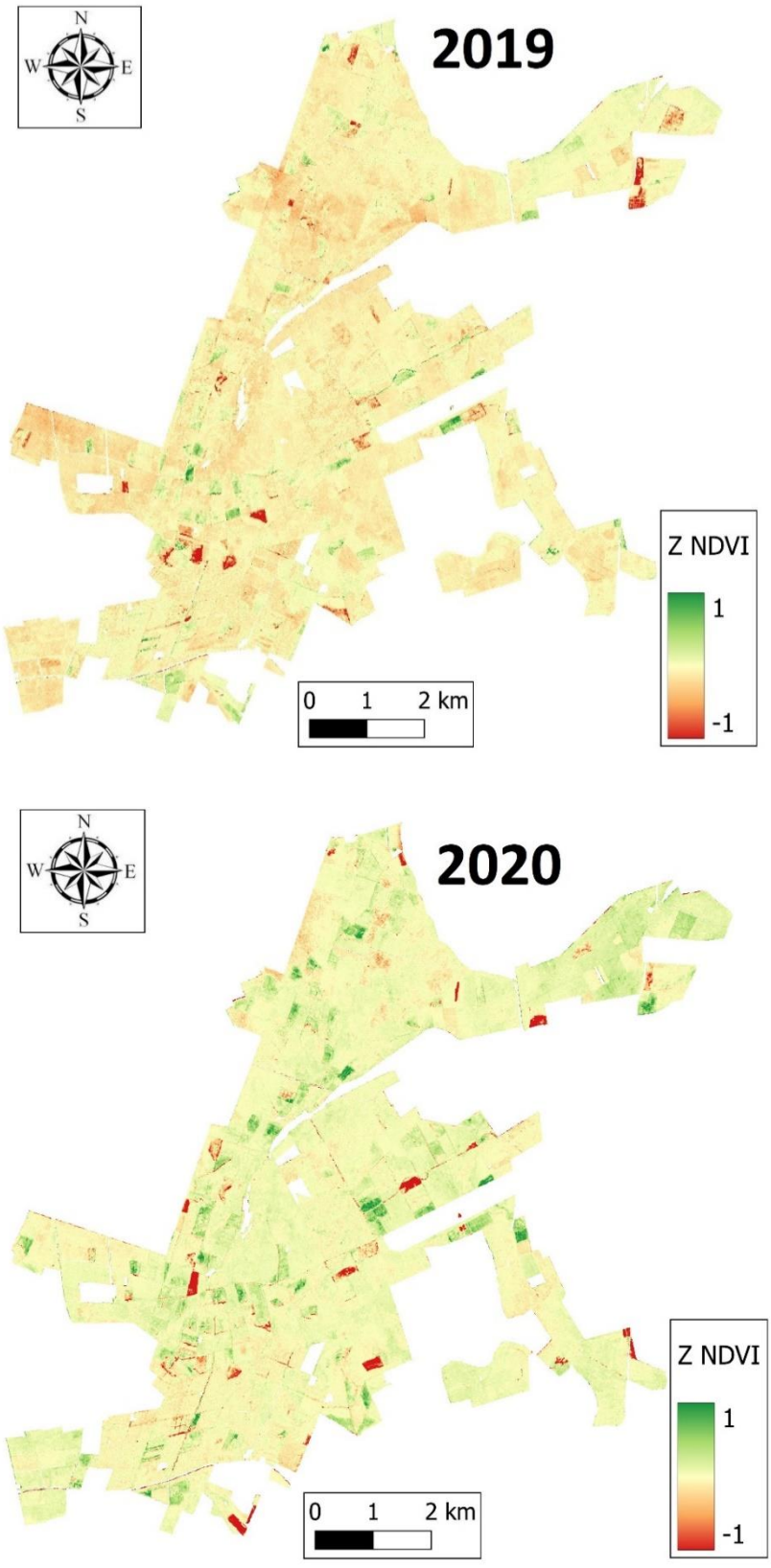

Figure 27. Z NDVI maps of Farkas-erdő of Sárvár in 2019, 2020 in the GEE monitoring system.

The ice break in 2017 and the drought in 2018 affected several forest stands in Bejcgyertyános (central part) which were visible on maps made for 2019 and 2020 as well (indicated with orange colour). In 2020 damage was registered in another five stands (marked with red), although regeneration was visible on previously damaged areas with green colours. Game damage was also reported from Farkas-erdő but it was not directly detectable since the satellites survey the canopy and the damage on the roots or trunks is not visible. Indirectly the foliage also shows the damaging, but it generally takes a longer time.

When the initial state of water content in 2017 was compared to the years 2018 and 2019, general drought was observed in NDWI maps as well, which was followed by a wetter year in 2020. The difference is conspicuous between the tree species as well, the coniferous stands have significantly higher water content compared to oak-hornbeam stands. Thus, the monitoring system is suitable to detect differences between tree species as well.

The high resolution of VI maps made it possible to see changes at the compartment level (Figure 28). For instance, in 2019 the field surveyed damage polygons only partially agree with remotely sensed pixels representing mostly negative changes, although severe damage was shown by both the RS-based and ground-based methods. Good examples of the agreement are Bejcgyertyános 68A and 71A compartments, but clearcut can be seen in Bejcgyertyános 64A, 66C, 67C, and 69B too which have low VI values, however not due to forest damage but to forest cover change. The weak and scattered damage is hardly detectable like in the case of Bejcgyertyános 64B, thus the RS has its limitations for this aim.

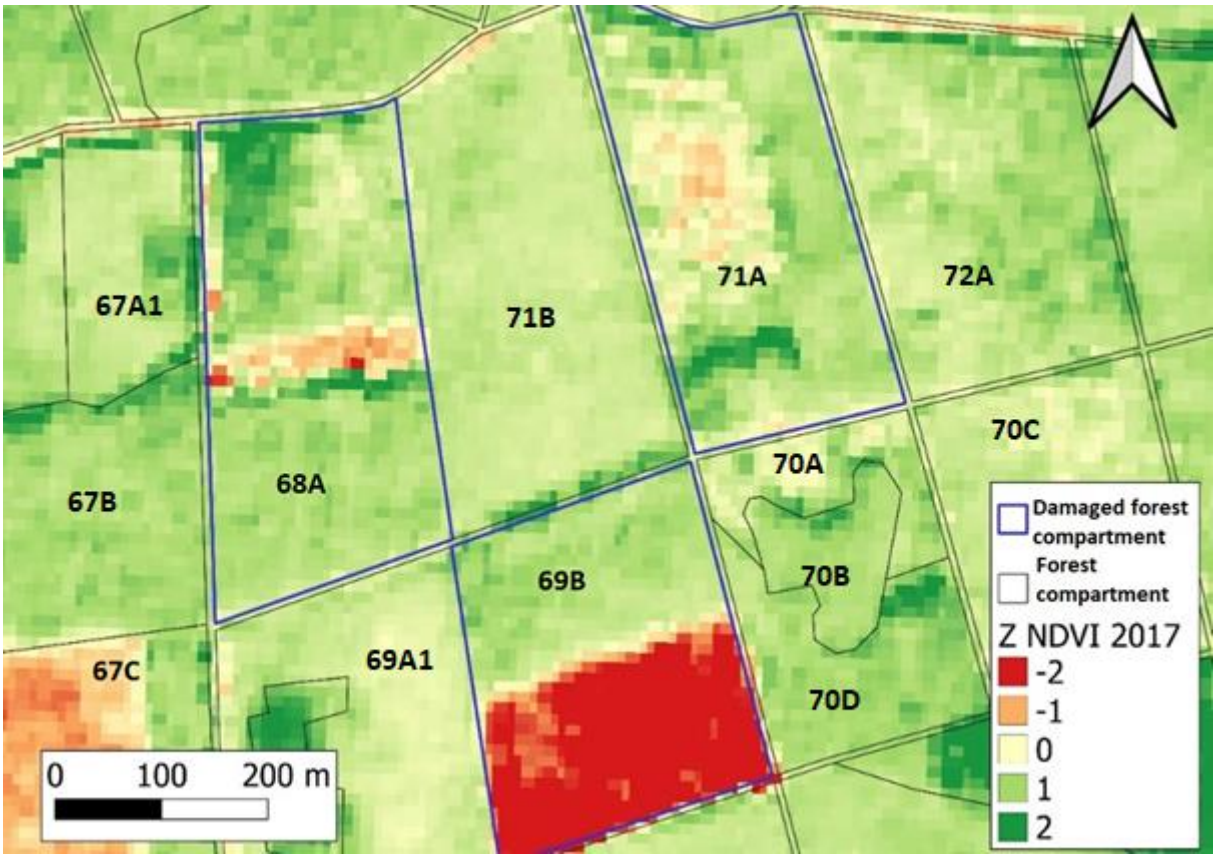

Figure 28. Forest health of Farkas-erdő of Sárvár on Z NDVI map of 2019, where differences are visible on subcompartment level. There is a clearcut in 69B, 67C and forest damage in 68A and 71A.

Charts were created from VI values as part of the detailed analysis based on the time series of 2017-2020 (Figure 29). Drought was registered in August 2017, August and September 2018 and 2019, and July and September 2020. Frost damaged Farkas-erdő in April and May of 2017. The drought in 2018, 2019 and 2020 was detected in the form of NDVI decline which referred to the decline of photosynthetic activity as well. However, the shape of the curve depends also on the number of utilized satellite images, which is to be improved.

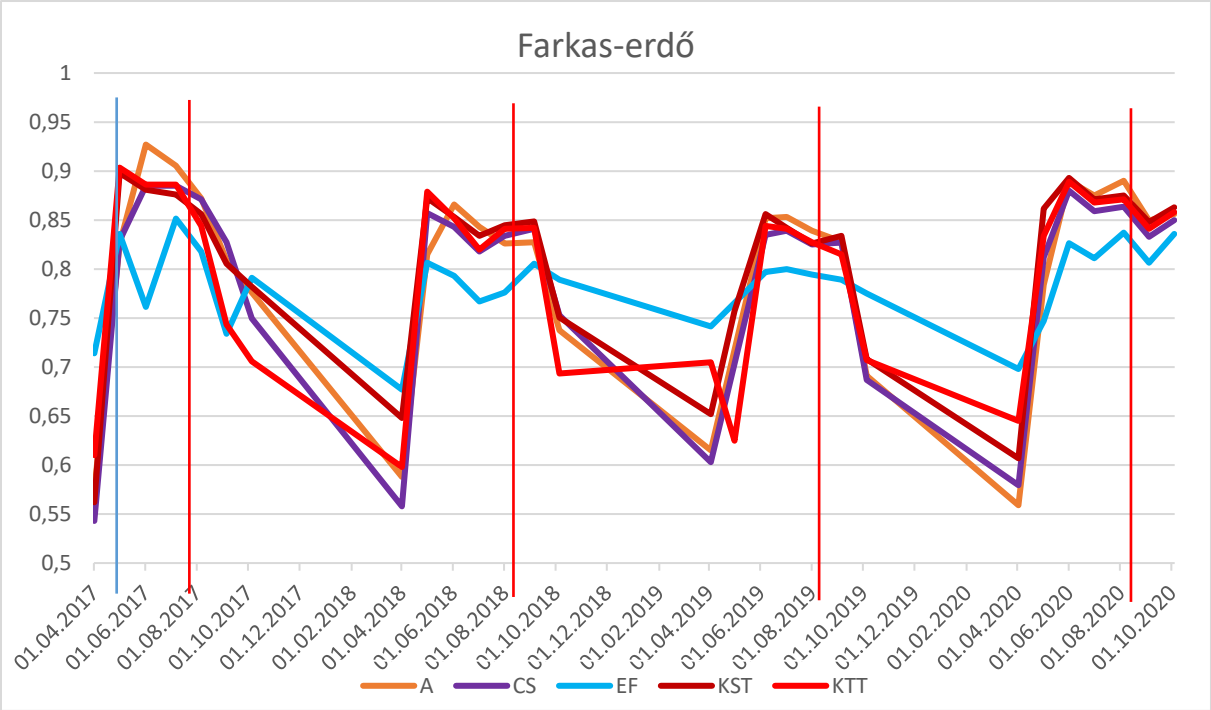

Figure 29. NDVI median graph of Farkas-erdő of Sárvár between 2017 and 2020 in the GEE monitoring system. Frost and droughts are marked with vertical blue and red lines respectively.

These yearly aggregated damage reports were compared to S-2 images, and in 2018 an NDVI break was detected in the curve, referring to a drop in the photosynthetic activity caused probably by the drought. While the curve of year 2019 seemed to be closer to the ideal, in 2020 data gap was visible, thus the cloud filtering algorithms shall be improved to provide more cloud-free observations.

4.1.7. Satellite-based damage of Central Bükk

According to our previous studies made for this area, severe abiotic damage took place in Bükk. The natural disaster in 2017 caused by severe ice and wind damage, was examined on MODIS and S-2 images (Molnár et2019a, 2019b), where 4410 ha of forests were damaged. NDVI, EVI, and Z NDVI were calculated for Bükk Mountains and Machine Learning was applied as well on S-2 imagery with QGIS SCP, where the damaged forest showed out with 87.3% producer and 94.2% user accuracy. While the ground-based damage reports stated 0.5% damage to the study area, the satellites showed more, 1.8-2.2%. Digital Terrain Model was utilized as well to describe site conditions of the study area like elevation, slope, and aspect

based on 10x10 m pixels. It was visible on the -ground-based maps made for 2017, that the windfall and snow break made serious damage.

The most severe damage was caused by snow break and windfall in April 201. In May and June, the same was reported as well as in April 2018 and 2019. While drought affected Bükk in August and September 2017 and 2018, and in September and October in 2019 and 2020. Spruce dieback was registered in September 2018 and June 2019. While different kinds of biotic agents damaged the Bükk, in August 2019 and 2020 presence of spruce bark beetle was reported, while in September 2019 and 2020 oak lace bugs appeared in larger numbers and caused damage. Both insects are keen to attack in waves after drought periods, which can be seen in these cases as well.

By the GEE method, new maps were made for this area (Figure 30, Figure 31) and showed agreement with previous studies, the damage in 2017 was visible on these maps as well, however to a smaller extent and intensity. In the novel GEE method, 0.56 % of the Bükk area was damaged when Z NDVI was < -0.5. It was similar to damage reports but not to our previous studies with different methods, where 1.8-2.2 % damaged area was shown. The differences had several reasons. The resolution is finer than in the case of MODIS and the investigated period is only four years compared to the twenty years, which is important in the calculation of Z NDVI, where the long-term mean is one of the key factors.

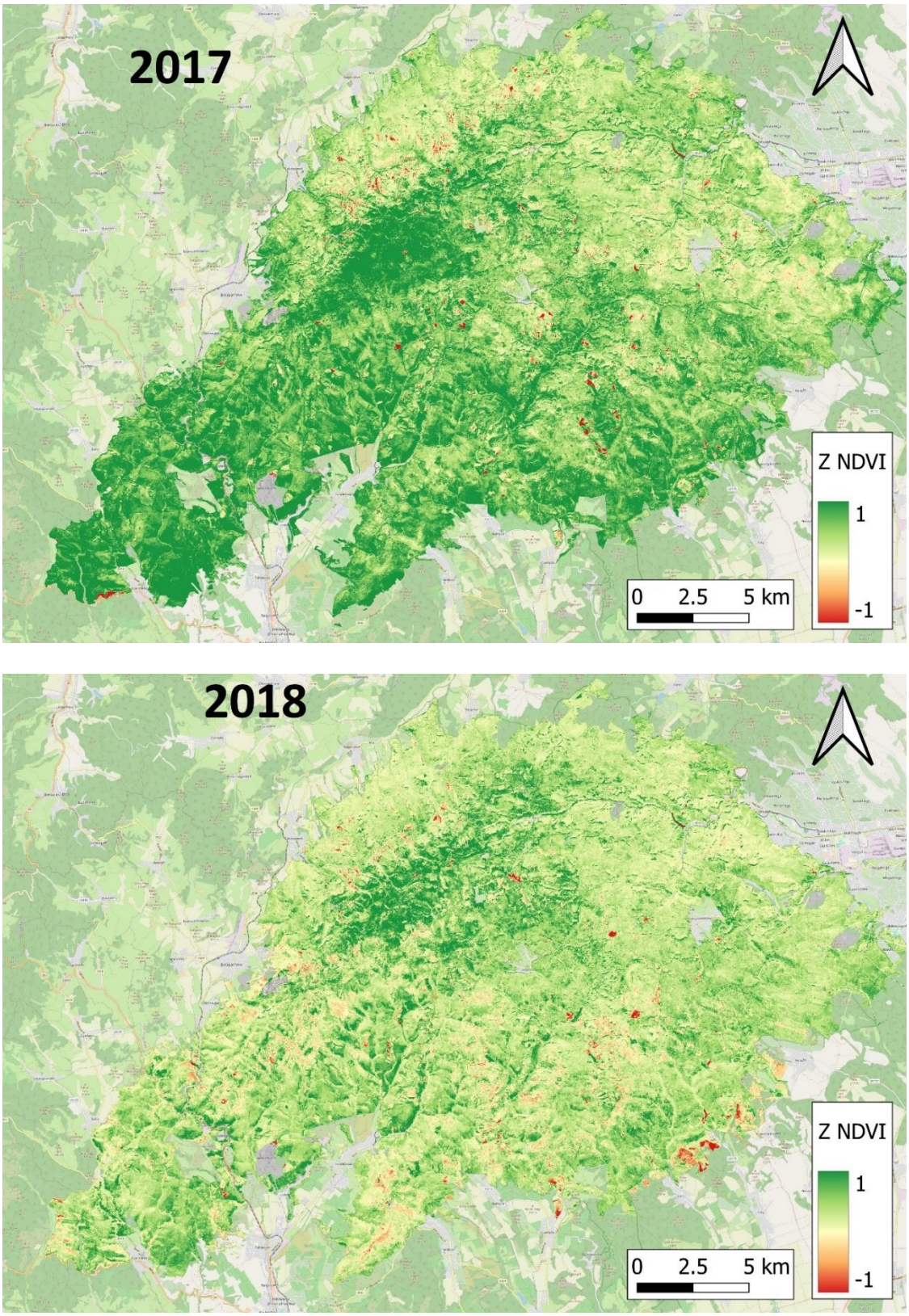

Figure 30. Z NDVI maps of the Bükk Mountains in 2017 and 2018 in the GEE monitoring system.

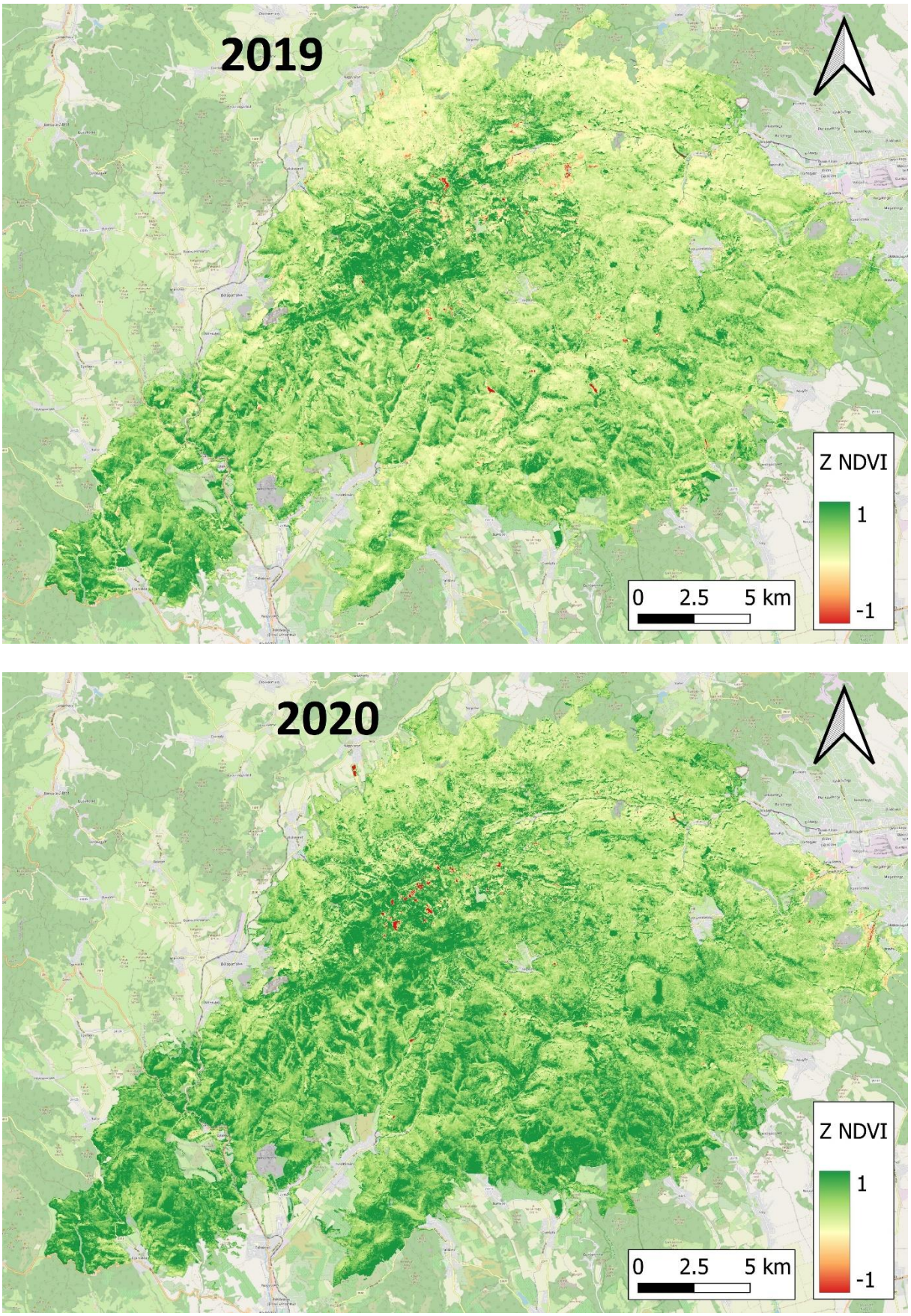

Figure 31. Z NDVI maps of the Bükk Mountains in 2019, and 2020 in the GEE monitoring system.

The most severe damage was caused by snow break and windfall in April 2017 (Figure 32) in the northern part of the mountain, but in May and June, the same was reported as well as in April 2018 and 2019. While drought affected Bükk in August and September 2017 and 2018, and in September and October in 2019 and 2020. Spruce dieback was registered in September 2018 and June 2019. While different kinds of biotic agents damaged the Bükk, in August 2019 and 2020 presence of spruce bark beetle was reported, while in September 2019 and 2020 oak lace bugs appeared in larger numbers and caused damage. Both insects are keen to attack in waves after drought periods, which can be seen in these cases as well (Figure 33).

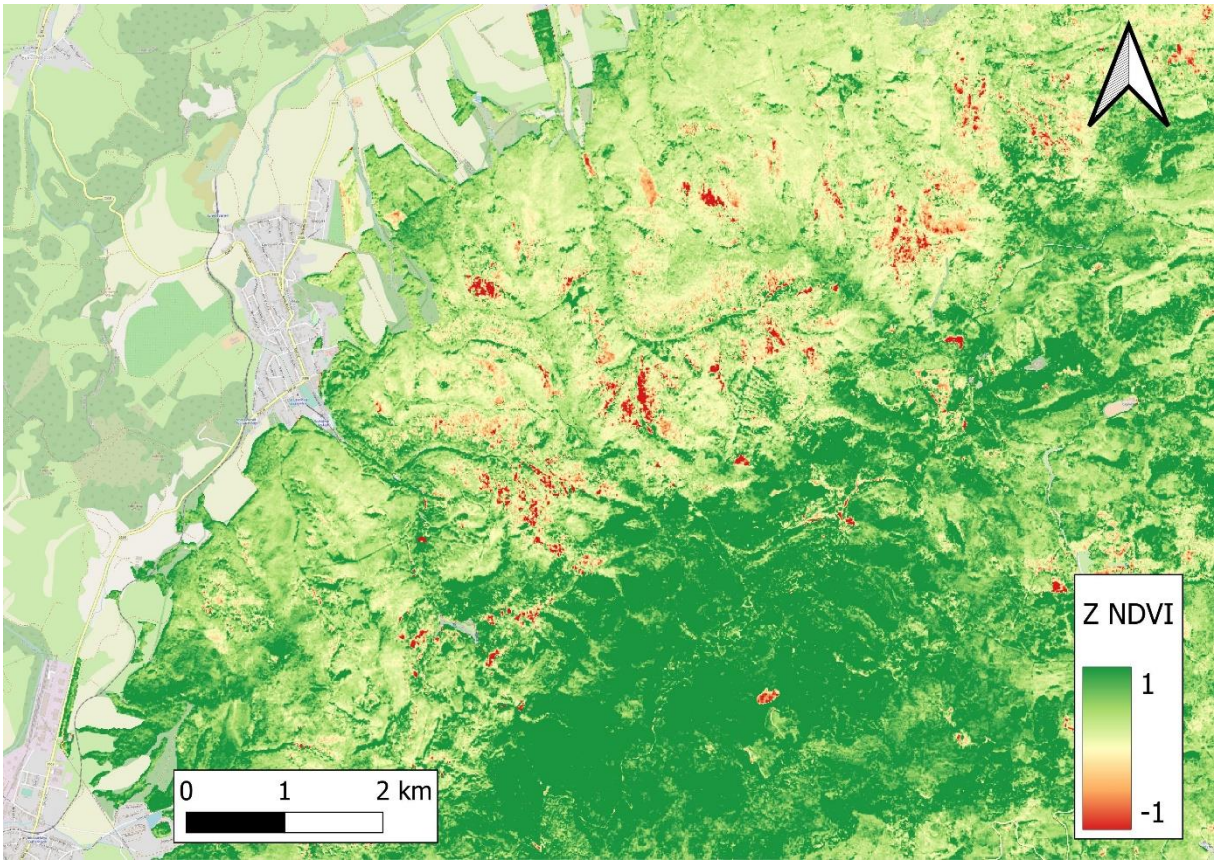

Figure 32. Z NDVI map of northern Bükk where snow break and windfall took place in April 2017.

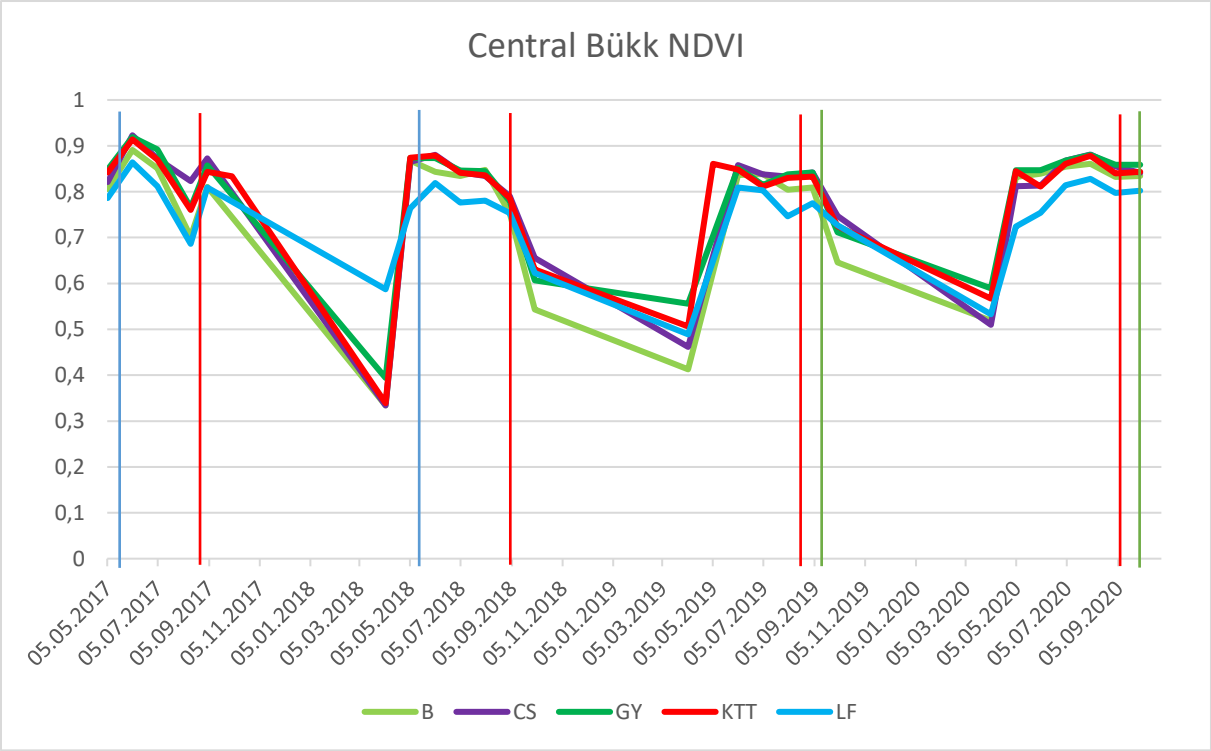

Figure 33. NDVI median graph of Central Bükk showing forest health between 2017 and 2020 tree species like beech (B), Turkey oak (CS), hornbeam (GY), sessile oak (KTT) and Norway spruce (LF). Frost, drought and dieback are marked with vertical blue, red and green lines respectively.

4.2. Accuracy assessment of study areas

Confusion matrices were created for each year to compare classified Z NDVI values to reference ground-based damage reports at the pixel level. Thresholds were selected to focus on severe damage; thus, the damage frequency was > 30% and Z NDVI was < – 0.5. According to these thresholds, every pixel was reclassified and was given a value of 0 in the case of damage and 1 in the case of no damage. User's, Producer's, and Total Accuracy were calculated for all years.

In the confusion matrix, accuracy assessment was calculated based on the classified, RS-based and reference, ground-based datasets, where the RS dataset was compared to damage frequency, intensity, and ratio values as well. The calculations were made for each year and study site and on pixel level.

Nagyerdő (Table 6), Farkas-erdő (Table 7), and Central Bükk (Table 8) all differed from each other, but all study sites' mean total accuracy values showed that frequency has the highest mean TA at 78%, followed by damage ratio with 46% and damage intensity with 30%. Although, the damage frequency-based matrix showed altering accuracy for each year and study area (Table 9). Regarding each study site, Nagyerdő showed 94.3% mean total accuracy in the surveyed four years, while Farkas-erdő did 79.82% and Central Bükk 60.66% (Table 9).

Table 6. Accuracy assessment of Nagyerdő for years 2017-2020 in confusion matrices, given in pixel and ratio (%).

Year		2017						2018			
		Reference						Reference			
		Damaged		Non damaged				Damaged		Non damaged	
		pixel	%	pixel	%			pixel	%	pixel	%
	Damaged	6811	88,71	276	3,59		Damaged	4879	80,34	500	0,00
Classified	Non damaged	554	7,22	37	0,48	Classified	Non damaged	629	10,36	65	0,00
Year		2019						2020			
		Reference						Reference			
		Damaged		Non damaged				Damaged		Non damaged	
		pixel	%	pixel	%			pixel	%	pixel	%
	Damaged	1253	100	0	0		Damaged	7085	92,95	514	6,74
Classified	Non damaged	0	0	0	0	Classified	Non damaged	22	0,29	1	0,01

Table 7. Accuracy assessment of Farkas-erdő for years 2017-2020 in confusion matrices, given in pixel and ratio (%).

Year		2017						2018			
		Reference						Reference			
		Damaged		Non damaged				Damaged		Non damaged	
		pixel	%	pixel	%			pixel	%	pixel	%
	Damaged	3363	6,12	1616	2,94		Damaged	0	0	2579	8,36
Classified	Non damaged	24054	31,81	25887	47,14	Classified	Non damaged	211	0,68	28056	90,96
Year		2019						2020			
		Reference						Reference			
		Damaged		Non damaged				Damaged		Non damaged	
		pixel	%	pixel	%			pixel	%	pixel	%
	Damaged	478	1,57	1490	4,89		Damaged	230	0,95	334	1,38
Classified	Non damaged	3087	9,33	25406	83,41	Classified	Non damaged	2127	8,16	21489	88,87

Table 8. Accuracy assessment of Central Bükk for years 2017-2020 in confusion matrices, given in pixel and ratio (%).

Year		2017				Year		2018			
		Reference						Reference			
		Damaged		Non damaged				Damaged		Non damaged	
		pixel	%	pixel	%			pixel	%	pixel	%
Classified	Damaged	8890	0,91	7722	0,79	Classified	Damaged	1523	0,70	3389	1,57
	Non damaged	360151	36,84	600741	61,46		Non damaged	73661	34,07	137623	63,66
Year		2019				Year		2020			
		Reference						Reference			
		Damaged		Non damaged				Damaged		Non damaged	
		pixel	%	pixel	%			pixel	%	pixel	%
Classified	Damaged	498	0,25	271	0,14	Classified	Damaged	250401	81,48	56483	18,38
	Non damaged	127943	65,24	67413	34,37		Non damaged	409	0,13	40	0,01

Table 9. Accuracy assessment of forest damage datasets for the years 2017-2020 in the three study areas, showing Producer's accuracy (PA), Users' accuracy (UA), Total Accuracy (TA) and mean values based on Z NDVI and field reports.

Year	2017						2018					
Study area	Nagyerdő		Farkas-erdő		Central Bükk		Nagyerdő		Farkas-erdő		Central Bükk	
Damage category	Positive	Negative	Positive	Negative	Positive	Negative	Positive	Negative	Positive	Negative	Positive	Negative
PA (%)	98.94	1.73	13.23	94.12	0.79	99.58	98.35	1.66	0	91.59	2.02	97.60
UA (%)	96.11	6.26	69.39	51.84	53.52	62.22	90.70	9.37	0	99.25	31.01	65.14
TA (%)	95.13		53.51		62.17		89.36		90.97		64.36	
Year	2019						2020					
Study area	Nagyerdő		Farkas-erdő		Central Bükk		Nagyerdő		Farkas-erdő		Central Bükk	
Damage category	Positive	Negative	Positive	Negative	Positive	Negative	Positive	Negative	Positive	Negative	Positive	Negative
PA (%)	100	0	13.31	94.51	0.38	99.60	99.55	0.28	9.99	98.43	99.84	0.07
UA (%)	100	0	24.29	89.17	64.76	34.51	93.24	4.35	40.78	90.99	81.59	8.91
TA (%)	99.86		85.01		34.62		92.85		89.79		81.49	

Table 9. Accuracy assessment of forest damage datasets for the years 2017-2020 in the three study areas, showing mean values of Producer's accuracy (PA), Users' accuracy (UA) and Total Accuracy (TA).

Study area	Nagyerdő		Farkas-erdő		Central Bükk	
Damage category	Positive	Negative	Positive	Negative	Positive	Negative
PA (%)	99.21	0.92	9.13	94.66	25.76	74.21
UA (%)	95.01	4.99	33.61	82.81	57.72	42.69
TA (%)	94.30		79.82		60.66	

4.3. Statistical analysis

I performed the Shapiro-Wilk test for normality on 100 randomly selected points from all four Z NDVI rasters of all study areas. This method was described in the original paper of the Z NDVI formula (Peters et al., 2002). The sample points were created with random points in the layer bounds and sample raster values functions of QGIS and analysed in Past 4.11 statistics software (Hammer et al., 2001).

The analysis of Nagyerdő showed (Table 10), that the distribution was normal ($p<5\%$) in the case of at least 95% of the points in the years 2017, 2018 and 2019 with 0.37, 0.3, and 0.11 p values (Figure 34). In 2020 it was not (0.01) but not due to the outliers (the Grubbs test was performed); the distribution of bins is rather even. The W values were between 0.97 and 0.99.

While in Farkas-erdő (Figure 35) and Central Bükk (Figure 36), the distribution was only normal in 2019 and 2018 with 0.53 and 0.52 p values respectively. The other years did not show normality with $p<5\%$ but again not due to the outliers, and neither the distribution was even. Moreover, at $p <10\%$ significance level four more years had normal distribution (2020 in Nagyerdő, 2017 and 2020 in Farkas-erdő and 2017 in Central Bükk). The W values varied between 0.96 - 0.99.

Table 10. Normality tests of study areas.

Area	Test	2017	2018	2019	2020
Nagyerdő	Z NDVI median	0.84	-0.08	0.15	0.08
	Shapiro-Wilk W	0.99	0.98	0.98	0.97
	p(normal)	0.37	0.3	0.11	0.01
Farkas-erdő	Z NDVI median	0.4	0.03	-0.09	0.05
	Shapiro-Wilk W	0.97	0.96	0.99	0.97
	p(normal)	0.01	0	0.53	0.03
Central Bükk	Z NDVI median	0.25	-0.17	-0.49	0.1
	Shapiro-Wilk W	0.97	0.99	0.93	0.94
	p(normal)	0.04	0.52	0	0

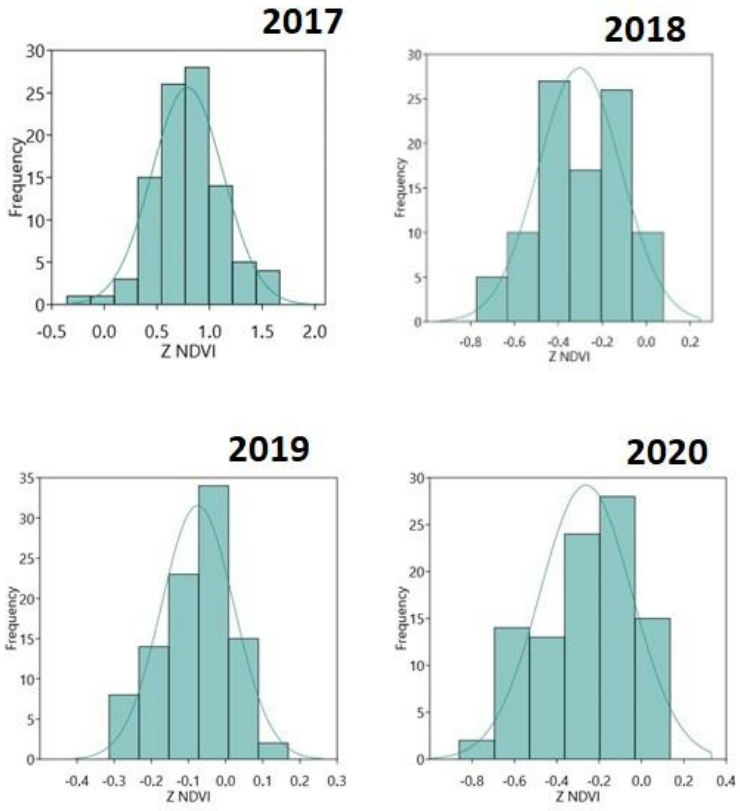

Figure 34. Z NDVI histograms of Nagyerdő in 2017, 2018, 2019 and 2020.

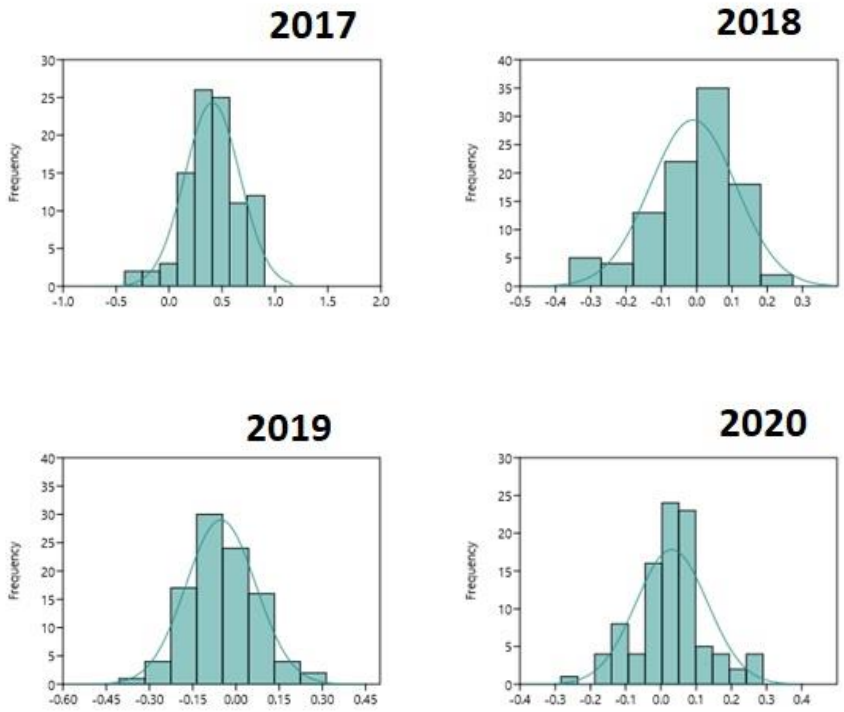

Figure 35. Z NDVI histograms of Farkas-erdő in 2017, 2018, 2019 and 2020.

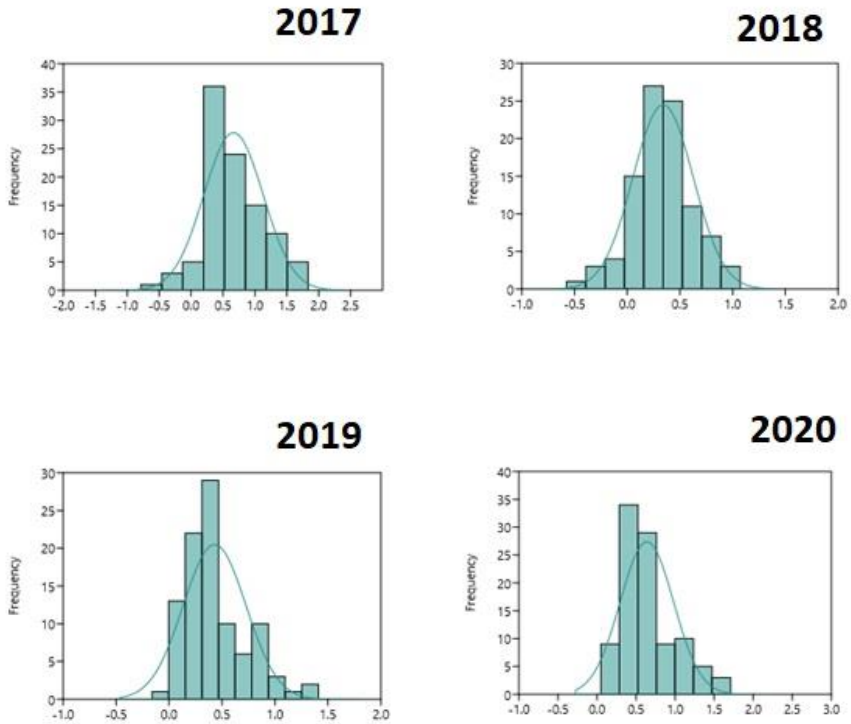

Figure 36. Z NDVI histograms of Central Bükk in 2017, 2018, 2019 and 2020.

4.4. Time-series analysis

Time series were suitable to be analysed in charts as well, thus we used Sentinel-2 imagery to show median NDVI values of study areas between 2017 and 2020. When the actual NDVI values were compared to the ideal NDVI curve of the vegetation period, deviations from the ideal state were detected. When forest damage occurred, the shape of the NDVI curve changed according to the severity of the damage. Most damage types affected the NDVI curve, which is visible on the graph in the form of a decline.

The different abiotic damage types were analysed based on NDVI change, where the difference between monthly, pixel-based median values was calculated for each species (Table 11) and aggregated for all study sites and years. Three of the four most frequent damage types were shown with negative values referring to health declines, such as drought (-0.03), snow break (-0.02) and windfall (-0.06). Late frost always occurred at the start of vegetation season when NDVI increased intensely, thus the positive 0.07 mean value is due to that phenological phase, however in the case of Turkey-oak, Norway spruce and beech negative values were successfully shown.

Table 11. Damage analysis based on NDVI time-series of tree species.

	KST	EF	A	VT	HNY	B	CS	GY	KTT	LF	mean
drought	-0.03	-0.02	-0.03	-0.02	-0.03	-0.04	-0.02	-0.03	-0.03	-0.01	-0.03
frost	0.25	0.03	0.17			-0.02	-0.05	0.01	0.21	-0.03	0.07
snow						-0.02	-0.05	0.01	-0.03	-0.03	-0.02
wind						-0.07		-0.04	-0.06		-0.06

As expected, different species reacted differently to drought, frost, snow and wind. Beech proved to be the least tolerant against windfall and break (-0.07 value) followed by sessile oak (-0.06) also against the wind. Turkey oak suffered mostly from late frost and snow break (both -0.05). Pedunculate oak, black locust and Hungarian poplars were affected mainly by drought (-0.03 for all). The negative impact of drought was observed in the case of red oak, beech, hornbeam, Scots pine and also Norway spruce, to a different extent. Norway spruce was damaged by frost and snow too (-0.03 both). The differences might be considered as not significantly large ones, however, the magnitude of abrupt NDVI changes detected by the

BFAST algorithm in the study of de Jong et al. (2012) showed similar results worldwide (-0.04 – +0.04), between 1982 and 2008.

Compartments also differ in tree species; thus, the different VI values do not mark necessary damage but heterogeneity in species, which was detected both on the RF-based classified and the VI maps. Tree species classification of Nagyerdő by RF-based method showed the dominant presence of pedunculate oak in the western part of the forest while coherent patches of black locust, red oak, and Scots pine were detected in the eastern quarters of the forest (corresponding to forest compartment borders).

The majority-based tree species comparison on forest compartment level indicated 76.1% accuracy in the case of five classes: four dominant tree species and clearcut. In 258 compartments we found agreement on the species from the 339 total. It is worth mentioning that we aimed to classify only the dominant tree species while there are several compartments with secondary, tertiary, quaternary, or even more mixed species, which made the result less accurate. It is also important to note that there is ongoing tree species change in several compartments due to nature conservation when black locust and Scots pine are exchanged with pedunculate oak. This process resulted in compartment-sized clearcuts and lower classification accuracy. Removing the clearcut class and only focusing on forest-covered compartments, resulted in 81.79 % accuracy instead of 76.1 %.

4.5. Comparison to existing maps

The new country-wide maps were compared to already existing forest maps made by the ESA and the Hungarian Ministry of Agriculture. Analysis of reasons for differences is needed to deduce conclusions for the future monitoring system which is the most accurate one.

Ecosystem Map of Hungary (“NÖSZTÉP” in Hungarian) shows the distribution, extent, and frequency of ecosystems on the national level relying on existing thematic databases and remote sensing images (Sentinel-1 and 2) (Agrárminisztérium, 2019).

The difference between maps of Forestry Database, Copernicus forest cover, and Ecosystem map was given in ha and % as well for all three study areas and it showed that Copernicus maps were smaller with 6.54 % in extension while Ecosystem map is also smaller with 10.4 %, when we take mean values of study sites (Table 12).

Table 12. Comparison of forest maps for Hungary.

Study area	Reference (ha)	Copernicus (ha)	NÖSZTÉP (ha)	Difference between ref. and Cop. (ha, %)	Difference between ref. and NÖSZTÉP (ha, %)
Nagyerdő	1027.30	996.04	955.28	31.26 (3.04)	72.02 (7.01)
Farkas-erdő	5664.62	4796.75	4548.48	867.87 (15.32)	1116.14 (19.7)
Central Bükk	49152.11	48530.25	46946.24	621.86 (1.27)	2205.87 (4.49)

The difference was expected since they are all based on different methods and have different formats: the Forestry Database units are polygons, while Copernicus and Ecosystem maps are rasters with 10x10 and 20x20 spatial resolution (Figure 37). Other differences showed up as well on a larger scale, discussed in the next chapter.

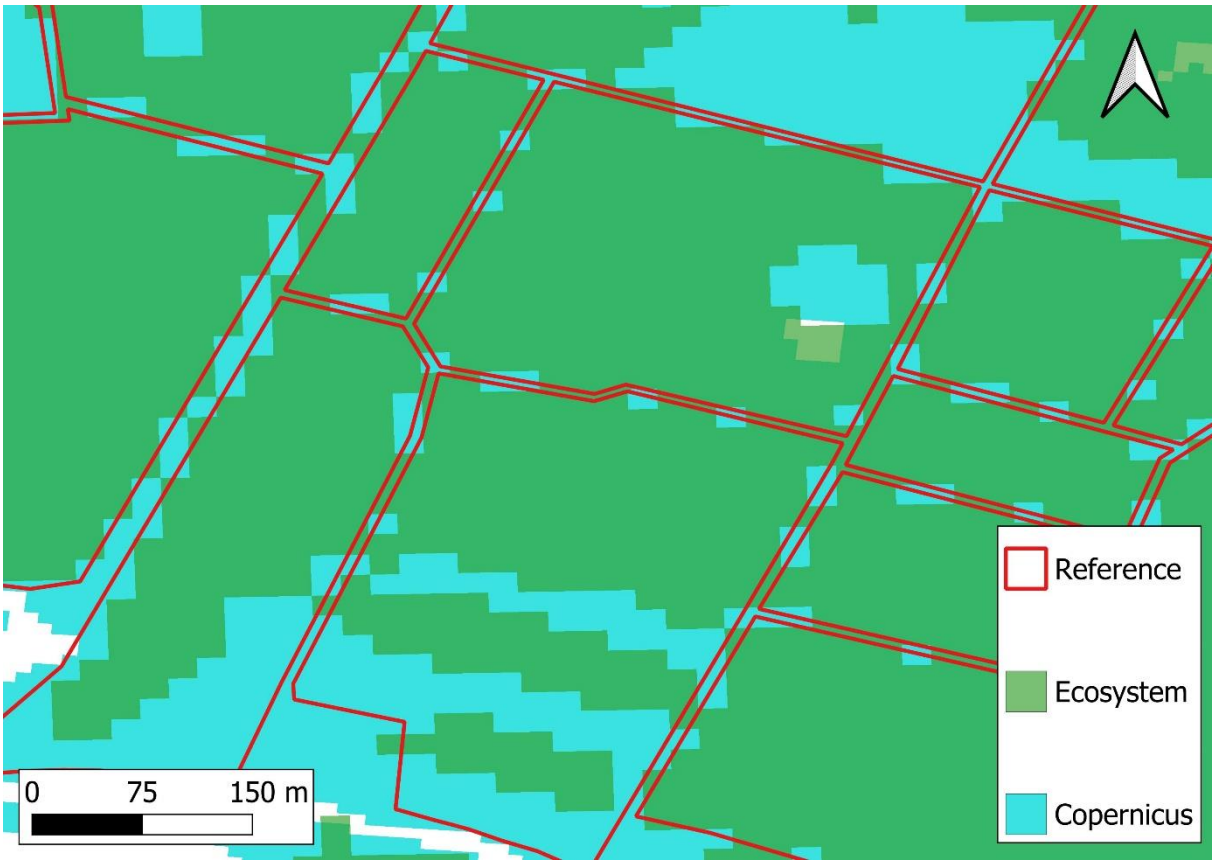

Figure 37. Comparison of three forest maps, the reference, the ecosystem, and the Copernicus in Farkas-erdő. The differences are visible in the extent, borders of compartments and spatial resolution.

4.6. Country-wide expansion

When the forest monitoring algorithms proved to be working for the study sites, it was expanded and tested for the whole of forested Hungary, which is about 2 million hectares. However, modifications had to be done to achieve the expansion. The creation and visualization of maps and index charts cannot be done in the same way described in the methods since too many vertexes are not allowed in the AOI polygons and the imagery has to be resampled to a coarser resolution to be visualized on charts since the number of points in them is limited.

Due to data policy and security publicly available forest masks had to be used, thus the polygons from the Hungarian Forestry Database were replaced with the ESA Copernicus Pan-European forest cover maps. These 10x10 m resolution Tree Cover Density rasters were filtered (above 75% forest cover) and vectorized, finally, the separate tiles were merged into one polygon and uploaded to GEE, and the Z NDVI maps were made on country level (Figure 38). The charts required imagery resampling, in the *ee.chart* function the original 10x10 m resolution was changed to 100x100 for the whole of Hungary (Table 13).

Table 13. Forest maps in Hungary

Map name	Map type	Area [ha]	Area [%]
Forestry Database	10x10 m rasterised	2060819	100
Copernicus (75% Tree Cover Density)	10x10 m raster	2329707	113,05
Ecosystem map of Hungary (trees and bushes)	20x20 m raster	2129733	103,34

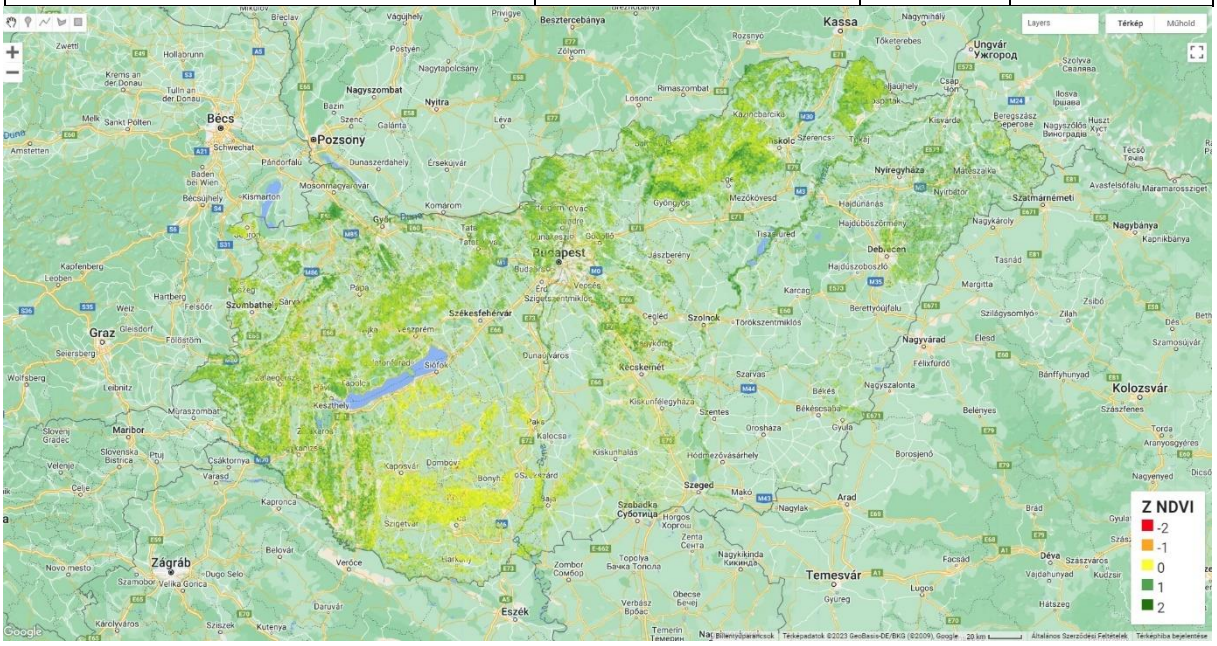

Figure 38. Z NDVI map of Hungary in 2021 made in the GEE.

Copernicus map differed by 13% for the whole country compared to reference but only 1-3% for two study sites, Nagyerdő and Bükk. The Farkas-erdő was out of line compared to the other two site, hence it differed with 15%, which could have different reasons.

The ecosystem map was more similar to reference, on country level it was 3% larger, but on study site level 4-7%, and 19%, where Farkas-erdő was outstanding again.

Reason of differces were that Copernicus is based on RS, which is a significant difference compared to the Forestry Database of Hungary. RS detects which are not part of the Forestry Database of Hungary, also, areas with forest management plans contain non-forested Moreover, clearcuts are detected on the exact year of the RS-based map making, wish are constant forest cover according to the Forestry Database.

Eventually, the definition of forest differs as well in all cases. Tree cover reaches at least 50% or 30% in the case of open forest, the average height is more than two metres, and occupied by a stand which is legally sustainable under these criteria and has an area of 5000 m^2 or an average 20 m width (Jogtár, 2017).

The Copernicus Tree Cover Density raster provides information on the crown coverage per pixel at 10m spatial resolution and ranges from 0% to 100% (Copernicus, 2022) and I filtered forests above 75% of TCD like in TEMRE.

While NÖSZTÉP determinates forest as an area under forest management planning, including all areas classified as forest, including clearcuts. In addition, all areas covered by woody vegetation (e.g woody patches, forest strips, spontaneously afforested areas) belong here (Agrárminisztérium, 2019).

5. Discussion

The forest monitoring approach based on Sentinel-2 imagery was successful, although besides several advantages of GEE, there are some limitations as well. Utilizing the remotely sensed and field-surveyed datasets simultaneously in this monitoring system was possible, also in a semi-automatized way but improvements are needed to fix the problems before running an operational system on a wall-to-wall level.

The comparison was made on study site and country level regarding the forest maps. Different types of satellite data were investigated in order to inspect their suitability for future monitoring. Regarding further expansion, biotic forest damage shall be surveyed as well in the future since in this thesis I focused on abiotic ones.

5.1. Discussion of analysis

The combined dataset of VIs derived from satellite images and ground-based reports was proved to be suitable input for forest damage monitoring made in GEE. Machine Learning was applied also successfully on Sentinel-2 data aiming for tree species classification to support VI maps. The combination of cloud systems and ML shows the distribution of different forest types and forest damage types in all the investigated years.

The availability of ground-based datasets was a great asset and they were compared to RS data, but results indicated problems too. The disadvantage of the ground-based dataset is the large sampling area (several hectares) compared to satellite pixels (100 m^2), resulting in the uneven distribution of data. This different sampling method is visible when scattered pixels are compared to whole forest compartments. To solve this problem, mean or median values could be calculated on a zonal basis from the pixels for the whole compartments, but it would reduce the diversity of VI values significantly which makes it harder to detect any changes in forest health state.

The availability of time series of ground-based data is beneficial, the another problem is the date of ground-based registration since if data is collected after the satellite image acquisition, the overlapping will not be visible on the maps dedicated to showing the same year. The RS could show the damage before the ground survey in time, which could be a useful tool to use before going out to the field. The collection period of the methods differ thus it happened that changes in forest state (damage or logging) were not visible always on the satellite images since they were created after the disturbance event, or it is visible on the satellite image but was not registered in the reports of the same year, only in the following one. However, the finer temporal resolution of satellite imagery is a huge asset in monitoring which can be exploited in EMMRE (chapter 2.8.1.1) in the future to detect early stage disturbances.

5.2. Discussion of accuracy assesment

Accuracy assessment was made on pixel level for all study sites, overally with high accuracy. The problem with the creation of confusion matrices used for accuracy assessment was that while RS data was in raster format and made of pixels, damage reports were originally in vector thus the shape differed and also the resolution since RS pixels hold unique values but the converted ones from reports are homogenous within the compartments. This can be solved by manual field-survey with high-precision GPS devices, even on single tree level, but the goal of this Thesis was not that, but the study site-wide and eventually the country-wide monitoring which does not require that precision. Also, the labour and time demand of this GPS method worth to be considered before doing field survey.

5.3. Time series analysis

Time series were studied to find seasonality in vegetation indices, and I found some seasonality with high reliability, but I found problems as well. The largest problem where the gaps in series caused by clouds. Cloud masking partly helped in that issue, but new datasets should be tested. The great advantage of GEE is flexibility and resilience: with a working method, a new study site can be surveyed easily and rapidly if the new area is also covered by the same RS dataset. However mountainous areas are too often clouded to have dense time series when clouds don't interfere.

5.4. Machine Learning

I applied the ML for tree species classification with 82% Total Accuracy. But when I studied the literature of forest degradation and species distribution which was studied using GEE based on S-2 and Landsat imagery, different accuracies appeared. A study made in Georgia by Chen et al. (2021a) found the UA of the forest degradation class was 69%, while PA was 83%. We found in the literature that in Latvian study site higher TA values were achieved (92-94% TA) by Siņica- Siņavskis et al. (2020) using S-2 imagery and K-means clustering and DynLand methods on Scots pine, Norway spruce, silver birch, and black alder (*Alnus glutinosa*). In Italy Puletti et al. (2017) obtained 86.2% TA with the RF method on four mixed forest types, emphasizing that the collection of multitemporal images at different phenological periods is required. Based on these studies, it is evident that multi-temporal imagery provided better

results than single images. Similar results (88.2% TA) were reported by Persson et al. (2018) after the classification of pedunculate oak, Scots pine, silver birch (*Betula pendula*), dunkeld larch (*Larix × marschlinsii*), and Norway spruce in Sweden with RF on multi-temporal S-2 imagery. Also in Sweden, 87% TA was obtained for the same species (Axelsson et al., 2021) with the Bayesian inference method using S-2 images. These are also similar to my results, 82% accuracy of species classification.

4.2. Comparison to existing maps

The new country-wide maps were compared to already existing forest maps made by the ESA and the Hungarian Ministry of Agriculture. Analysis of reasons for differences is needed to deduce conclusions for the future monitoring system which is the most accurate one.

Ecosystem Map of Hungary ("NÖSZTÉP" in Hungarian) shows the distribution, extent, and frequency of ecosystems on the national level relying on existing thematic databases and remote sensing images (Sentinel-1 and 2) (Agrárminisztérium, 2019).

The difference between maps of Forestry Database, Copernicus forest cover, and Ecosystem map was given in ha and % as well for all three study areas and it showed that Copernicus maps were smaller with 6.54 % in extension while Ecosystem map is also smaller with 10.4 %, when we take mean values of study sites (Table 12).

The difference was expected since they are all based on different methods and have different formats: the Forestry Database units are polygons, while Copernicus and Ecosystem maps are rasters with 10x10 and 20x20 spatial resolution (Figure 35). The year of creation also differed, since the FD was updated in 2016, the Copernicus in 2018, and the Ecosystem was based on data from 2015. Other differences showed up as well on a larger scale, discussed in the next chapter.

5.5. Expansion to other satellite data

The expansion of possible with both freely available and paid datasets. Landsats, MODIS and Sentinel-3 is for free but Planetscope is not, however it offer multisprectral imagery with higher resolution.

5.5.1. Landsat

Landsat data can provide longer times series compared to S-2 but in lower spatial resolution. For the Landsat-based analysis I used the USGS Landsat 8 Level 2, Collection 2, Tier 1 collection in the same way as S-2 except the different bands. For the calculation of NDVI bands B4 and B5 were used, for cloud maskingg the QA_PIXEL bands' 1,2,3,4 and 5 bits, where 0 refers cloud free value. The investigated period prolonged compared to S-2 and eight years were surveyed from 2013 to 2020. In this period the winter months were also excluded and a 30 days time window was applied to flatten the collection with mean values. In addition to the future application, the Landsat 9 was launched in 2021 and the data is available since October.

The Harmonized Landsat and Sentinel dataset (HLS) could be ideal for monitoring, since it covers the Earth's mainland in 2-3 days (USGS, 2022) which is a significant improvement compared to either Landsat or Sentinel alone, even if resolution is moderate 30x30 m.

5.5.2. MODIS

MODIS data is available since 2000 by Terra, and 2002 by Aqua satellites in moderate resolution. The preprocessed long-term datasets are ideal for monitoring since they can be used easily. The MOD13Q1 product contains NDVI already and cloud masking as well for 16 days periods. It was filtered for the vegetation periods from 2000 to 2020, thus it is the longest, 20-year long time-series, I used in this study. Due to this parameter MODIS has been popular among scientists who worked on time-series and forest monitoring systems. Kern et al. (2017) used for finding extreme events in vegetation condition in long term, while we used it for determining forest damage extent after a certain event in Hungary (Molnár et al., 2019a), and built a whole monitoring system on it (Somogyi et al., 2018) to have constantly updated geodatabase about Hungary. While in the USA (USDA 2020), or in Germany (Buras et al., 2020) other similar systems operate using MODIS data. But since its lifespan ended in 2022 it shall be replaced with other satellites like Sentinel-3 or Suomi NPP.

5.5.3. Sentinel-3

The Sentinel-3 A and B twin satellites are equipped with five instruments to measure sea-surface topography, temperature, and colour used for environmental and climate monitoring (ESA, 2020d). Sentinel-3A was launched in 2016 and Sentinel-3B in 2018. For forest

monitoring the Ocean and Land Colour Instrument (OLCI) is the most suitable with a 1270 km swath, 300x300 m spatial resolution in 21 bands with 1-2 days revisit time. In the new version of the TEMRE, this dataset is used to replace the former the MODIS.

5.6. GEE limitations

The GEE is a powerful geospatial tool to process and visualize data, with multpy functions and development possibilities, it has no unlimited capacities. In order to serve more clients at the same time the GEE has certain computing limitations and exceeding them results in errors. It is possible to avoid them with higher programming skills to a certain extent, but on nationwide level, the problems occur in high numbers and some functions and datasets cannot be applied to larger areas. The most frequent problems during my PhD work were the following ones:

- **Geometry has too many edges**: only 2 000000 edges are allowed thus large polygons need to be simplified with edge reduction before uploading them to GEE. GIS programs like QGIS or ArcGIS are capable of that. However, from a forestry point of view, the reduction results in less accurate forest masks for instance.
- **Geometry has too many vertices**: above the limit of 1 000000. Simplification and dissolution are needed before uploading.
- **Too many pixels in the region**: only 1 0000000 is allowed which can be exceeded by setting the *maxPixels* or the scale to a higher value or setting *bestEffort* to true which recomputes the scale of not to exceed the *maxPixels* limit.
- **Computation time out**: quota restrictions exist to ensure the availability of computing resources for the entire Earth Engine community and when too many rasters are loaded simultaneously or there are too many mathematical operations with several layers, the GEE stops the calculation since the algorithm can't be scaled. It can be solved by loading only a few maps at the same time and trying to use combined functions for computing such as *.normalizedDifference* for NDVI instead of calculation with separate subtraction, summation, and division of bands.
- **User memory limit exceeded**: when too long time series or large arrays are used, or unnecessary data conversion takes place the computation does not fit the given memory limits. This error can be solved by setting a narrower time window to reduce memory usage.

- **Downloading data**: too large datasets to be exported result in either computation time out or user memory limit exceeding. It can be solved with the above-mentioned methods or with further reducer application on the dataset before exporting.

Besides certain computation errors there were other issues with the cloud filtering, the validation of RS data, the time shift, the practical use of the novel system and the data security. These are all discussed here with methods to be tested in the future.

- **Cloud filtering**: a perfect could filtering method does not exist for Sentinel-2. The high cloud cover caused gaps in the dataset, especially in spring and early summer. In the vegetation period April, May, and June are particularly important marking the start of the growing season with increasing photosynthetic activity. This phenological stage has valuable health information about forests and the forest type classification is more accurate if these months are included, according to Persson et al. (2018) and Axelsson et al. (2021). In addition, more advanced cloud filtering algorithms could be applied to datasets like Cloud Probability, s2cloudless, or Fmask (Tarrio et al., 2020). Barton (2021) developed a specified forest cloud filtering where sen2core had problems.
- **Validation**: Due to the different scales of RS and ground-based datasets the validation could be problematical. The large sampling area (several hectares and/or whole forest compartments) is certainly a disadvantage of the ground-based dataset when compared to fine-resolution satellite pixels (10x10 m), which causes uneven data distribution. When we compared scattered pixels to whole forest compartments, it often caused a matching problem. To solve it, pixels were transformed into polygons, namely zonal statistics were calculated from the pixels for the compartments based on mean or median values. This method helped to compare the datasets having the same scale but reduced the diversity of pixel values within the compartment and made it harder to detect changes in the forest health state.
- **Timeshift**: The date of the ground-based registration is another problem. The field data is collected throughout the year but published next year after summarizing the whole year's dataset thus time shift is always present. Also, the exact date of satellite image acquisition does not match the ground survey and the overlap will not be visible on the maps dedicated to showing the same forest damage in the same period. RS could be a useful tool to survey the damaged area before going out into the field since it

could show the damage before it's visible on the ground, however, drought effects can appear in the coming year rather than the given year; thus, it is not always completely evident which datasets should be compared to each other.

- **Practical use**: the compartment-based comparison method would be suitable for practical use since the rescaled VI maps and forest protection reports of the Forestry Database are similar in scale and can be used by forest managers. The RS could reduce the workload both of researchers and practical foresters since RS offers an alternative to repetitive fieldwork triggered by each new survey or research.
- **Uploading protected data**: if the dataset is transformed before uploading into GEE the decompilation will not be possible, thus it's a way to keep it safe. For instance, forest polygons were simplified, and the attributes were reduced to the necessary ID columns or transformed into rasters with the reclassification of vector attribute values of forest damage.
- **Public version**: making the system public is not recently possible in Google Apps without sharing the code since the web browser's network traffic can be accessed. This is due to Google's policy of sharing valuable research results and making methods easily reproducible, but it is certainly a drawback when one cope with private data and is not allowed to share.

5.7. Expansion with biotic damage

Due to the limited amount of time and capacity, in this Thesis I focused on surveying abiotic forest damage but since biotic ones have more and more significant importance nowadays it would be desirable to try the GEE-based method on these damage types as well.

Several studies were made identifying bark beetle damage with different datasets. I surveyed the Sopron mountains in Western Hungary, which was affected by bark beetle since 2017, which was the latest gradation. The Sentinel-2 satellite images were created using Mosaic Hub, Anaconda, and Jupyter Notebook web-based computing environments for the period 2017-2020 (Molnár & Király, 2022a). Biotic forest damage was detected by vegetation (NDVI) and moisture (Moisture Stress Index - MSI, NDWI) indices derived from S-2 images. The spatial and temporal change of damage was observed in the image series, resulting in information about the level of degradation and regeneration. 84 affected forest

compartments were surveyed, which showed degradation in the index mean values (MSI = - 0.14, NDWI = - 0.2, NDVI= - 0.19) almost in every studied forest compartment when years were compared to each other. The remote sensing-based survey was validated with the forest database of the Hungarian National Land Centre and the forest protection damage reports of the Hungarian National Forest Damage Registration System.

Another possible application of this RS-based method could be the expansion of the survey for the whole of Hungary to check the damage caused by a relatively new invasive species, the oak lace bug. According to Paulin et al. (2020), this new biotic agent is present all around the country posing multiple threats to oak ecosystems, which gives one-third of Hungarian forests. The problem is even more severe in southern Hungary and in Croatia for example and RS was successfully applied to investigate the impacts in both countries by Kern et al. (2021).

Since the drought has been an increasing problem both worldwide and in Hungary and the invasion of insect species is often triggered by drought, it would be interesting to apply climatic and meteorological datasets (precipitation, temperature, soil moisture) in the studies, which could be compared to VI values to show correspondence between them, as Birinyi et al. (2021) suggested with corn yield comparison to NDVI and EVI in Hungary with GEE.

5.8. Expansion with machine learning

Aiming to improve research efficiency, I wish to involve more ML methods into my future works. Since in this Thesis, I solely applied Random Forest, with satisfying results but yet it can be improved, and I see two ways of achieving it.

The first would be a more advanced way of determining Z NDVI damage thresholds by ML. Instead of the recent, empirical threshold, dynamic threshold based on the VI histogram of each year could be used. Based on the histogram, the VI values could be divided into quantiles or percentiles, standing for the intensity of VI change.

The second way would concern testing other ML methods, for instance, pixel-based algorithms like Minimum Distance Estimation, Support-Vector Machine, Gradient Boost Regression, Naïve Bayes, or object-based methods like K-means, X-means, Cobweb or Learning Vector Quantization, which is a case of the neural network and used in the latest and highest end developed technique, Deep Learning.

6. Conclusions

To conclude my PhD thesis, I briefly report the results in connection with the research goals, plans, hypotheses, and questions I stated in the introduction.

At the beginning of my PhD, the first and second questions and hypothesis were if it is possible to monitor forest health in Hungary based on high-resolution satellite images. I successfully achieved to have Sentinel-2-based annual composites for all study areas (Nagyerdő, Farkas-erdő, Central Bükk) and years (2017-2020). Even the wall-to-wall expansion worked, which could be a great asset in future monitoring.

In the third hypothesis I asked if cloudless annual and monthly satellite image composites can be created for the entire vegetation season and with the adequate spatial, temporal and cloud filtering methods. I also managed to create nearly cloud-free annual S-2 imagery. The monthly temporal resolution was not yet possible to achieve due to the cloud-cover and the drawbacks of recent cloud-masking algorithms used in this Thesis.

Fourthly, I was interested if interannual disturbances in forest health due to biotic and abiotic damage can be detected by vegetation and water indices and I tested NDVI, NDVI change, Z NDVI, EVI, and NDWI, all derived from annual S-2 composites. All indices were suitable showing disturbances in different extent and severity, but Z NDVI showed the most differences from the long term mean and thus it was used in comparison of RS and ground-based maps.

Fifthly, I was keen to know if it is necessary to develop new methods for reaching agreement between RS and ground-based datasets and yes, not only the different existing methods had to be combined to achieve the goals, but new codes had to be implemented as well for the specific vegetation indices used in the monitoring system. Developing a specific computer code system as a base for a novel forest monitoring system was done and several VI-s were tested for disturbance detecting. From the several indices the Z NDVI was the most suitable for the monitoring goals, thus it was used as base for the RS damage detection and accuracy assessment was made based on this dataset.

My results indicated that the combined dataset of satellite imagery and ground-based data provided suitable input for forest damage monitoring conducted with GEE. The applied method successfully identified different types of forest damage (abiotic, biotic and

anthropogenic) on Z NDVI maps in the surveyed period with 78% Total Accuracy. This mean accuracy was based on all years between 2017 and 2020 and all study areas and can be considered satisfactory. However, the study sites and years differed from each other. The accuracy was excellent in the case of Nagyerdő (94%), hight in Farkas-erdő (80%) and moderate in Central Bükk (61%).

The satisfactory and moderate Total Accuracy results of Farkas-erdő and Central Bükk have to be improved to reach the state-of-the-art level. Further developments are also needed to introduce this method in a wall-to-wall, operational system, namely, to improve the forest masking, cloud filtering, the density, the accuracy of damage threshold determination, eventually to use Machine Learning for damage detection.

The seasonality in vegetation indices was studied on time series as well. Cloud masking already helped in that issue, but new datasets should be tested. The great advantage of GEE is flexibility and resilience: with a working method, a new study site can be surveyed easily and rapidly if the new area is also covered by the same RS dataset.

In the sixth hypothesis about if Copernicus forest maps can support my monitoring system by providing novel, satellite-based forest masks for both the study areas and the whole of Hungary and it turned out that these masks can be used in the GEE system and could improve monitoring speed since they are already built in, but the accuracy differed with the designation of forested areas in 1-20% compared to reference maps. However, it has great importance since RS-based maps can be updated more frequently than tradition ones plus on European level the monitoring would be easier on a map which is available for all countries. But even on study site level the masks could differ significantly, and the possible reasons are explained below.

Better quality forest mask is needed and can be created by excluding areas with a regularly updated clearcut class and only focusing on actual forest-covered compartments. Cloud filtering is also essential part of and forest monitoring and even a small amount of remaining cloud cover can cause problems but to achieve completely cloudless image is very challenging. A cloud filtering (cloudy pixel percentage and QA 60 bitmask) method was used in this PhD Thesis, and it provided high-quality mosaics for each study area and period. Nevertheless, cloudy springs and summers caused gaps in the dataset due to the high cloud cover. To solve

this problem, novel cloud-filtering algorithms like Fmask or s2cloudless can be applied to S-2 images, and with the adequate cloudless images created by the novel cloud filtering, eventually it will be possible to increase monitoring frequency and analyse forest health on a weekly or at maximum monthly basis instead of annual composites.

The wall-to-wall expansion worked for maps made for Hungary, some functions, like displaying data on a graph, did not work at that scale. Also, native S-2 resolution had to be rescaled from 10x10 m to 100x100 m to be able to display data on this scale.

Regarding the seventh hypothesis, I hypothesized that the ground-based reports can be used for validation of RS data, and these reports were probed to be useful indeed, however, the accuracy can be improved. Problems occurred due to the varied reasons.

I tested different parameters which could be compared to pixels of satellite images but nor the damage frequency, intensity and ratio gave very accurate results of all study areas and all years. The frequency was proved to be the best marking the number of damage trees in the compartment; however, it doesn't concern how badly they were damaged. While the intensity is the opposite of that, which is less accurate on spatial based analysis. This was the reason why I created the damage ratio based on damaged area and total area of the compartment, but despite the idea it did not work as well as I expected but was still better than the intensity. Yet it would be needed to register the location of the damage core with GPS coordinates in the Hungarian National Forest Damage Registration System which would be a great help to match ground-based survey with RS. The time matching is also problematic since reports are delivered sometimes a year after the actual damage while in theory S-2 could provide new data in every 2-5 days, from what the composites are made.

The question of reliability emerged, if the system is robust enough for forest authorities and managers to forest damage monitoring or not. The answer is that, before we recommend it for operational use, the system has to be tested in several areas, but regarding the results of the analysed three study areas and four years it can be said that 94, 80 and 61 % Total Accuracy values are promising enough to put more effort into the development.

The lack of workforce in the forestry sector Since nowadays is a serious problem, thus it is very important to support fieldwork with RS to enhance effectiveness. The RS could reduce the workload of the forestry labour force as well and provide forest data quicker and more

accurately than the traditional methods used in fieldwork. The usage of field reports and forestry data from national forest damage databases could enhance the possibility of expanding the method into other regions of Hungary, since the datasets are available for the entire country in a uniform way, and no extra field measurements would be needed. That is one of the reasons why this database was used in this PhD instead of own field measurements.

Yet before reaching the operational level, the suitability of the proposed monitoring approach should be tested on a larger scale as well. The expansion of this GEE-based monitoring method into a wall-to-wall monitoring system is possible, for Hungary or even Europe. The similar conditions and similar forest damage types in Europe could be monitored in a uniform way regarding data collection, processing, analysis, and visualization which would be a novel solution instead of national approaches. Cloud computing and ML both have great relevance in this plan, with them the entire monitoring process can be made online. It would be ideal to compute the dynamic damage threshold for forest damage by ML algorithms in GEE. To enhance accuracy the thresholds of damage could be determined by ML instead of manual setting. ML could detect trends in anomalies of time series which sit outside these patterns and identify the thresholds automatically.

7. Thesis

7.1. Forest health state was successfully monitored based on high resolution, annual Sentinel-2 satellite image series from 2017 until 2020 in the selected study areas (Nagyerdő, Farkas-erdő, Central Bükk) in Hungary, using Google Earth Engine online, cloud computing system. The study sites differed in location (east, west, and north), terrain (plain, hilly, mountainous), size (1092, 5500, 52000 ha), and species composition (oak, hornbeam, beech – dominated forests) to represent different forest site types.

7.2. Forest damage was shown on vegetation and water index maps (NDVI, Z NDVI, NDWI, EVI) and charts derived from cloudless, Sentinel-2 composites of the entire vegetation season (April - October). Both biotic (insect) and abiotic (wind, snow, ice, frost, drought) damage resulted in negative changes in the index values. In the case of Z NDVI, the threshold of -0.5 was chosen for forest damage, where all equal or lower values refer to negative change, while the ground-based damage frequency was set at least 30%.

7.3. Remotely sensed forest damage was validated with systematically collected ground-surveyed forest damage reports based on the damaged area, intensity, frequency, and sanitary logging data. The remotely sensed dataset was compared to damage frequency, intensity, and ratio values. The ratio was a novel field surveyed data type which was based on the damaged and total area of the compartments. In that would be desired to have the location of damage registered with GPS coordinates in the reports. All study sites' mean total accuracy values showed that frequency has the highest accuracy with 78%, followed by the ratio at 46% and intensity at 30%. Regarding each study site, Nagyerdő showed 94% total accuracy in the surveyed four years, while Farkas-erdő did 80% and Central Bükk 61%.

7.4. The Google Earth Engine-based method for forest health assessment is capable of running a nationwide monitoring system. The Sentinel-2-based method was successfully tested for Hungary on the country level using Copernicus forest cover maps and Sentinel-based Z NDVI maps. The satellite-based forest cover maps were generally more up to date but larger in extension with 1-20 % in the mean for the study areas and country-wide scale compared to the land-use-based Copernicus maps of the National Forest Database or National Ecosystem map. However, they are all based on different methods, have different formats (vector vs raster, 10x10 vs 20x20 m resolution) and made in different years. Definition of forest and forest masking technique is not the same either.

7.5. Machine Learning can be applied for forest species classification in the GEE system. Species composition can be mapped on pixel level using Random Forest method on Sentinel-2 composites and validated by ground-based datasets. In the case of Nagyerdő 82% Total Accuracy was achieved for the four dominant tree species (pedunculate oak, red oak, Scots pine and Black locust).

7.6. The novel approach could be integrated into the operating TEMRE system or the Forestry Subsystem of the Hungarian Earth Observation Information System since both utilize S-2 imagery.

Acknowledgement

I would like to express my gratitude to my supervisors, Dr. Géza Király and Dr. Zoltán Somogyi (Hungarian Forest Research Institute) for their support and supervision of my work. Their

knowledge helped me complete my academic research by conducting my PhD. The same applies to my opponents Dr. Kornél Czimber, Dr. Anikó Kern (Eötvös Loránd University) and Dr. Péter Burai (University of Debrecen) who all helped me to produce quality work.

I am grateful to my employee, the Hungarian Forest Research Institute of the University of Sopron, formerly of the Hungarian National Agricultural Research and Innovation Centre, especially Dr. Attila Borovics (institute director) and Dr. Gábor Illés (vice director), who supported my work from the beginning. I am grateful for the field damage reports from Dr. György Csóka and Dr. Anikó Hirka (Department of Forest Protection). I also want to thank all colleagues at the Department of Ecology and Silviculture who helped in any way during these years. My staying in Sopron was supported by the Department of Economy.

I would like to thank four Hungarian forestry companies, namely the Nyírerdő Forestry PLC. (especially Zoltán Gencsi), the Szombathely Forestry PLC., the Északerdő Forestry PLC. and the TAEG Forestry PLC. for providing practical forest data for the study areas of my research.

I would like to offer my special thanks to Dr. Svein Solberg from the Norwegian Institute of Bioeconomy Research (Ås, Norway) for accepting me as PhD trainee in 2020 and 2021 when I spent half a year in Norway and got involved in various forest research projects. My appreciation also goes to all my other colleagues in Norway who conversed a lot with me about scientific topics and whom with I had a great time in NIBIO.

Eventually, I would like to express my gratitude to my parents, grandparents, sister, and brother. Without their understanding and encouragement during these years, completing the PhD would have been even harder. I especially thank the feedback from my father and younger brother who both hold PhD degree and are completely aware of its difficulty. I wish to thank my friends as well, who helped me in their ways and believed in me during these years that I will be able to accomplish the PhD. This applies to my personal trainers, Szonja Szőke and Anita Reszegi in gym and my dance partner, Réka Krisztina Farkas as well who contributed to maintaining my physical and mental health with their positive attitude, during the very challenging period resulting in to achieve the Doctoral degree.

My PHD research was supported with the following grants:

- QUALITAS ”Development of Higher Education in Sopron, Szombathely and Tata grant” (EFOP) - 2019
- QUALITAS ”Development of Higher Education in Sopron, Szombathely and Tata grant” (EFOP) – 2020
- QUALITAS “Development of Higher Education in Sopron, Szombathely and Tata grant” (EFOP) - 2021
- Campus Mundi foreign internship - 2020
- Campus Mundi foreign internship - 2021
- New National Excellence Program of the Ministry for Innovation and Technology from the source of the National Research, Development and Innovation Fund (ÚNKP) – 2022

List of abbreviations

Abbreviation	Definition
A	Akác – black locust – *Robinia pseudoacacia*
AI	Artificial Intelligence
AOI	Area of Interest
API	Application Programming Interface
ASTER	Advanced Spaceborne Thermal Emission and Reflection Radiometer
B	Bükk – beech – Fagus sylvatica
CB	Central Bükk
CLC	Corine Land Cover
CNDM	Canada the National Deforestation Monitoring System
CS	Csertölgy - Turkey oak – *Quercus cerris*
DI	Difference Index
DLT	Dominant leaf type
DLTC	Dominant Leaf Type Change
EF	Scots pine
EF	Erdei fenyő – Scots pine – Pinus sylvestris
ELM	Elegyedés módja - tree species mixture
EMMRE	Erdővédelmi Mérő- és Megfigyelő Rendszer
ESA	European Space Agency
EVI	Enhanced Vegetation Index

FAFN	Main tree species
FD	Forestry Database of Hungary
FE	Farkas-erdő
FIR	Földmegfigyelési Információs Rendszer
FN	False Negative
FP	False Positive
FTY	Forest type product
GEE	Google Earth Engine
GEO	Geosynchronous orbit
GFW	Global Forest Watch
GMES	Global Monitoring for Environment and Security
GNDVI	Green Normalized Difference Vegetation Index
GNSS	Global Navigation Satellite Systems.
GPS	Global Positioning System
GSL	growing season length
GY	Gyertyán – hornbeam – Carpinus betulus
HEO	the High Earth orbit
HLS	Harmonized Landsat and Sentinel dataset
IBLES	Instytut Badawczy Leśnictwa (Polish Forest Research Institute)
IDE	Integrated Development Environment
JSZ	index - jelzőszám
KNN	k-Nearest Neighbours
KST	Kocsányos tölgy – pedunculate oak – *Quercus robur*
KTT	Kocsánytalan tölgy – sessile oak – Quercus *petraea*
L	Landsat
L1C	Top Of Atmosphere reflectances
L2A	Bottom Of Atmosphere
LAI	Leaf Area Index
LEO	Low Earth orbit
LF	Lucfenyő – Norway spruce – *Picea abies*
LIDAR	Light Detection and Ranging
MEO	Medium Earth orbit
MKGP	Slovenian Ministry of Agriculture, Forestry and Food
ML	Machine Learning
MODIS	Moderate Resolution Imaging Spectroradiometer

MSI Moisture Stress Index

MSI Multispectral Instrument

MTCI Terrestrial Chlorophyll Index

NASA National Aeronautics and Space Administration

NDII Normalized Difference Infrared Index

NDII Normalized Difference Infrared Index

NDVI ch Normalized Difference Vegetation Index change

NDVI Normalized Difference Vegetation Index

NDWI Normalized Difference Water Index

NFDRS Forest Damage Registration System (in Hungarian Országos Erdőkár Nyilvántartási Rendszer)

NFDRS Hungarian National Forest Damage Registration System

NFK EI Forestry Department of Hungarian National Land Centre

NIR Near-Infrared

NÖSZTÉP Ecosystem Map of Hungary

PA Producer's Accuracy

PLC Privite Limited Company

Radar Radio Detection and Ranging

REIP Red Edge Inflection Point

RF Random Forest

RGB Red Green Blue (true colour)

ROI Region of Interest

RS Remote Sensing

S-2 Sentinel-2

SCP Semi-Automatic Classification Plugin

SO Synchronous orbit

Sonar Sound Navigation Ranging

SOS Start of the growing Season

SPOT Satellite Pour l'Observation de la Terre

SSO Semi-synchronous orbit

SVM Support Vector Machines

SWIR Short-wave infrared

TA Total Accuracy

TCCM Tree Cover Change Mask

TCD Tree cover density

TEMRE Hungarian Remote Sensing based Forest Health Monitoring System

TN True Negative

TP True Positive

UA User's Accuracy

ÚHÚL Czech Forest Management Institute – (Ústav pro hospodářskou úpravu lesů Brandýs nad Labem)

USDA United States Department of Agriculture

VI Vegetation Index

VT Vörös tölgy – red oak – *Quercus rubra*

Z NDVI Standardized Normalized Difference Vegetation Index

List of figures and tables

List of figures

List of tables

References

Abdullah, H., Skidmore, A., Darvishzadeh, R., Heurich, M. (2018): Sentinel-2 accurately maps green-attack stage of European spruce bark beetle (Ips typographus, L.) compared with Landsat-8. 10.1002/rse2.93.

Agrárminisztérium (2019): Ökoszisztéma-alaptérkép és adatmodell kialakítása. Magyarország Ökosztisztéma-alaptérképe. [Establishing Ecosystem Map of Hungary by the Ministry of Agriculture]. DOI: 10.34811/osz.alapterkep.

Axelsson, A., Lindberg, E., Reese H., Olsson, H. (2021). Tree species classification using Sentinel-2 imagery and Bayesian inference. International Journal of Applied Earth Observation and Geoinformation, Volume 100, 2021, 102318, ISSN 0303-2434, https://doi.org/10.1016/j.jag.2021.102318.

Banskota, A., Kayastha, N., Falkowski, M.J., Wulder, M.A., Froese, R.E., White, J.C. (2014): Forest Monitoring Using Landsat Time Series Data: A Review, Canadian Journal of Remote Sensing, 40:5, 362-384, DOI:10.1080/07038992.2014.987376

Bar, S., Parida, B.R., Chandra Pandey, A. (2020): Landsat-8 and Sentinel-2 based Forest fire burn area mapping using machine learning algorithms on GEE cloud platform over Uttarakhand, Western Himalaya. Remote Sensing Applications: Society and Environment, 100324. doi:10.1016/j.rsase.2020.100324.

Barka I., Bucha, T. (2010): Processing and Utilization of Remote Sensing Data in the Regional Information System (RIS) of Ecological and Productive State of Forest. GIS Ostrava 2010.

Barka, I., Bucha, T. Molnár, T., Móricz, N., Somogyi, Z., Koreň, M. (2019): Suitability of MODIS-based NDVI index for forest monitoring and its seasonal applications in Central Europe. Central European Forestry Journal. 66. 206-217. 10.2478/forj-2019-0020.

Barka, I., Lukeš, P., Bucha, T., Hlásny, T., Strejček, R., Mlčoušek, M., Křístek, Š. (2018): Remote sensing-based forest health monitoring systems-case studies from Czechia and Slovakia. Lesnícky Časopis. 64. 259 – 275. 10.1515/forj-2017-0051.

Bárta, V., Lukeš, P., Homolova, L. (2021): Early detection of bark beetle infestation in Norway spruce forests of Central Europe using Sentinel-2. International Journal of Applied Earth Observation and Geoinformation. 100. 10.1016/j.jag.2021.102335.

Bartold, M., 2012: Monitoring of forest damage in Poland and Slovakia based on Terra MODIS satellite images. Geoinformation Issues, Vol. 4, No 1 (4), 23 – 31/2012

Barton, I., Király, G., Czimber, K. (2017): Képfeldolgozó program fejlesztése nagy mennyiségű földmegfigyelési adat feldolgozásához és kiértékeléséhez; In: Bidló, A; Facskó, F (szerk.) Soproni Egyetem Erdőmérnöki Kar VI. Kari Tudományos Konferencia; Sopron, Magyarország: Soproni Egyetem Kiadó (2017) pp. 164-167., 4 p.

Barton, I., Király, G., Czimber, K. (2018): Sentinel-2A űrfelvétel-idősorozat sűrűség vizsgálata az országos erdőállományra; [Density analysis of the Sentinel-2A spaceborne time series on national forests] In: Bidló, A; Facskó, F (szerk.) Soproni Egyetem Erdőmérnöki Kar VI. Kari Tudományos Konferencia; Sopron, Magyarország: Soproni Egyetem Kiadó, (2018) pp. 123-127., 5 p.

Barton, I., Király, G., Czimber, K., Hollaus, M., Pfeifer, N. (2017c): Treefall Gap Mapping Using Sentinel-2 Images. Forests 2017, 8, 426.

Barton, I (2021): Faállományok felmérése és modellezése távérzékelési és geoinformatikai módszerekkel. [Survey and modelling of tree stands using remote sensing and geoinformatics methods]. PhD Theses, University of Sopron.

Belényesi, M., Burai, P., Czimber, K., Kristóf, D., Király, G., Tanács, E. (2013): Távérzékelési adatok és módszerek erdőtérképezési célú felhasználása. [Use of remote sensing data and methods for forest mapping.] SH/4/13 – WP1 Megvalósíthatósági tanulmány, Budapest, 2013.

Bucha, T., Barka, I. (2010): Processing and Utilization of Remote Sensing Data in the Regional Information System (RIS) of Ecological and Productive State of Forest. GIS Ostrava 2010.

Bucha, T., Koreň, M. (2014): Phenology of the beech forests in the Western Carpathians from MODIS for 2000-2015 In. Bucha (ed): Satelity v službách lesa. SAP-Slovak Academic Press Bratislava, 202 s.

Buras, A., Rammig, A., & Zang, C. S. (2020): Quantifying impacts of the 2018 drought on European ecosystems in comparison to 2003. Biogeosciences, 17(6), 1655-1672. doi:10.5194/bg-17-1655-2020

Buras, A., Rammig, A., Zang, C. S. (2021): The European Forest Condition Monitor: Using Remotely Sensed Forest Greenness to Identify Hot Spots of Forest Decline. Frontiers in Plant Science, 12. https://doi.org/10.3389/fpls.2021.689220

Canada's National Deforestation Monitoring System (CNDMS) (2015): System Description. 2015. Dyk, A.; Leckie, D.; Tinis, S.; Ortlepp, S. Natural Resources Canada, Canadian Forest Service, Pacific Forestry Centre, Victoria, British Columbia. Information report BC-X-439. 30p.

Chen N, Tsendbazar NE, Hamunyela E, Verbesselt J, Herold M (2021b). Sub-annual tropical forest disturbance monitoring using harmonized Landsat and Sentinel-2 data, International Journal of Applied Earth Observation and Geoinformation, Volume 102, 2021, 102386, https://doi.org/10.1016/j.jag.2021.102386.

Chen S, Woodcock CE, Bullock EL, Arévalo P, Torchinava P, Peng S, Olofsson P (2021a). Monitoring temperate forest degradation on Google Earth Engine using Landsat time series analysis. Remote Sensing of Environment, Volume 265, 2021, 112648, https://doi.org/10.1016/j.rse.2021.112648.

Congalton, R., Green, K. (2019). Assessing the Accuracy of Remotely Sensed Data: Principles and Practices, Third Edition. 10.1201/9780429052729. pp 17.

Copernicus (2022): Tree Cover Density status maps. Online: https://land.copernicus.eu/pan-european/high-resolution-layers/forests/tree-cover-density/status-maps

Csóka, Gy., Hirka, A., Koltay, A., Kolozs, L. (2013): Erdőkárok - képes útmutató. [Forest damage – guide with pictures]. Agroinform Press, Budapest. ISBN 978-963-7349-37-9. pp 40,41,45, 48,84,127,141.

CzechGlobe (2019): Mapserver. Online: http://mapserver.czechglobe.cz/en/map

de Jong, R., Verbesselt, J., Schaepman, M.E., de Bruin, S. (2012): Trend changes in global greening and browning: Contribution of short-term trends to longer-term change. Global Change Biology 2012, 18, 642 – 655. DOI: https://doi.org/10.1111/j.1365-2486.2011.02578.x.

Egererdő (2021): Az EGERERDŐ Zrt. erdészetei. [Forestry units of Egererdő PLC.] Online: http://client4.springmedia.hu/index.php?tpl=page&cID=10

ESA (2019): Biomass mission. Online: https://www.esa.int/ESA_Multimedia/Images/2019/02/Biomass_mission

ESA (2020a): Current and future missions. Online: https://www.esa.int/Enabling_Support/Operations/Current_and_future_missions

ESA (2020b): Flex mission. Online: https://earth.esa.int/web/guest/missions/esa-future-missions/flex

ESA (2020c): Multispectral Instrument (MSI) Overview. Online: https://sentinel.esa.int/web/sentinel/technical-guides/sentinel-2-msi/msi-instrument

ESA (2020d): Sentinel-3 mission summary. Online: https://sentinel.esa.int/web/sentinel/missions/sentinel-3/overview/mission-summary

ESA (2020e): Copernicus overview. Online: https://www.esa.int/Our_Activities/Observing_the_Earth/Copernicus/Overview4

Északerdő (2021): ÉSZAKERDŐ Erdőgazdasági Zrt. [Egererdő Forestry PLC.] Online: http://www.eszakerdo.hu/magyar/menu/ceginfo_uj.htm

Fernandez-Carrillo, A., Patocka, Z., Dobrovolný, L., Franco-Nieto, A., Revilla-Romero, B. (2020): Monitoring Bark Beetle Forest Damage in Central Europe. A Remote Sensing Approach Validated with Field Data. Remote Sensing. 12. 3634. 10.3390/rs12213634.

Gao, B.C. (1996): NDWI—A Normalized Difference Water Index for Remote Sensing of Vegetation Liquid Water from Space. Remote Sensing of Environment, 58, 257-266. https://doi.org/10.1016/S0034-4257(96)00067-3

Garonna, I., De Jong, R., De Wit, A.J.W., Mücher, C.A., Schmid, B., Schaepman, M.E. (2014): Strong contribution of autumn phenology to changes in satellite-derived growing season length estimates across Europe (1982 – 2011). Global Change Biology, 20(11): 3457-3470.

Gencsi, Z. (2021): Debreceni Erdőskönyv. [Forest book of Debrecen] Kiadó: Nyírerdő Zrt. Felelős kiadó: Dr. Szalacsi Árpád.

GISGeography (2018): Geosynchronous vs Geostationary Orbits. Online: https://gisgeography.com/geosynchronous-geostationary-orbits/

Global Forest Watch (2019): Forest Monitoring Designed for Action. Online: https://www.globalforestwatch.org/

Gómez, D., Ritger, H., Pearce, C., Eickwort, J., Hulcr, J. (2020): Ability of Remote Sensing Systems to Detect Bark Beetle Spots in the Southeastern US. Forests. 11. 1167. 10.3390/f11111167.

Google (2019): Introduction of Google Earth Engine. Online: https://developers.google.com/earth-engine

Google (2020a): Sentinel-2 MSI: MultiSpectral Instrument. Online: https://developers.google.com/earth-engine/datasets/catalog/COPERNICUS_S2#description

Google (2020b): Sentinel-2: Cloud Probability. Online: https://developers.google.com/earth-engine/datasets/catalog/COPERNICUS_S2_CLOUD_PROBABILITY

Google (2020c): Datasets tagged borders in Earth Engine. Online: https://developers.google.com/earth-engine/datasets/tags/borders

Google (2021): Google App Engine. Online: https://cloud.google.com/appengine

Gorelick, N., Hancher, M., Dixon, M., Ilyushchenko, S., Thau, D., Moore, R. (2017): Google Earth Engine: Planetary-scale geospatial analysis for everyone, Remote Sensing of Environment, Volume 202, 2017, Pages 18-27, ISSN 0034-4257, https://doi.org/10.1016/j.rse.2017.06.031

Grubbs, F. (1969): Procedures for Detecting Outlying Observations in Samples, Technometrics, 11(1), pp. 1-21.

Hamunyela, E., Rosca, S., Mirt, A., Engle, E., Herold, M., Gieseke, F. & Verbesselt, J. (2020): Implementation of BFASTmonitor Algorithm on Google Earth Engine to Support Large-

Area and Sub-Annual Change Monitoring Using Earth Observation Data. Remote Sens. 2020, 12, 2953.

Hamunyela, E., Verbesselt, J., Roerink, G., Herold, M. (2013): Trends in Spring Phenology of Western European Deciduous Forests. Remote Sensing, 5: 6159-6179.

Hawryło, P., Bednarz, B., Wężyk, P., Szostak, M. (2018): Estimating defoliation of Scots pine stands using machine learning methods and vegetation indices of Sentinel-2, European Journal of Remote Sensing, 51:1, 194-205, DOI: 10.1080/22797254.2017.1417745

Hirka, A (2018): A 2017. évi biotikus és abiotikus erdőgazdasági károk, valamint a 2018-ban várható károsítások. [Biotic and abiotic forest damage in 2017 and expected ones in 2018]. Online: http://www.erti.hu/images/erti/Publikaciok/EV-Prognzis-2017-2018_3.pdf

Hirka, A. (2019): A 2018. évi biotikus és abiotikus erdőgazdasági károk, valamint a 2019-ban várható károsítások. [Biotic and abiotic forest damage in 2018 and expected ones in 2019]. Online: https://erti.naik.hu/sites/default/files/uploads/2019-09/prognozis_2018-2019.pdf

Hirka, A. (2020): A 2019. évi biotikus és abiotikus erdőgazdasági károk, valamint a 2020-ban várható károsítások. [Biotic and abiotic forest damage in 2019 and expected ones in 2020]. Online: https://erti.naik.hu/system/files/uploads/2020-09/prognozis_2019-2020.pdf

Hirka, A. (2023): A 2022. évi biotikus és abiotikus erdőgazdasági károk, valamint a 2023-ban várható károsítások. [Biotic and abiotic forest damage in 2022 and expected ones in 2023].

Hirka, A., Pödör, Z., Garamszegi, B., Csóka, Gy. (2018): A magyarországi erdei aszálykárok fél évszázados trendjei (1962-2011) - 50 years trends of the forest drought damage in Hungary (1962-2011). Erdészettudományi Közlemények. 8. 11-25. 10.17164/EK.2018.001.

Hlásny, T., Barka, I., Sitková, Z., Bucha, T., Konôpka, M., Lukac, M. (2014): MODIS-based vegetation index has sufficient sensitivity to indicate stand-level intra-seasonal climatic stress in oak and beech forests. Annals of Forest Science. 72. 10.1007/s13595-014-0404-2.

Ho, T.K. (1995): Random decision forests. Proceedings of 3rd International Conference on Document Analysis and Recognition, 1995, pp. 278-282 vol.1, DOI: 10.1109/ICDAR.1995.598994.

Honkavaara, E., Näsi, R., Alves de Oliveira, R., Viljanen, N., Suomalainen, J. & Khoramshahi, E., Hakala, T., Nevalainen, O., Markelin, L., Vuorinen, M., Kankaanhuhta, V., Paivi, L-S., Haataja, L. (2020): Using multitemporal hyper- and multispectral UAV imaging for detecting bark beetle infestation on Norway spruce. ISPRS - International Archives of the Photogrammetry, Remote Sensing and Spatial Information Sciences. XLIII-B3-2020. 429-434. 10.5194/isprs-archives-XLIII-B3-2020-429-2020.

Hortobágyi Nemzeti Park (HNP) (2020): Debreceni Nagyerdő TT. Online: http://www.hnp.hu/hu/szervezeti-egyseg/termeszetvedelem/oldal/debreceni-nagyerdo-tt

Huete, A. R. (2012): Vegetation Indices, Remote Sensing and Forest Monitoring. Geography Compass, 6(9), 513 – 532. doi:10.1111/j.1749-8198.2012.00507.x

Huete, A., Didan, K., Shimabukuro, Y. Ratana, P., Saleska, S., Hutyra, L., Yang, W., Nemani, R., Myneni, R. (2006): Amazon green-up with sunlight in the dry season. Geophysical Research Letters - GEOPHYS RES LETT. 33. 10.1029/2005GL025583.

Huo, L., Persson, H., Lindberg, E. (2021): Early detection of forest stress from European spruce bark beetle attack, and a new vegetation index: Normalized distance red & SWIR (NDRS). Remote Sensing of Environment. 255. 112240. 10.1016/j.rse.2020.112240.

Hycza, T., Stereńczak K., Bałazy, R. (2018): Black-Bridge data in the detection of forest area changes in the example of Sudety and Beskidy

ICP Forest (2011): International Co-operative Programme on Assessment and Monitoring of Air Pollution Effects on Forests. Online. http://icp-forests.net/

Instytut Badawczy Leśnictwa (IBLES) [Polish Forest Research Institute] (2019): Mapping portal. Online: https://www.ibles.pl/mapa/index.html

Jensen, J. R. (1996): Introductory digital image processing: a remote sensing perspective. Upper Saddle River, N.J., Prentice Hall. pp 573-576.

Jensen, J. R. (2016): Introductory digital image processing: a remote sensing perspective (4th ed.). Pearson Education.

Jin, H., Jönsson, A.M., Olsson, C. et al. (2019): New satellite-based estimates show significant trends in spring phenology and complex sensitivities to temperature and precipitation at northern European latitudes. Int J Biometeorol. https://doi.org/10.1007/s00484-019-01690-5

Jogtár (2017): 2017. évi LVI. törvény az erdőről, az erdő védelméről és az erdőgazdálkodásról szóló 2009. évi XXXVII. törvény és egyéb kapcsolódó törvények módosításáról. [Act LVI of 2017 amending Act XXXVII of 2009 on Forest, Forest Protection and Forest Management and other related acts.]. Online: https://mkogy.jogtar.hu/jogszabaly?docid=A1700056.TV

Justice, C.O., Townshend, J.R.G., Vermote, E.F., Masuoka, E., Wolfe, R.E., Saleous, N., Roy, D.P., Morisette, J.T. (2002): An overview of MODIS land data processing and product status. Remote Sensing of Environment, 83: 3-15.

Justice, C.O., Vermote, E., Townshend, J., Defries, Ruth, Roy, David, Hall, D.K., Salomonson, V.V., Privette, J.L., Riggs, G., Strahler, A., Lucht, W., Myneni, R.B., Knyazikhin, Y., Running, S.W., Nemani, R., Wan, Z.M., Huete, A., Van Leeuwen, W., & Wolfe, R., Barnsley, M.J. (1998): The moderate resolution imaging spectroradiometer (MODIS): Land remote sensing for global change research. IEEE Transactions Remote Sensing Geoscience and Remote Sensing. 36. 1228-1249. 10.1109/36.701075.

Kern, A., Barcza, Z., Hollós, R., Birinyi, E., Marjanović, H. (2022): Critical Climate Periods Explain a Large Fraction of the Observed Variability in Vegetation State. Remote Sens. 2022, *14*, 5621. https://doi.org/10.3390/rs14215621

Kern, A., Marjanović, H., Csóka, Gy., Móricz, N., Pernek, M., Hirka, A. & Matošević, D., Paulin, M., Kovač, G. (2021): Detecting the oak lace bug infestation in oak forests using MODIS and meteorological data. Agricultural and Forest Meteorology. 306. 108436. 10.1016/j.agrformet.2021.108436.

Kern, A., Marjanović, H., Dobor, L., Anić, M., Hlásny, T., Barcza, Z. (2017): Identification of Years with Extreme Vegetation State in Central Europe Based on Remote Sensing and Meteorological Data. South-east European forestry. 8. 10.15177/seefor.17-05.

Király, G. (2007): A távérzékelés erdészeti alkalmazása. [Application of remote sensing in forestry]. Phd Thesis, Sopron, 2007., p 121.

Király, G., Balla, Cs., Barton, I., Mészáros, Gy., Petrányi, B., Szabó K. (2017): Borított felszínmodellek erdészeti felhasználása. [Application of Digital Surface Models in forestry]. In Bidló A. – Facskó F. (szerk.): Soproni Egyetem Erdőmérnöki Kar VI. Kari Tudományos Konferencia. Soproni Egyetem Kiadó, Sopron, 118 – 122.

Koltay, A. (2006): Az erdők egészségi állapotának változásai az erdővédelmi monitoring rendszerek adatai alapján [Changes in forest health based on data from forest protection systems]. Tájökológiai lapok 4 (2): 327-337.

Koreň, M., Jakuš, R., Zápotocký, M., Barka, I., Holuša, J., Ďuračiová, R., Blaženec, M. (2021): Assessment of Machine Learning Algorithms for Modeling the Spatial Distribution of Bark Beetle Infestation. Forests 2021, *12*, 395. https://doi.org/10.3390/f12040395

Kovács, F., Gulácsi, A. (2018): MODIS EVI/NDVI alapú monitoring erdőterületeken 2000 – 2017 között a klímaváltozás földrajzi hatásának kimutatásában. [MODIS EVI/NDVI-based monitoring in forest areas between 2000-2017 aiming to show geographical impacts of climate change]. Geodézia és Kartográfia. 19-27. 10.30921/GK.70.2018.5.3.

Lakatos, M., Bihari, Z., Szentimrey, T. (2014): A klímaváltozás magyarországi jelei. [Sings of climate change in Hungary]. Légkör 59 (4), pp. 158 – 163.

Lausch, A., Erasmi, S., King, D., Magdon, P., Heurich, M. (2016): Understanding Forest Health with Remote Sensing -Part I & II.- A Review of Spectral Traits, Processes, and Remote sensing Characteristics. Remote Sensing. 8. 1029. 10.3390/rs8121029.

Lukeš, P., Strejček, R., Křístek, Š., Mlčoušek, M. (2018): Hodnocení zdravotního stavu lesních porostů v České republice pomocí dat Sentinel-2. [Forest health assessment in Czech Republic using Sentinel-2 satellite data]. Online: http://www.uhul.cz/images/aktuality_doc/Metodika_-_final.pdf

Makki, I. (2017): Hyperspectral Imaging for Landmine Detection. PhD Thesis, 2017.

Ministrstvo za kmetijstvo, gozdarstvo in prehrano (MKGP) [Slovenian Ministry of Agriculture, Forestry and Food] (2019): Publish Graphic Data Viewer. Online: http://rkg.gov.si/GERK/WebViewer

Molnár T., Király G. (2021): A Sárvári Farkas-erdő Sentinel-2 űrfelvétel alapú erdőmonitoring terve. [A forest monitoring plan of Farkas-erdő of Sárvár based on Sentinel-2 satellite images]. Erdészettudományi Közlemények, 11(2): 83-94. DOI: 10.17164/EK.2021.009

Molnár, T., Birinyi, M., Király, G., Móricz, N., Koltay, A., Hirka, A., Csóka, Gy., Somogyi, Z. (2019a): Egy bükki hótörés távérzékelési elemzése MODIS és Sentinel-2 műholdképek alapján. [Snow-break analysis in Bükk Mountains based on MODIS and Sentinel-2 satellite images]. Geomatikai Közlemények XXII. 2019. Sopron.

Molnár, T., Birinyi, M., Somogyi, Z., Király, G. (2019b): A 2017. áprilisi bükki hókárok felmérése és elemzése űrfelvételek alapján. [Snow-break analysis in Bükk Mountains based on

MODIS and Sentinel-2 satellite images]. Soproni Egyetem Erdőmérnöki Kar VII. Kari Tudományos Konferencia. Sopron.

Molnár, T., Király, G. (2022a): A Soproni-hegységet 2017-2020 között sújtó szúkárok távérzékelési felmérése Sentinel-2 műholdképeken. [Analysis of bark beetle damage in Sopron Mountains on Sentinel-2 satellite images]. IN Erdészeti Tudományos Konferencia Sopron. Szerk. Czimber Kornél. Sopron, 2022.

Molnár, T., Király, G. (2023): A satellite-based forest monitoring system based on Sentinel-2 imagery, Google Earth Engine cloud computing, and Machine Learning. iForest

Molnár, T., Koltay, A., Móricz, N., Somogyi, Z. (2018): Távérzékelésen alapuló Erdőállapot Monitoring Rendszer (TEMRE). [Hungarian Satellite-based Forest Monitoring System]. Alföldi Erdőkért Egyesület Kutatói Nap 2018. Tudományos eredmények a gyakorlatban. Lakitelek, 2018.

Molnár, T., Somogyi, Z., Király, G. (2021): A Debreceni Nagyerdő Sentinel-2 űrfelvételeken alapuló erdőmonitoring rendszer terve. [A forest monitoring plan of Nagyerdő of Debrecen based on Sentinel-2 satellite images]. IN Az elmélet és a gyakorlat találkozása a térinformatikában XII.: theory meets practice in GIS: Debreceni Egyetem, XII. Térinformatika Konferencia és Szakkiállítás. Szerk. Molnár Vanda Éva. Debrecen, 2021. ISBN 978-963-318-977-1

Móricz, N., Garamszegi, B., Rasztovits, E., Bidló, A., Horváth, A., Jagicza, A., Illés, G., Vekerdy, Z., Somogyi, Z., Gálos, B., 2018: Recent Drought-Induced Vitality Decline of Black Pine (PinusnigraArn.) in South-West Hungary—Is This Drought-Resistant Species under Threat by Climate Change? Forests 2018, 9, 414.

Nádor, G., László, I., Csornai, G. (2007): Monitoring of forest damage caused by gypsy moth in Hungary using Envisat MERIS data (2005-2006).

NASA (2000): Normalized Difference Vegetation Index (NDVI). Online: https://earthobservatory.nasa.gov/features/MeasuringVegetation/measuring_vegetation_2.php

NASA (2017): Earth Missions List. Online: https://www.nasa.gov/content/earth-missions-list

NASA (2019a): MODIS. Online: https://terra.nasa.gov/about/terra-instruments/modis

NASA (2019b): Aqua Earth-observing satellite mission. Online: https://aqua.nasa.gov/

NASA (2021): About Terra. Online: https://terra.nasa.gov/about

Nemzeti Földügyi Központ Erdészeti Főosztálya (NFK EF) (2004): Erdőrendezési útmutató kódjegyzéke és mellékletei. [Forest management code list and appendices]. Online: https://docplayer.hu/28170821-Erdorendezesi-utmutato-kodjegyzeke-es-mellekletei.html

Nemzeti Földügyi Központ Erdészeti Főosztálya (NFK EF) (2018): Országos Erdőkár Nyilvántartási Rendszer útmutatói. [Manuals of National Forest Damage Registration System]. Online: http://portal.nebih.gov.hu/documents/10182/1047730/Erdővédelmi+kárbejelentő_Útmutató_új_20180604.pdf/96c53f3a-89ca-967f-f40a-98b059115fad

Nemzeti Földügyi Központ Erdészeti Főosztálya (NFK EF) (2020): Országos Erdőkár Nyilvántartási Rendszer. [National Forest Damage Registration System]. Online: https://erdoterkep.nebih.gov.hu/erdokar/index.htm

Norman, S. P., Christie, W. M. (2020): Chapter 7 - Satellite-based evidence of forest stress and decline across the conterminous United States for 2016, 2017, and 2018. In: Potter, Kevin M.; Conkling, Barbara L., eds. Forest health monitoring: national status, trends, and analysis 2019. Gen. Tech. Rep. SRS-250. Asheville, NC: U.S. Department of Agriculture, Forest Service, Southern Research Station: 151-166.

Nyírerdő (2020): Debreceni Erdészet. [Forestry unit of Debrecen]. Online: http://www.nyirerdo.hu/Erd_dbr.aspx

OpenStreetMaps (OSM) (2021): Közigazgatási határok. [Administrative borders]. Online: https://data2.openstreetmap.hu/hatarok/index.php?admin=2

Osei, J.C., Andam-Akorful, S. & Osei Jnr, E. (2019). Long Term Monitoring of Ghana's Forest Reserves Using Google Earth Engine. 10.20944/preprints201909.0016.v1.

Paulin, M., Hirka, A., Eötvös, Cs., Csaba, G., Fürjes-Mikó, Á., Csóka, Gy. (2020): Known and predicted impacts of the invasive oak lace bug (Corythucha arcuata) in European oak ecosystems – a review. Folia Oecologica. 47. 131-139. 10.2478/foecol-2020-0015.

Paulin, M., Hirka, A., Eötvös, Cs., Csaba, G., Mikó, Á., Csóka, Gy. (2020): Known and predicted impacts of the invasive oak lace bug (Corythucha arcuata) in European oak ecosystems – a review. Folia Oecologica. 47. 131-139. 10.2478/foecol-2020-0015.

Persson, M., Lindberg, E., Reese, H. (2018): Tree Species Classification with Multi-Temporal Sentinel-2 Data. Remote Sensing. 2018, 10, 1794. https://doi.org/10.3390/rs1011179.

Peters, A. J., Walter-Shea, E.A., Andrés Viña, L.J., Hayes, M., Svoboda, M.D. (2002): Drought monitoring with NDVI-based standardized vegetation index. Photogrammetric Engineering and Remote Sensing 68.1:72-75.

Puletti, N., Chianucci, F., Castaldi, C. (2017): Use of Sentinel-2 for forest classification in Mediterranean environments. Annals of Silvicultural Research. 10.12899/ASR-1463.

QGIS.org (2021). QGIS Geographic Information System. QGIS Association. http://www.qgis.org

Qiu, S., Zhu, Z., He, B. (2019): Fmask 4.0: Improved cloud and cloud shadow detection in Landsats 4-8 and Sentinel-2 imagery. Remote Sensing of Environment. 231. 111205. 10.1016/j.rse.2019.05.024.

Riebeek, H. (2009): Catalog of Earth Satellite Orbits. Online: https://earthobservatory.nasa.gov/features/OrbitsCatalog

Rouse, J.W, Haas, R.H., Scheel, J.A., and Deering, D.W. (1974): Monitoring Vegetation Systems in the Great Plains with ERTS. Proceedings, 3rd Earth Resource Technology Satellite (ERTS) Symposium, vol. 1, p. 48-62.

Saarinen, N., White, J.C., Wulder, M.A., Kangas, A., Tuominen, S., Kankare, V., Holopainen, M., Hyyppä, J., Vastaranta, M. (2018): Landsat archive holdings for Finland: opportunities for forest monitoring. Silva Fennica vol. 52 no. 3 article id 9986. 11 p. https://doi.org/10.14214/sf.9986

Sandino, J., Pegg, G., Gonzalez, F., Smith, G. (2018): Aerial Mapping of Forests Affected by Pathogens Using UAVs, Hyperspectral Sensors, and Artificial Intelligence.Sensors 18 (4), 944

Shapiro, S. S., Wilk, M. B. (1965): An analysis of variance test for normality (complete samples). Biometrika, 52(3-4), 591 – 611. doi:10.1093/biomet/52.3-4.591

Siņica- Siņavskis J, Dinuls R, Zarins J, Mednieks I (2020). Automatic tree species classification from Sentinel-2 images using deficient inventory data. 17th Biennial Baltic Electronics Conference (BEC), 2020, pp. 1-6, DOI: 10.1109/BEC49624.2020.9276810.

Somogyi, Z., Koltay, A., Molnár, T., Móricz, N. (2018): Forest health monitoring system in Hungary based on MODIS products. In Theory Meets Practice in GIS; Molnár, V.É., Eds.; Proceedings of the 9. Térinformatikai Konferencia és Szakkiállítás, Debrecen, Hungary, 24-25 May 2018; Debrecen University Press: Debrecen, Hungary, 2018: 325-330.

Somogyi, Z., Koltay, A., Molnár, T., Móricz, N. (2018b): Távérzékelésen alapuló Erdőállapot Monitoring Rendszer (TEMRE). [Hungarian Satellite-based Forest Monitoring System]. Erdészeti Lapok CLIII. évf., 2018. szeptemberi szám, p. 277-279.

Swinburne Astronomy Online (2019): Orbital Eccentricity. Online: http://astronomy.swin.edu.au/cosmos/O/Orbital+Eccentricity

Szombathelyi Erdészeti Zrt. (2020): Farkas-erdő. Online: http://www.szherdeszet.hu/kozjoleti-letesitmenyek/farkas-erdo.html

Szostak, M., Hawryło, P., Piela, D. (2018): Using of Sentinel-2 images for automation of the forest succession detection, European Journal of Remote Sensing, 51:1, 142-149, DOI: 10.1080/22797254.2017.1412272

Teshome, D.T., Zharare, G.E., Naidoo, S. (2020): The Threat of the Combined Effect of Biotic and Abiotic Stress Factors in Forestry Under a Changing Climate. Front Plant Sci. 2020 Nov 30;11:601009. DOI: 10.3389/fpls.2020.601009. PMID: 33329666; PMCID: PMC7733969.

Tobak, Z, Szatmári, J., van Leeuwen, B., Papp, L.: (2017): Az erdőtüzet követő szukcessziós folyamat és a fajösszetétel vizsgálata légi- és műholdas távérzékelési módszerekkel. [Investigation of post-fire succession and species composition using aerial and satellite remote sensing]. In: Blanka, V; Ladányi, Zs (eds.) Interdiszciplináris tájkutatás a XXI. században: a VII. Magyar Tájökológiai Konferencia tanulmányai. Szeged, Hungary: SZTE TTIK Földrajzi és Földtudományi Intézet (2017) 656 p. pp. 605-610. , 6 p.

USDA Forest Service (2020): ForWarn II. Online: https://forwarn.forestthreats.org/

USGS (2019): Landsat Satellite Missions. Online: https://www.usgs.gov/landresources/nli/landsat/landsat-satellite-missions?qt-science_support_page_related_con=2#qt-science_support_page_related_con

USGS (2022): HLS Overview. Online: https://lpdaac.usgs.gov/data/get-started-data/collection-overview/missions/harmonized-landsat-sentinel-2-hls-overview/

Varga, Z., Varga-Haszonits, Z., Enzsölné Gerencsér, E., Lantos, Zs., Milics, G. (2012): A fehér akác (Robinia pseudoacacia L.) fejlődésének bioklimatológiai elemzése. [Analysis of bioclimatological development of black locust] Acta Agronomica Óváriensis 54 (1), pp. 35 – 52.

Vojtkó, A. (2002): A Bükk hegység növényvilága. [Flora of Bükk Mountains] Online: https://www.researchgate.net/publication/336278611_A_Bukk_hegyseg_novenyvilaga

Waldzustandsmonitor (2019): German Forest Condition Monitor. Online: https://waldzustandsmonitor.de/en/forest-condition-monitor/

Wang, J., Sammis, T.W., Gutschick, V.P., Gebremichael, M., Dennis, S. O., Harrison, R. E. (2010): Review of Satellite Remote Sensing Use in Forest Health Studies

White, J.C., Tompalski, P., Vastaranta, M., Wulder, M.A., Saarinen, S., Stepper, C., Coops, N.C. (2017): A model development and application guide for generating an enhanced forest inventory using airborne laser scanning data and an area-based approach. White N.C. CWFC Information Report FI-X-018, 38 pp.

Wood, M.S., Keightley, E.K., Lee, A., and Norman, P. (2006): Continental Forest Monitoring Framework, Technical Report - Design and Pilot Study. National Forest Inventory, Bureau of Rural Sciences, Canberra.

Wulder, M. A., Roy, D. P., Radeloff, V. C., Loveland, T. R., Anderson, M. C., Johnson, D. M., Hansen, M.C., Cook, B. D. (2022): Fifty years of Landsat science and impacts. Remote Sensing of Environment, 280, 113195.

WWF (2017): The Kedr forest monitoring system. Online: https://wwf.ru/en/resources/news/lesa/v-primore-deystvuet-sistema-monitoringa-lesov-kedr

Xiong, X., Butler, J. (2018): Comprehensive Remote Sensing. 2018, Elsevier, ISBN: 978-0-12-803221-3

Yang, S (2021). Detecting bark beetle damage with Sentinel-2 multi-temporal data in Sweden. Msc Thesis, Department of Physical Geography and Ecosystem Science Lund University, Lund, Sweden. 2021.

Zavod za gozdove Slovenije (ZGS) [Slovenian Forest Service] (2019): Forest data viewer. Online: https://prostor.zgs.gov.si/pregledovalnik/?locale=en

Zhang K, Liu N, Chen Y, Gao S (2019). Comparison of different machine learning method for GPP estimation using remote sensing data. IOP Conference Series: Materials Science and Engineering. 490. 062010. 10.1088/1757-899X/490/6/062010.

Zhang, Y., Jiang, X., Wang, S. (2022): Fingerspelling Recognition by 12-Layer CNN with Stochastic Pooling. Mobile Networks and Applications. 10.1007/s11036-021-01900-8.

Zhu, Z., Fu, Y., Woodcock, C., Olofsson, P., Vogelmann, J. Holden, C., Wang, M., Dai, S., Yu, Y. (2016): Including the land cover change in the analysis of greenness trends using all

available Landsat 5, 7, and 8 images: A case study from Guangzhou, China (2000 – 2014). Remote Sensing of Environment. 185. 10.1016/j.rse.2016.03.036.

Zöld Kör (2019): A Debreceni Nagyerdő és környéke. [Nagyerdő of Debrecen and its surroundings]. Center-Print Nyomda. Debrecen.

Zoltán, L., Friedl, Z., Pacskó, V., Orbán, I., Tanács, E., Magyar, B., Kristóf, D., Standovár, T. (2021): Application of Sentinel-1 radar data for mapping ice disturbance in a forested area. European Journal of Remote Sensing 54(1): 568-587. https://doi.org/10.1080/22797254.2021.1982407